Preliminary Study of Russian River Estuary: Circulation and Water Quality Monitoring

2009 DATA REPORT

Report to
Sonoma County Water Agency (SCWA)

Prepared by

Dane K. Behrens & John L. Largier

Bodega Marine Laboratory (BML)
University of California Davis

15 February 2010

1. Introduction

This report is a summary of data collected in the Russian River Estuary during the summer and fall of 2009. As outlined in the Statement of Work, the purpose of this study is to provide a view of circulation, stratification, residence and salinity in the Russian River estuary during a period when river flows were lower than normal.

As planned, two Acoustic Doppler Current Profilers (ADCPs) were deployed in the estuary to collect data on current velocities through the water column. In addition, repeat boat-based CTD surveys were conducted to characterize the vertical structure of salinity, dissolved oxygen (DO) and temperature in the estuary. The deployment locations for the moored ADCPs and sites where CTD profiles were taken are given in Figure 1.1. Further, the timing of these deployments and profiles is summarized in Table 1 and Figure 1.2.

To supplement these efforts, several additional tasks were performed:

- Four data loggers were used to measure water level and surface temperature at high temporal resolution in different sections of the estuary
- Three stationary sondes were deployed to measure temperature and salinity at the channel bottom in sections of the river (sites chosen to complement data collected by sondes deployed by the SCWA. The purpose of this was to track the upstream movement of saline water.
- Nearshore waves were estimated, and data of river flow and nearby wind speed were collected to provide context for changes in estuary behavior

An extended mouth closure event during the months of September and October allowed for the study of prolonged closure conditions at high temporal resolution. Enough data were collected to provide a comparison between fully tidal conditions and closed-inlet conditions.

The remaining sections outline the data, with each data type presented separately. Sections 2 and 3 summarize the results of the water level and temperature loggers. Section 4 describes the results of the stationary sondes in the estuary. Sections 5 and 6 present wave and wind measurements, respectively. Section 7 is a summary of river flow conditions during the study period. Current velocity profiles are described in Section 8. Section 9 is divided into three subsections describing the spatial CTD results for DO, temperature, and salinity, respectively. Analysis and interpretation of these data will be addressed in a subsequent report.

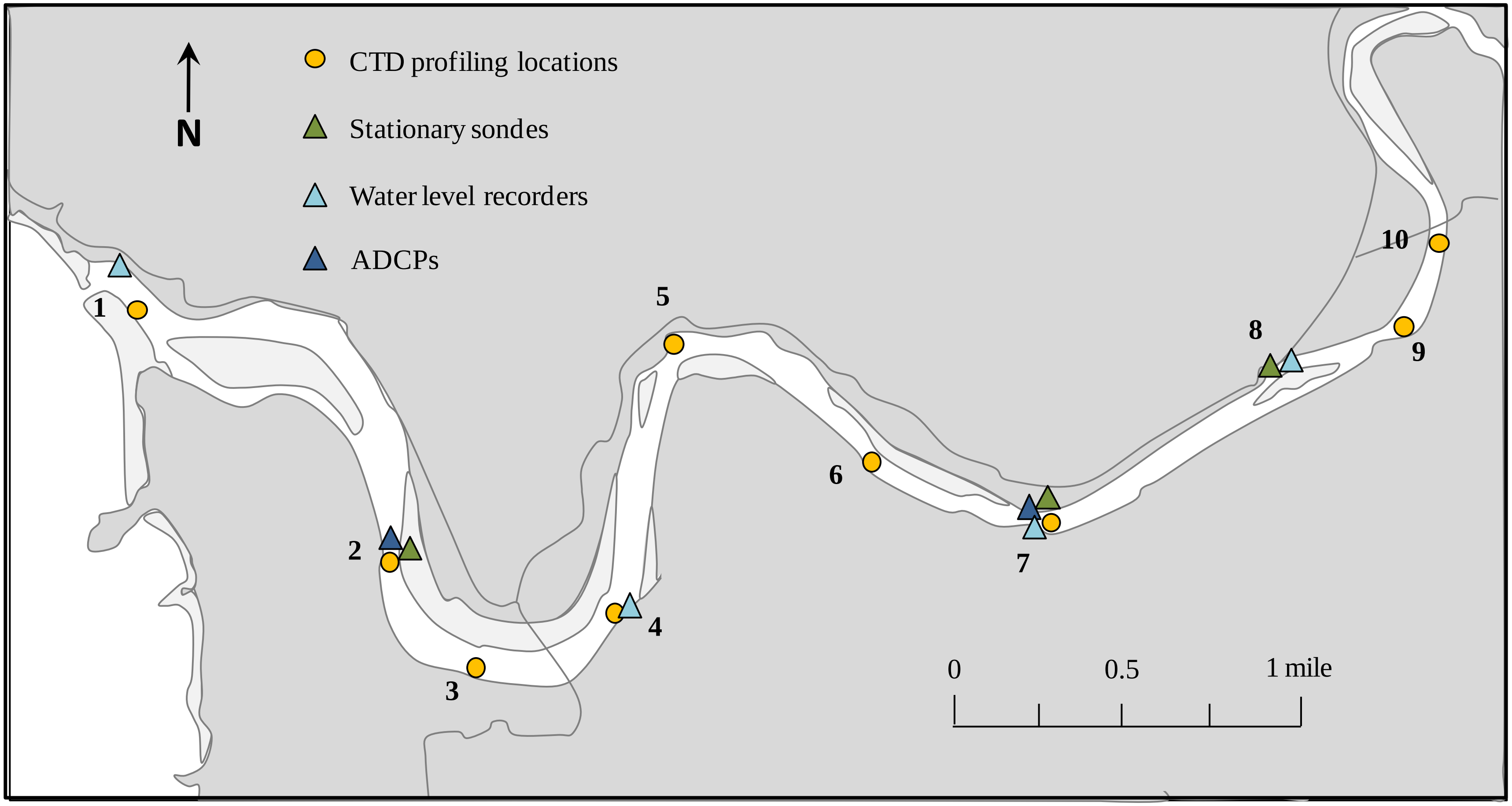

Figure 1.1 Locations of deployed devices and CTD profiling locations. Numbered locations are explained in Table 1.

Table 1. Data collection sites

Station No. (Fig X)	Station Name	Data Collection	Approx. Location	Installation Date	Extraction Date
1	--	WL[1]/ temp	38.451339 N 123.127301 W	8/11/2009	10/24/2009
2	"Mouth"	CTD	38.450056 N 123.126883 W	--	--
3	"Patty's Rock"	CTD	38.439431 N 123.111656 W	--	--
		ADCP	38.439431 N 123.111656 W	7/3/2009	7/24/2009[2]
		Salinity/temp (sonde)	38.439431 N 123.111656 W	7/3/2009	7/24/2009
4	"Bridgehaven"	CTD	38.434181 N 123.106194 W	--	--
5	"Willow Creek"	CTD	38.437090 N 123.097855 W	--	--
		WL[1]/ temp	38.436731 N 123.098398 W	9/11/2009	10/10/2009
6	"Sheephouse Creek"	CTD	38.448496 N 123.095716 W	--	--
7	"Osprey Rookery"	CTD	38.444066 N 123.085145 W	--	--
8	"Heron Rookery"	CTD	38.440674 N 123.074972 W	--	--
		ADCP	38.440661 N 123.075245 W	8/27/2009	10/27/2009
		WL[1]/temp	38.440389 N 123.074830 W	8/11/2009	10/9/2009
		Salinity/temp (sonde)	38.440661 N 123.075245 W	8/27/2009	10/27/2009
9	"Freezeout Island"	WL[1]/temp	38.446907 N 123.060572 W	8/29/2009	10/11/2009
		Salinity/temp (sonde)	38.446907 N 123.060572 W	8/29/2009	10/11/2009
10	"Freezeout Creek"	CTD	38.448858 N 123.052847 W	--	--
11	"Moscow Bridge"	CTD	38.453672 N 123.049217 W	--	--

[1] WL: "water level", as determined from pressure readings
[2] Battery shorted on this date

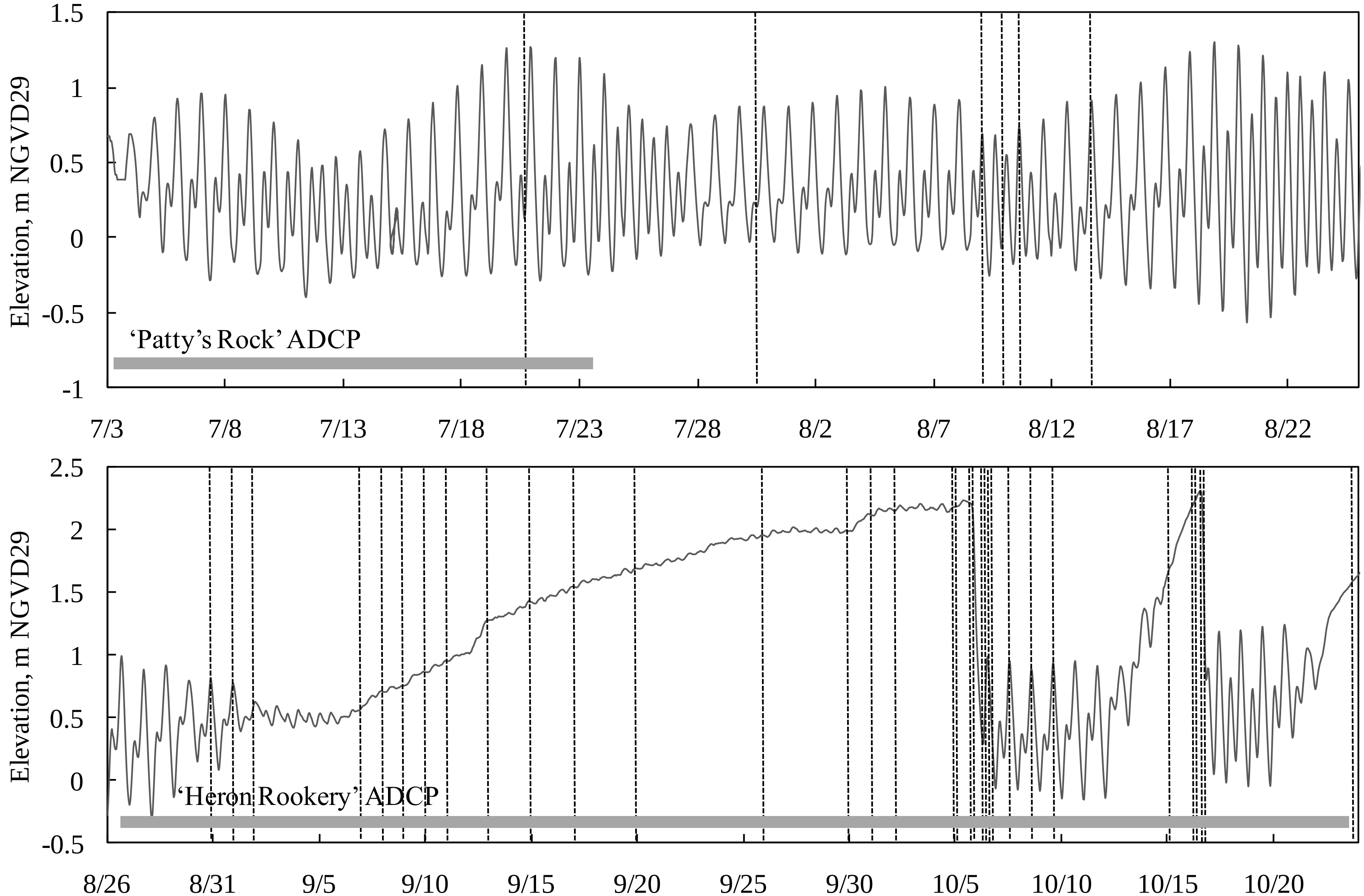

Figure 1.2 Timeline indicating periods of ADCP deployment (horizontal grey bars) and times that CTD profiles were taken (vertical dashed lines).

2. Water Level Data

Four U20-model HOBO water level loggers were deployed in the estuary between the months of August and October 2009. The stations where recorders were installed (as shown in Figure 1.1) are Freezeout Island, Heron Rookery, Willow Creek, and a Mouth station located roughly 300m upstream of the inlet, on the north side of the channel. The purpose of installing multiple recorders were (1) to observe the difference in tidal response of different sections of the estuary, and (2) to provide a continuous record of water surface elevation to be used for translating the depth values in CTD profiles (see Section 7) to actual elevations. Data were collected at two-minute intervals at each site.

The recorders output pressure and temperature data. The CTD profiles taken during the study were used to estimate the salinity in the water column above the recorders. The time-series pressure and temperature data, and the repeated salinity measurements, were used to calculate the density of the water above the recorders, using the UNESCO equation of state. All recorders were located at elevations between 0 and -1m from the NGVD29 datum. Shallow depths were chosen to minimize the effect of errors in the estimate of density. Recorder depths were referenced to the same datum by assuming that the elevation measured by the SCWA Jenner gage was accurate for the entire estuary during an hour-long period in late September when measured wind velocity was less than 2m/s, hour-to-hour water level increase was small (< 0.2 cm/hr), and Guerneville flow was small (<100 cfs), and assuming that the water surface had minimal slope throughout the estuary. Given these conditions, the error in the estimate of the water surface elevation for each station is assumed to be within the range of 0-5 cm.

The data indicate a difference in response to tides among different segments of the estuary. Figures 2.1 and 2.2 indicate that at Heron Rookery and upstream, the spring tide range is truncated to less than 70% of the range near the inlet, with a minimum elevation of about 10cm above NGVD. Figure 2.3 shows that the tide is similar near the mouth and at the Willow Creek station, 4 km upstream, whereas it begins to differ significantly at Heron Rookery (7.4 km upstream) and Freezeout Island (9.3 km) upstream. Although the flood limb of the tide curve is similar for all stations, the ebb is relatively slow at these two stations, with a delay of 1-2 hours at MLLW compared with the two stations nearest to the mouth.

Figures 2.4 and 2.5 illustrate an observed daytime gradient in estuary water surface elevations that occurred during closure conditions. This was only observed during closure conditions, between the hours of 11:00 AM and 4:00 PM, and often resulted in an increase in the elevation at Freezeout Island of 2-4cm and a simultaneous decrease in elevation at the Mouth of a similar magnitude.

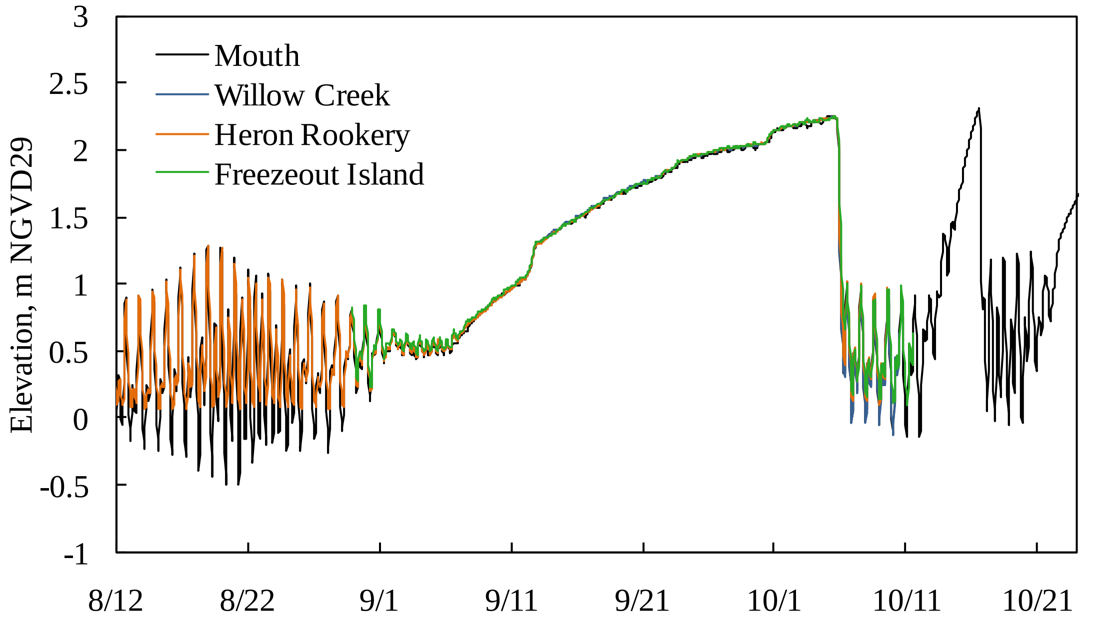

Figure 2.1 Water level data from the four gages deployed between 8/12 and 10/21 2009

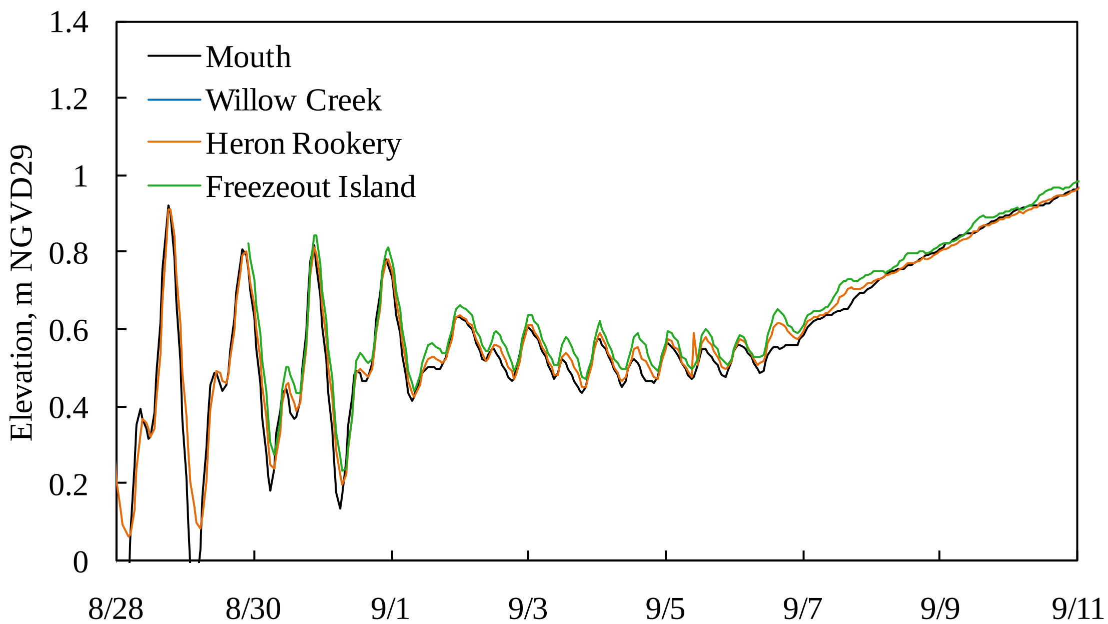

Figure 2.2 Water level data during the days prior to the prolonged September-October closure event

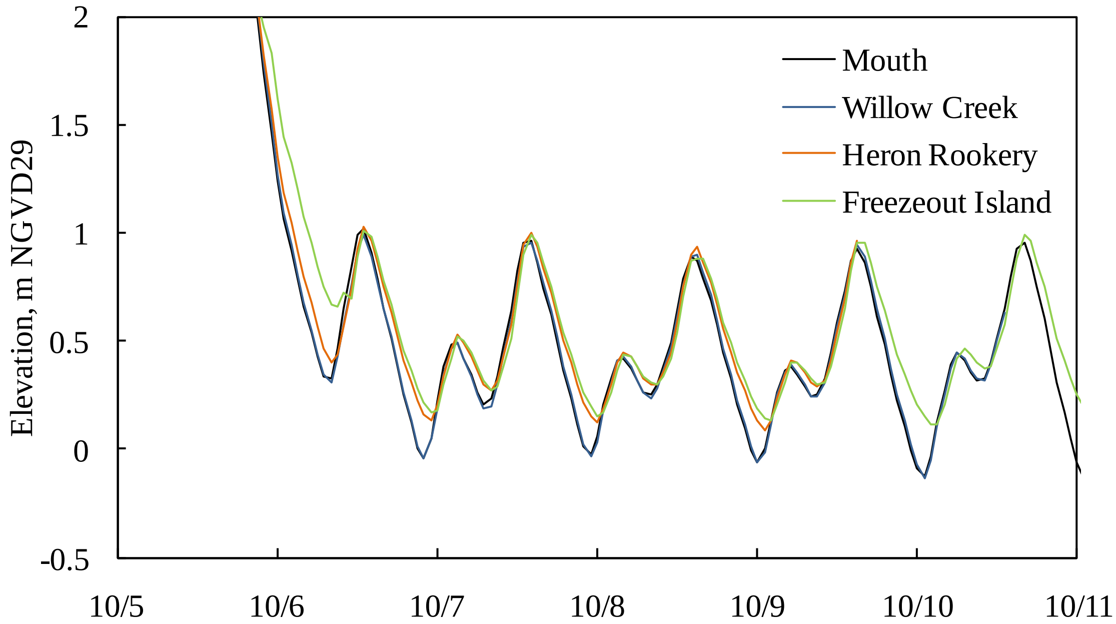

Figure 2.3. Variations in tidal response among gaging stations. Note that the "Mouth" and Willow Creek tidal curves overlap

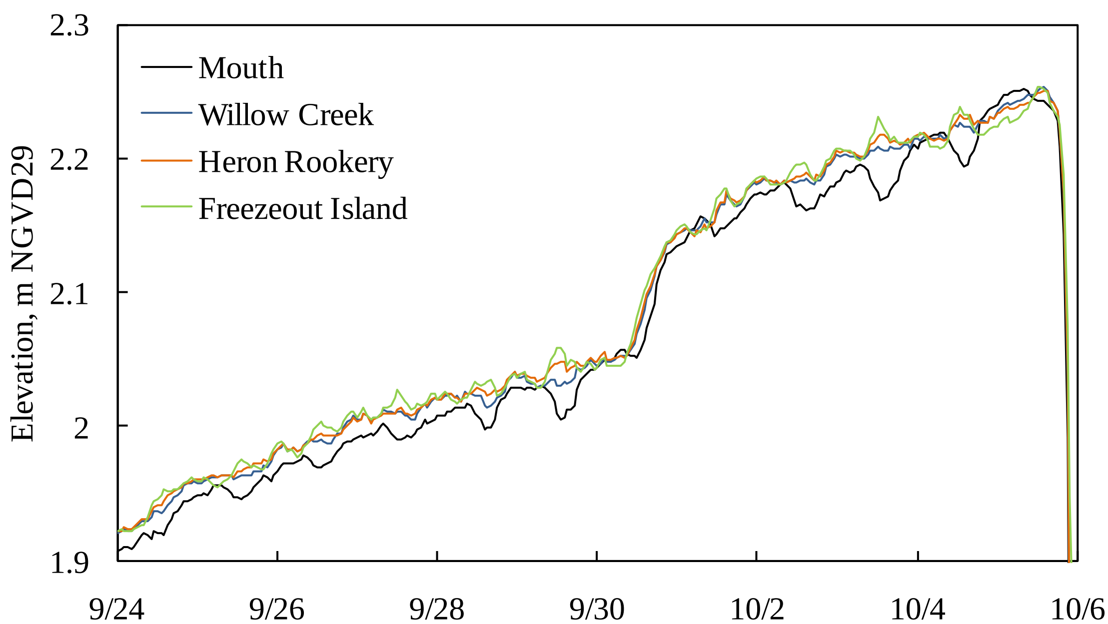

Figure 2.4 Observed fluctuations among surface elevations throughout the estuary during the closure period.

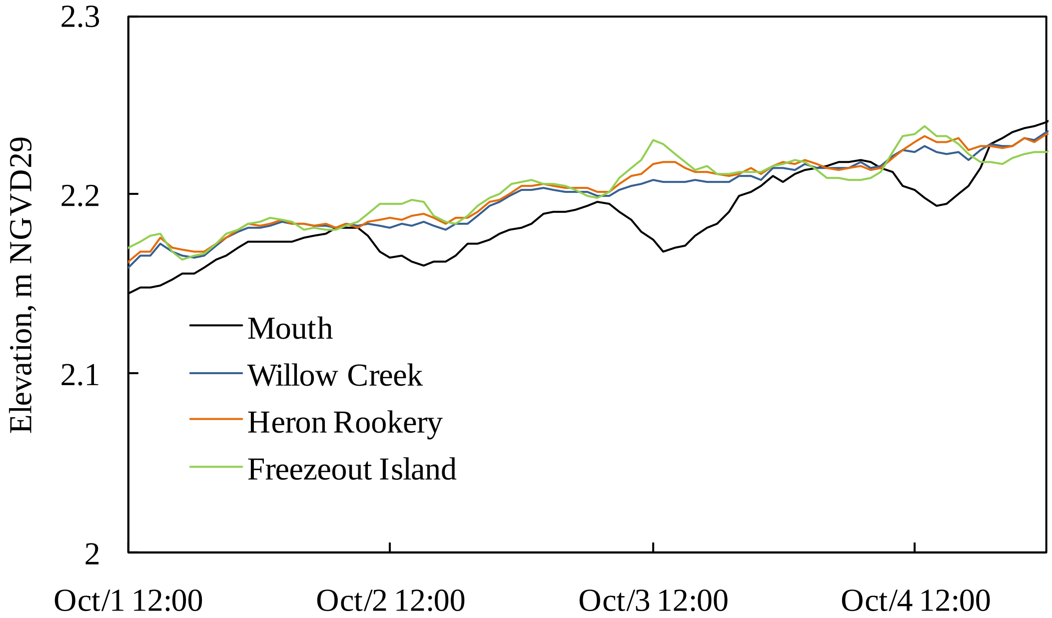

Figure 2.5 Surface fluctuations during the last several days of inlet closure, indicating gradients in estuary surface elevation during the middle of the day

3. Temperature Data

Temperature data collected from the four deployed water level loggers (see Section 2) were used to compare changes in temperature across the lower 10 km of the estuary between the elevations of 0 and -1m NGVD29 (see Figure 3.1). Since the individual elevation (and depth) of each logger was different, the differences in response to changes in estuary conditions are of more importance than the actual difference in temperature between stations.

Daily changes in temperature differed considerably between downstream locations (Mouth and Willow Creek) and upstream locations (Heron Rookery and Freezeout Island) where temperature was measured. During tidal conditions, the temperature at the Mouth station has a strong semidiurnal signal. At Willow Creek and Heron Rookery, the signal was also semidiurnal, but less prominently so. The temperature signal for the period of measurement at Freezeout Creek was diurnal, regardless of the inlet condition.

During periods of inlet closure (Figures 3.2-3.4), the temperature signal was diurnal at all stations. During the closure event lasting from September 7 to October 5, the temperature rose at all stations except during two events. The first event, shown in Figure 3.2, occurred during September 12-13. The temperature decreased at the Mouth and Willow Creek stations on September 12, and subsequently increased at the Heron Rookery and Freezeout Island stations on September 13. As shown in Figure 3.3, the mean temperature increased for each station between September 13 and September 30. Between September 30 and the October 5th inlet breach, Figure 3.4 indicates that the temperature decreased by 2-4 ºC at all stations. The breach event caused an additional mean decrease of 2-4 ºC at each station.

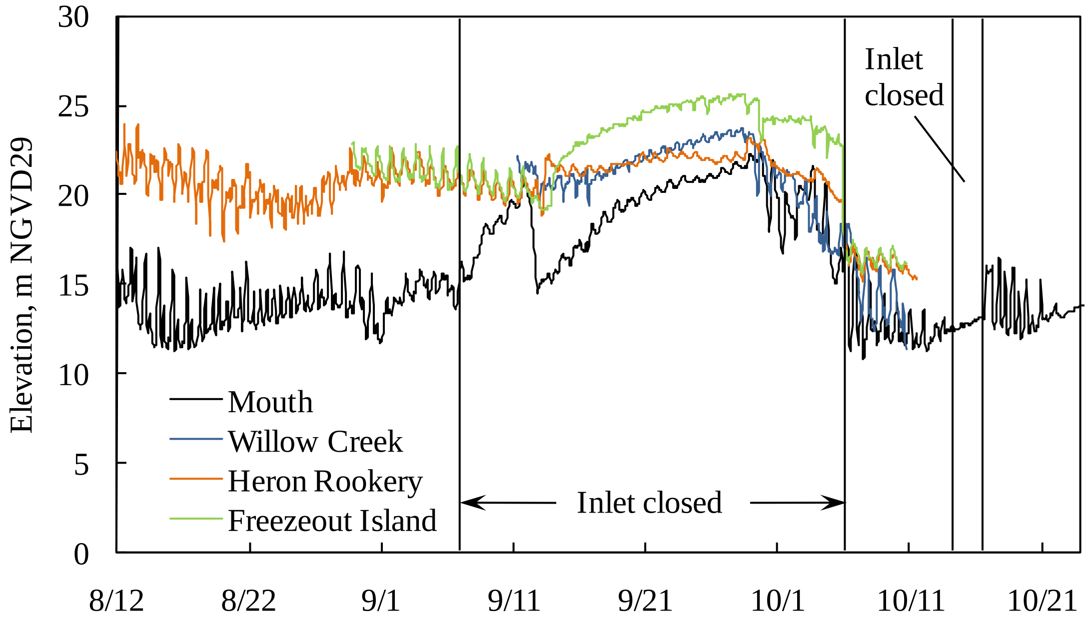

Figure 3.1 Full record of observed temperature from deployed HOBO recorders

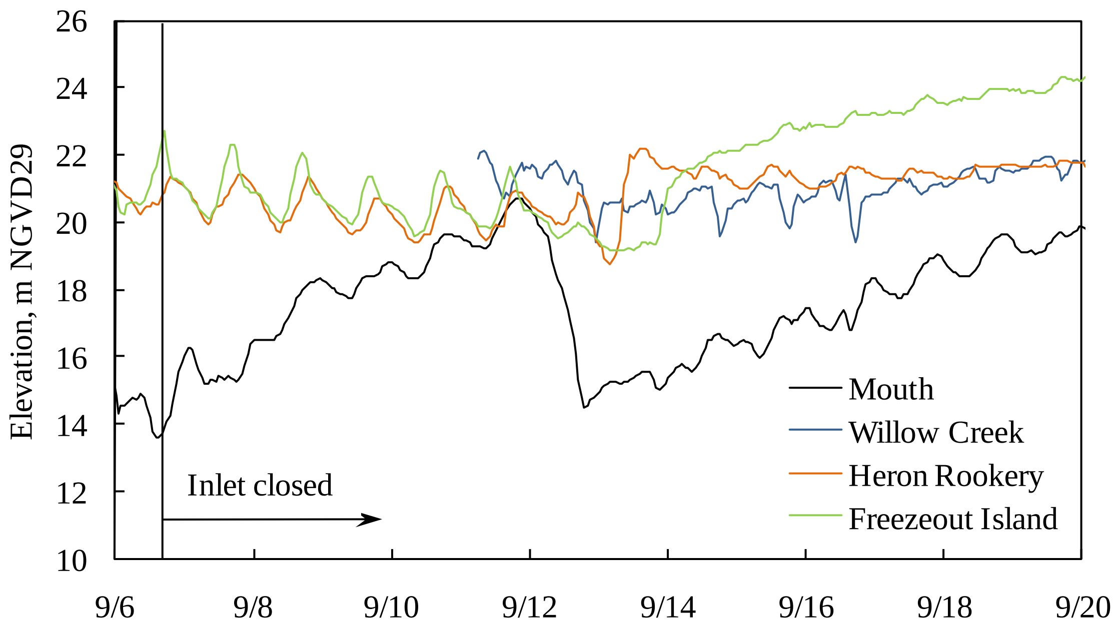

Figure 3.2 Observed temperature during the initial days after the September closure event

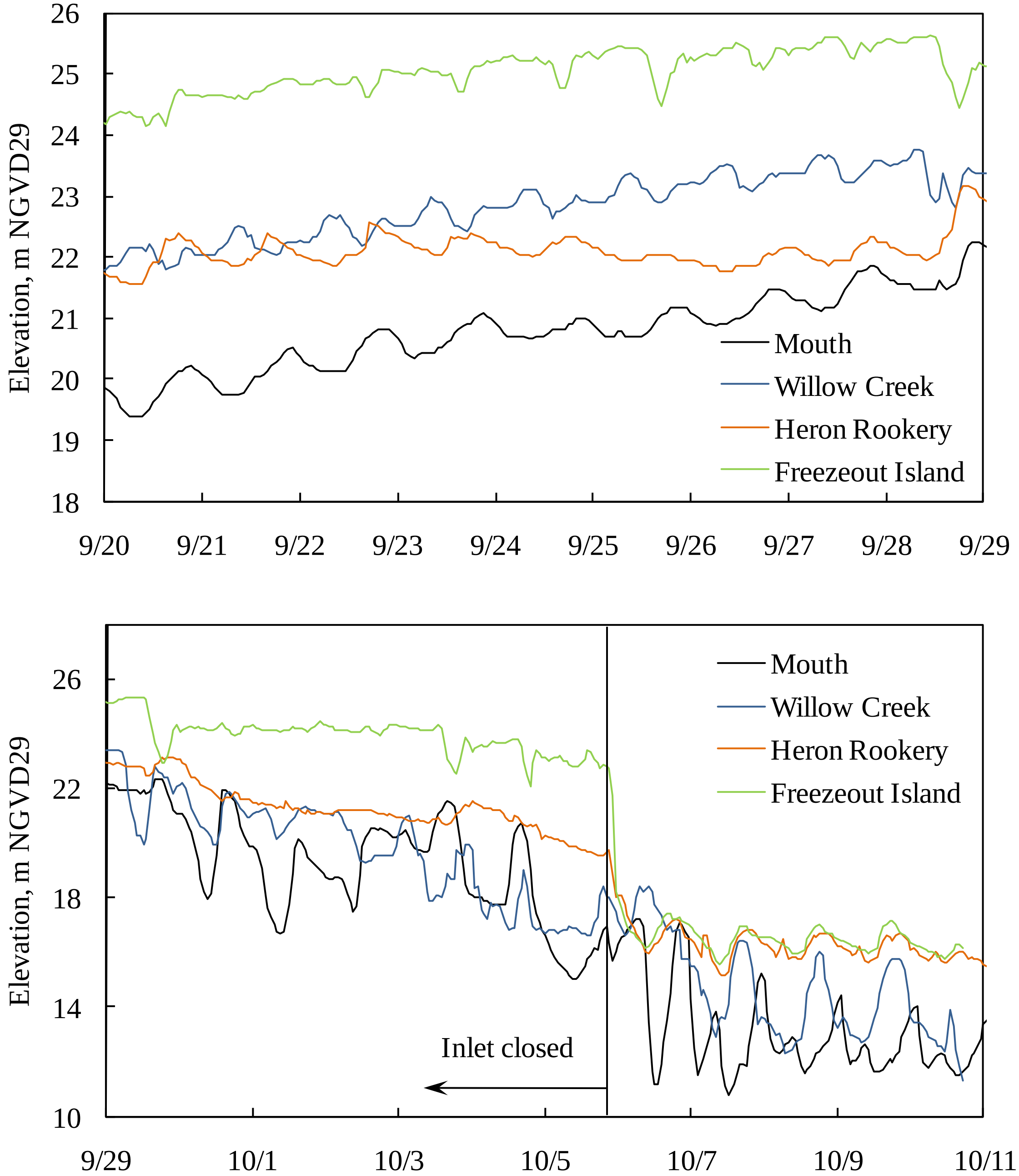

Figure 3.3 Observed temperature **(top)** during the several weeks after the September closure and **(bottom)** after the October breach even

4. Temperature-Salinity Data

Three SeaBird Electronics 37-SM MicroCat sondes were deployed in the estuary during the study period. One was attached to the frame of an ADCP tripod and deployed at the bottom of the river at Patty's Rock and another was deployed with the ADCP at Heron Rookery. A third was attached to a concrete weight and deployed at the Freezeout Island station. Sonde measurements included temperature and conductivity, from which salinity was estimated.

Figure 4.1 shows the observed bottom temperature and salinity at Patty's Rock from July 3 to October 28. During the open-inlet conditions of July and August, the change in salinity was minimal, while temperature varied by 2-3 ºC on a cycle of approximately two weeks. Closure events in the latter half of the study period held both temperature and salinity nearly constant, but an abrupt change (0.5-2 ºC) occurred for temperature after the subsequent breach events.

Figure 4.2 indicates that the most abrupt changes in salinity and temperature occurred during closure events for the Heron Rookery and Freezeout Island stations, rather than during tidal conditions. The sonde at Heron Rookery captured all three closure events between September and October. The September closure event initially caused no change in temperature or salinity, but two step-increases in both parameters occurred on September 8 and 13. Although these step responses occurred at this site for all three closure events, the changes in salinity and temperature were not always parallel, nor were they always increases. After the closure event on October 14, temperature and salinity both declined. For the closure event on October 22, the subsequent step increase in salinity was matched by a significant decrease in temperature.

The sonde at Freezeout Island only captured the September closure event, but showed the greatest change in salinity and temperature of all of the stations. A single, abrupt increase in salinity from 0 to 15 psu occurred between September 13 and 15. This event reversed a slow decline in temperature that had precluded it. From August 30 to September 14, the mean temperature had declined from 23 to 20 ºC. Between September 14 and September 29, the temperature slowly increased to 25 ºC. As seen with the water level loggers (see Section 3), an event on September 30 caused the temperature to decline again. After achieving a peak salinity of 15 psu on September 15, the salinity at this station decreased slowly until the date of the inlet breach, when salinity and temperature both decreased dramatically. During the subsequent tidal cycles, the salinity remained near 0 psu and showed only modest (0-0.5 psu) daily changes.

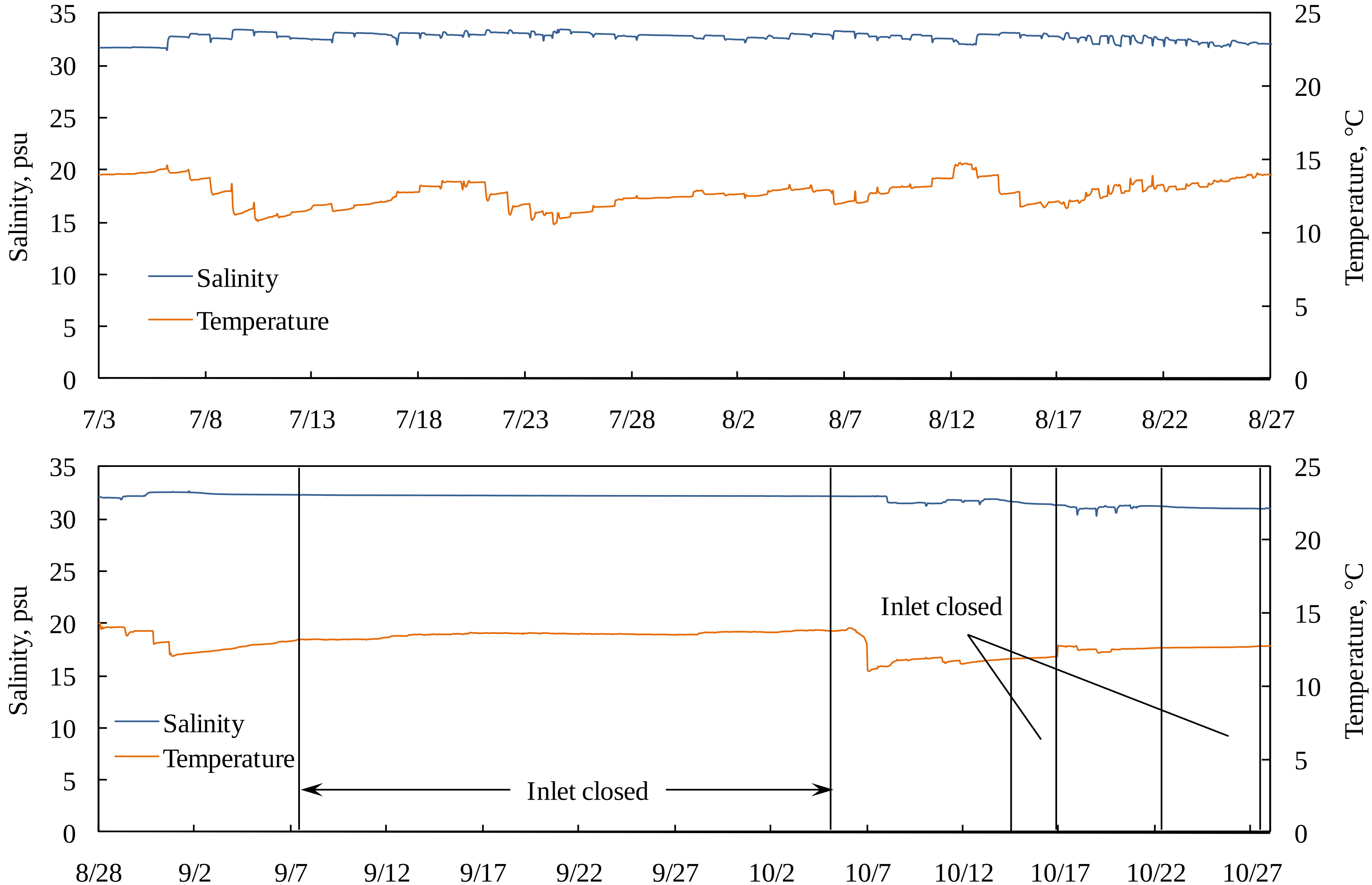

Figure 4.1. Time-series salinity data from the bottom sonde at Patty's Rock

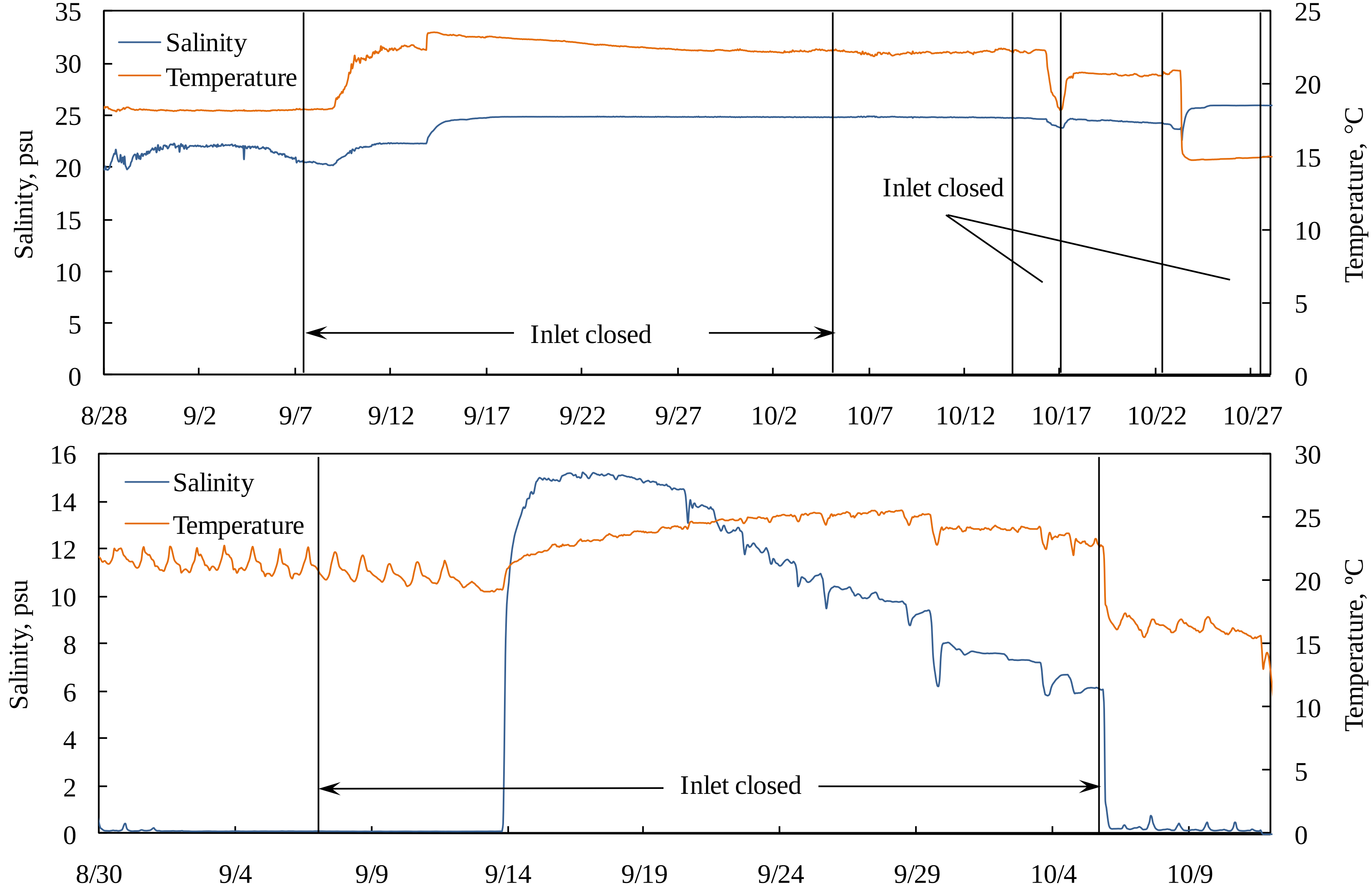

Figure 4.2 Time-series salinity data from the **(top)** bottom sonde at Heron Rookery and **(bottom)** at Freezeout Island

5. Wave Data

Deep-water wave heights were obtained from NDBC Buoy #46214 (http://cdip.ucsd.edu/?nav=historic&sub=data&stn=029&stream=p1), which is operated under the Coastal Data Information Program (CDIP) and located 39 miles southwest of the inlet. A wave transformation matrix provided by CDIP allowed for deep-water wave heights to be translated to nearshore values, taking into account wave refraction and shoaling. These estimates give the significant wave height (Hs) at 10m depth located directly offshore of the inlet.

Figure 5.1 presents a time-series of both nearshore and deepwater Hs values. Nearshore and deep-water values for this site vary significantly because of the high degree of refraction required for waves to approach the site from steep (northerly or southerly) angles. The nearshore Hs data shown for August is typical for summer conditions. Several large wave events occurred during the months of September and October. The most significant wave event during the extended September-October closure event occurred during the days of September 12-14, with Hs values exceeding 3m at 10m depth. A storm, generating nearshore wave heights in excess of 4m, coincided with the closure on October 14.

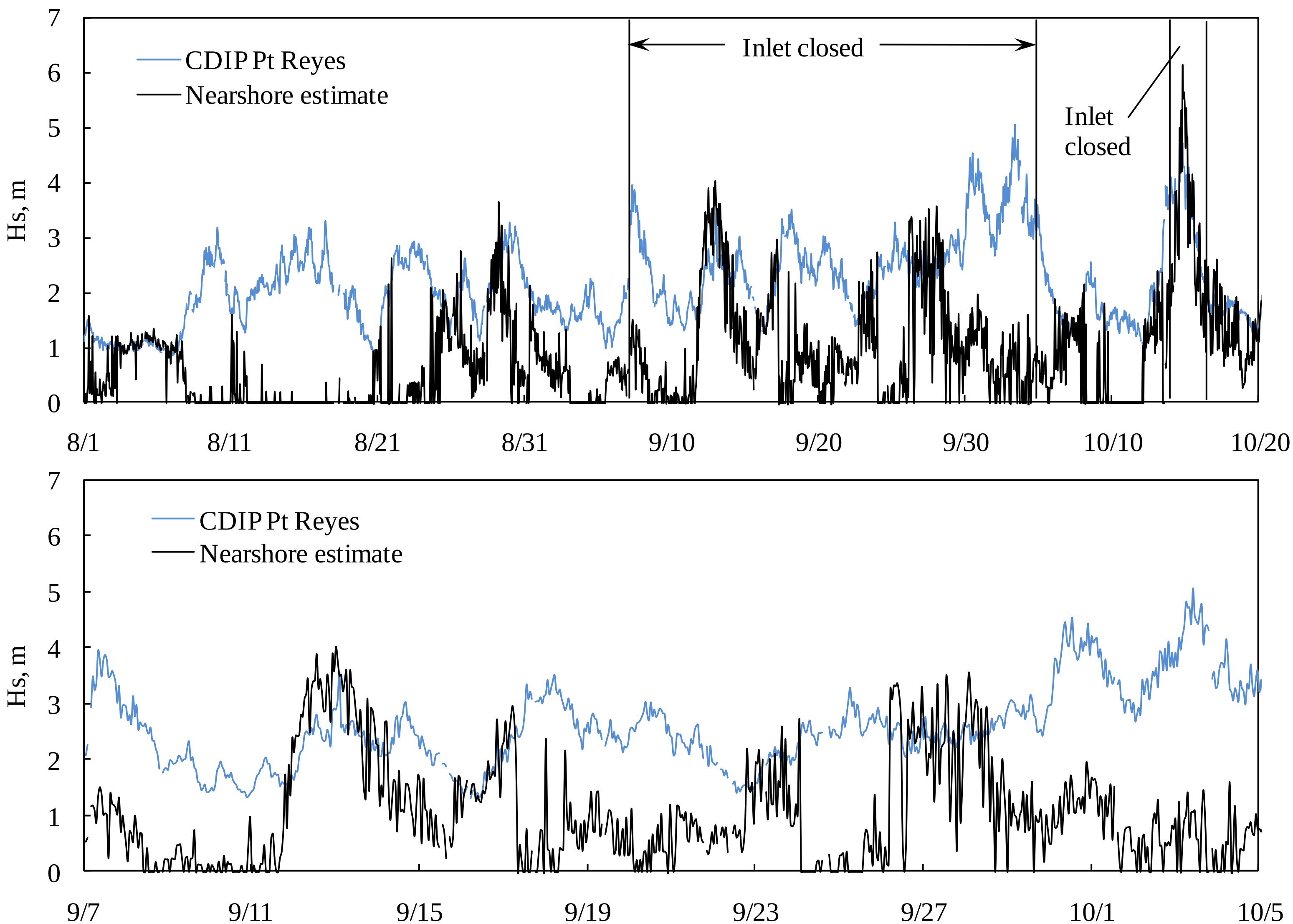

Figure 5.1. Significant wave heights (Hs) observed and modeled from **(top)** August to October, and **(bottom)** during the prolonged September-October inlet closure period

6. Wind Data

Wind data were collected from the Bodega Ocean Observing Node (BOON) through its website (http://www.bml.ucdavis.edu/boon/data_access.html). This sensor is an anemometer positioned at 10m elevation, and is located at the Bodega Marine Laboratory, 10 miles south of the estuary. These data are presented for reference only, and provide only an estimate of wind conditions at the estuary. Further, the wind conditions vary markedly along the estuary.

The data shown in Figure 6.1 indicate both diurnal and longer-term fluctuations in wind speed during the study period. It was most common for wind speed to reach 10-15 m/s between the hours of 10:00 AM and 4:00 PM on most days, and reduce to 0-5 m/s at night. Four events with wind speed exceeding 25 m/s occurred between July and October. The first event (Figure 6.2, top) occurred during the deployment period of the ADCP at Patty's Rock. The latter three occurred during closure events. During the final 10 days of the prolonged September-October closure event, there were five days when wind speed was consistently 15 m/s or higher (Figure 6.2, bottom).

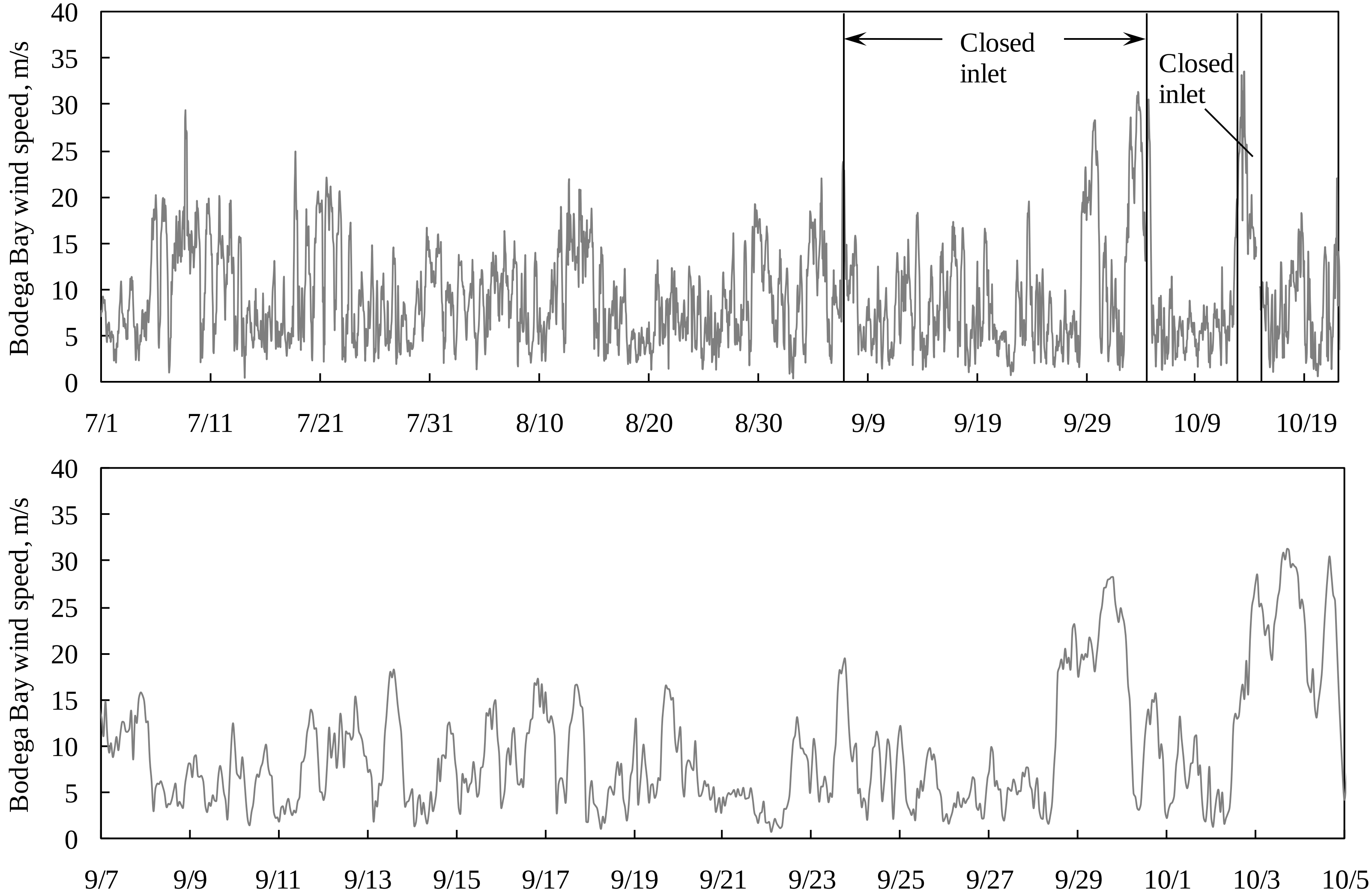

Figure 6.1. BOON wind speed during (top) the months of July-October 2009 and (bottom) the prolonged September-October inlet closure event.

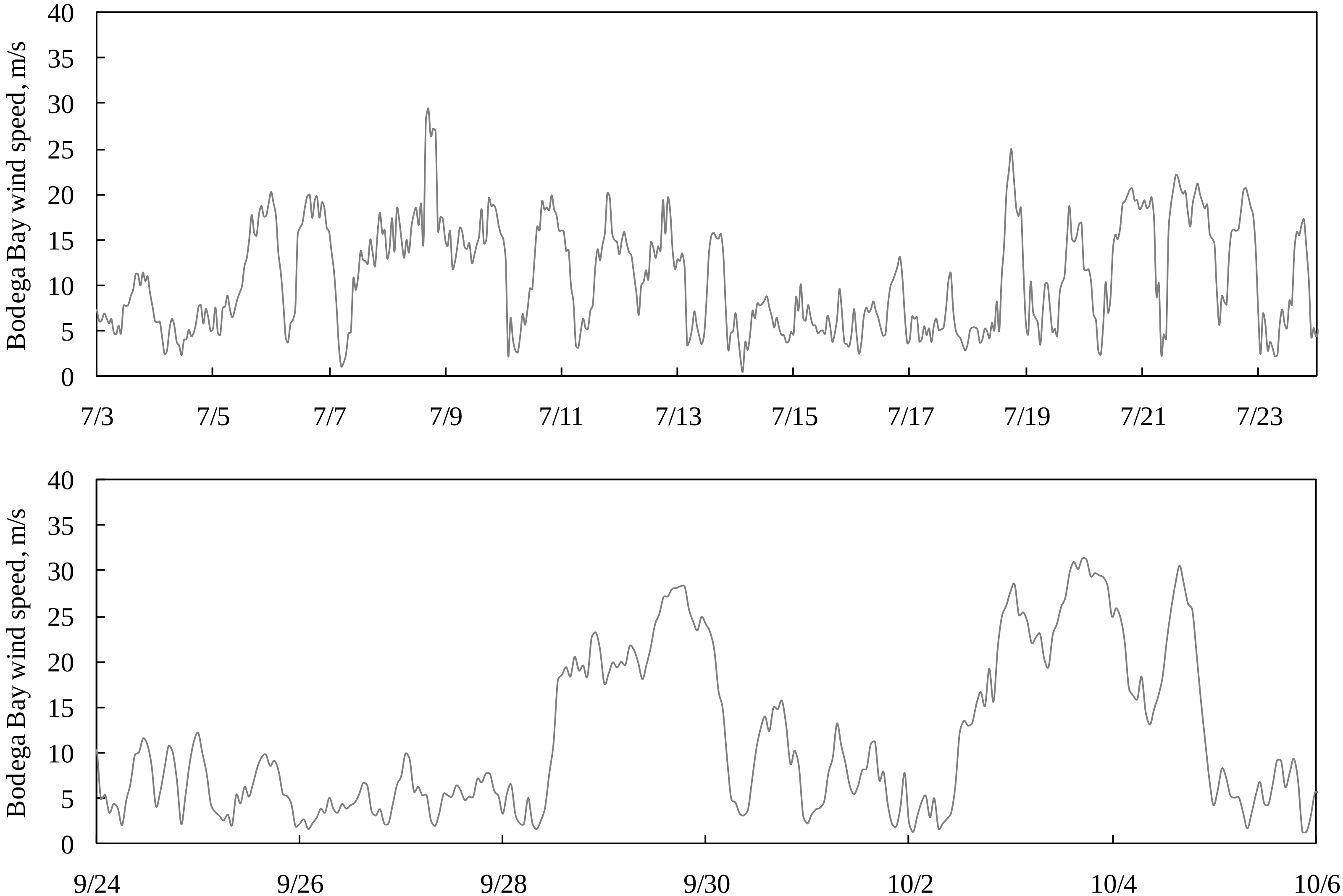

Figure 6.2. BOON wind speed coinciding with (top) the period of ADCP deployment at Patty's Rock and (bottom) during the final half of the prolonged September-October inlet closure event.

7. River Discharge Data

Measurements of river discharge were obtained from the gage operated by the U.S. Geological Survey (USGS) at Hacienda Bridge, approximately 20 miles upstream of the inlet. Data were downloaded from the California Data Exchange Center website (http://cdec.water.ca.gov/cgi-progs/selectQuery?station_id=HAC). At the time of this report, the data corresponding to the study period are listed as preliminary by the USGS.

A stage-flow relationship provided by SCWA for Vacation Beach was used for comparison with upstream flows. Vacation Beach is located near the upstream extent of the backwater effect caused by closure events. Flows estimated from the stage-flow curve that were higher than actual measured points were not used in this comparison, to prevent errors from extrapolation. The data, summarized in Figures 7.1 and 7.2, indicate that Vacation Beach flows were within 10 cfs of flows measured at Hacienda Bridge for the duration of the study period.

For the majority of the study period, estuary inflows were less than 100 cfs. Flows into the estuary did not exceed 150 cfs consistently until October 13 (Figure 7.1, top). Figure 7.2 (top) shows two spikes in flow between September 30 and October 2 caused by the opening of the Johnson Beach dam. Another, smaller dam removal on September 25, was not captured by the Vacation Beach dataset. Apart from these events, and a short-lived event with flows exceeding 130 cfs on September 8, flows were between 70 and 105 cfs during the prolonged September-October closure event (Figure 7.1, bottom).

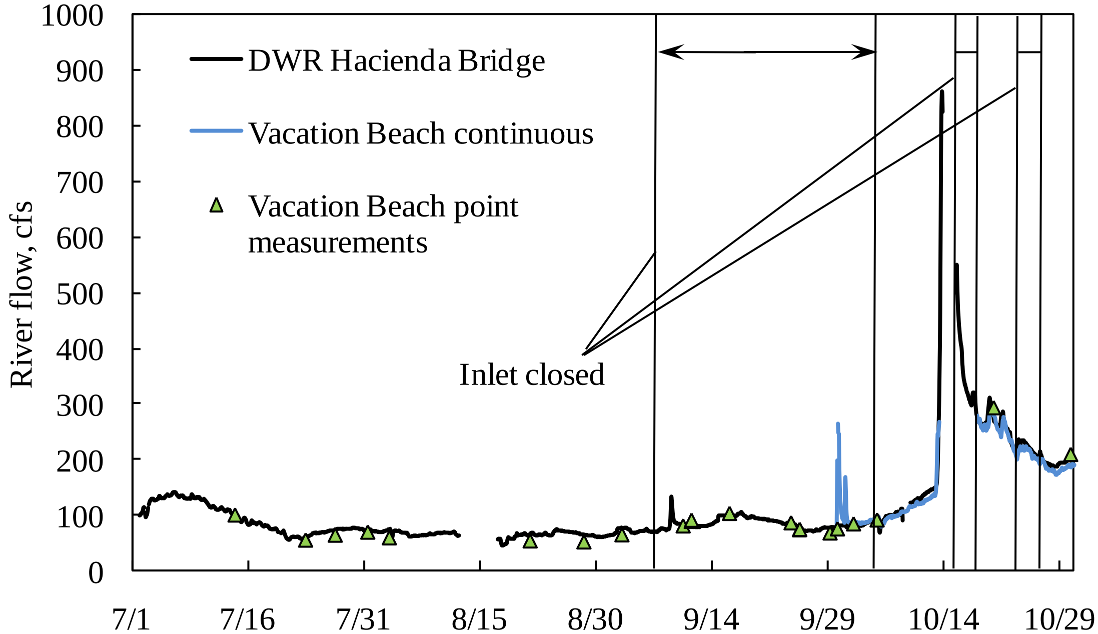

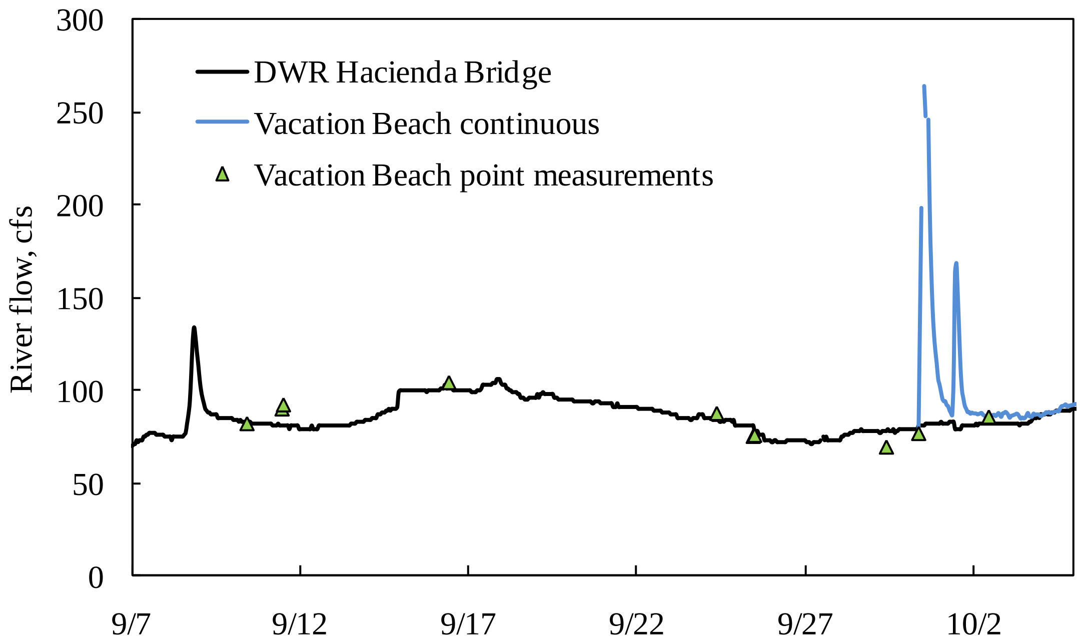

Figure 7.1 River discharge data for **(top)** the entire study period, **(bottom)** the September-October closure period.

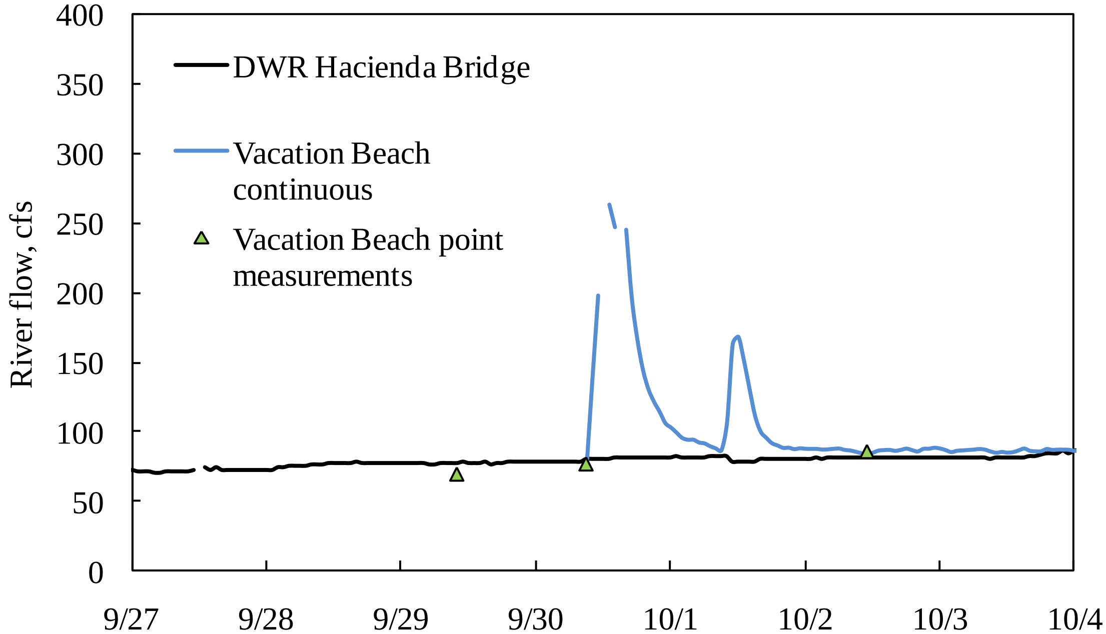

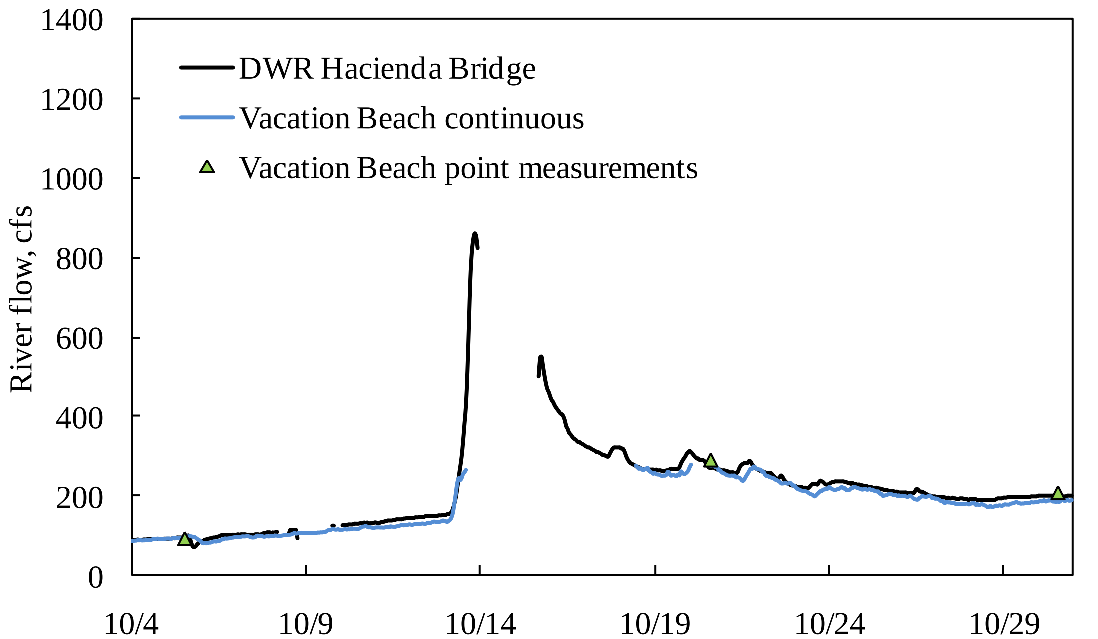

Figure 7.2 River discharge data for **(top)** the Johnson Beach dam removal and **(bottom)** the moderate flood event in October.

8. Current Velocity Data

Two Acoustic Doppler Current Profilers (ADCPs) were installed during the study period. The first was installed at Patty's Rock on June 26, and a second was installed at Heron Rookery on August 27. Both were stationed at the bottom of bathymetric lows, and were oriented upwards. Both took 10-minute ensemble averages of velocity and generated hourly averages. The Patty's Rock ADCP collected data with a vertical resolution of 1m for depth cells while the Heron Rookery ADCP had a vertical resolution of 0.25m. A battery malfunction caused the ADCP at Patty's Rock to delay the beginning of data collection until July 3, and caused it to lose full functionality by July 24, preventing the desired simultaneous data collection from both ADCPs in September and October.

Current velocity data are shown as along-channel speed (positive in the upstream direction) to compare flood and ebb tidal currents. A channel alignment (in degrees from north) was chosen for the location of each ADCP, and the velocity data was output in north and east directional components. These were projected onto the upstream/downstream channel alignment.

The 21-day set of current velocity data at Patty's Rock (Figure 8.1) indicate that tidal currents near Jenner regularly exceed 25 cm/s (~1 ft/s) in both the upstream and downstream directions when the inlet is fully open. When estuary tide range at Jenner exceeds 1m, an upstream directed current with a velocity of 10-20 cm/s appears along the bottom of the channel during flood tide. When this was not present, current velocities in excess of 5cm/s were typically confined to the upper 3m of the water column. The peak velocity observed during this period (~35 cm/s) was upstream-oriented, but in most cases, flood and ebb tidal current speed were within 1-2 cm of each other.

Velocity data at Heron Rookery are provided in two figures. Figure 8.2 omits data for which the error velocity exceeded 3 cm/s. Figure 8.3 keeps these values despite the associated error. Data collected when the inlet was open indicate that tidal velocities are similar to those at Patty's Rock. The magnitude of upstream and downstream components are typically 25 cm/s or less. Despite this, tidal currents penetrated deeper into the water column. Figures 8.2 (bottom) and 8.3(bottom) show both ebb and tidal currents extending 3-5 meters below the water surface.

During inlet closure, a 1-2m-deep flow of downstream-oriented water dominates the surface, whereas the lower water column is dominated by water moving slowly (< 5cm/s) upstream. A diurnal upstream-oriented velocity at the surface sometimes provides current speeds above 30 cm/s, which are superimposed over the downstream-oriented flow. The largest currents of the study period occurred during inlet breach events. All three October breach events resulted in downstream-oriented current velocities above 50 cm/s for at least one hour.

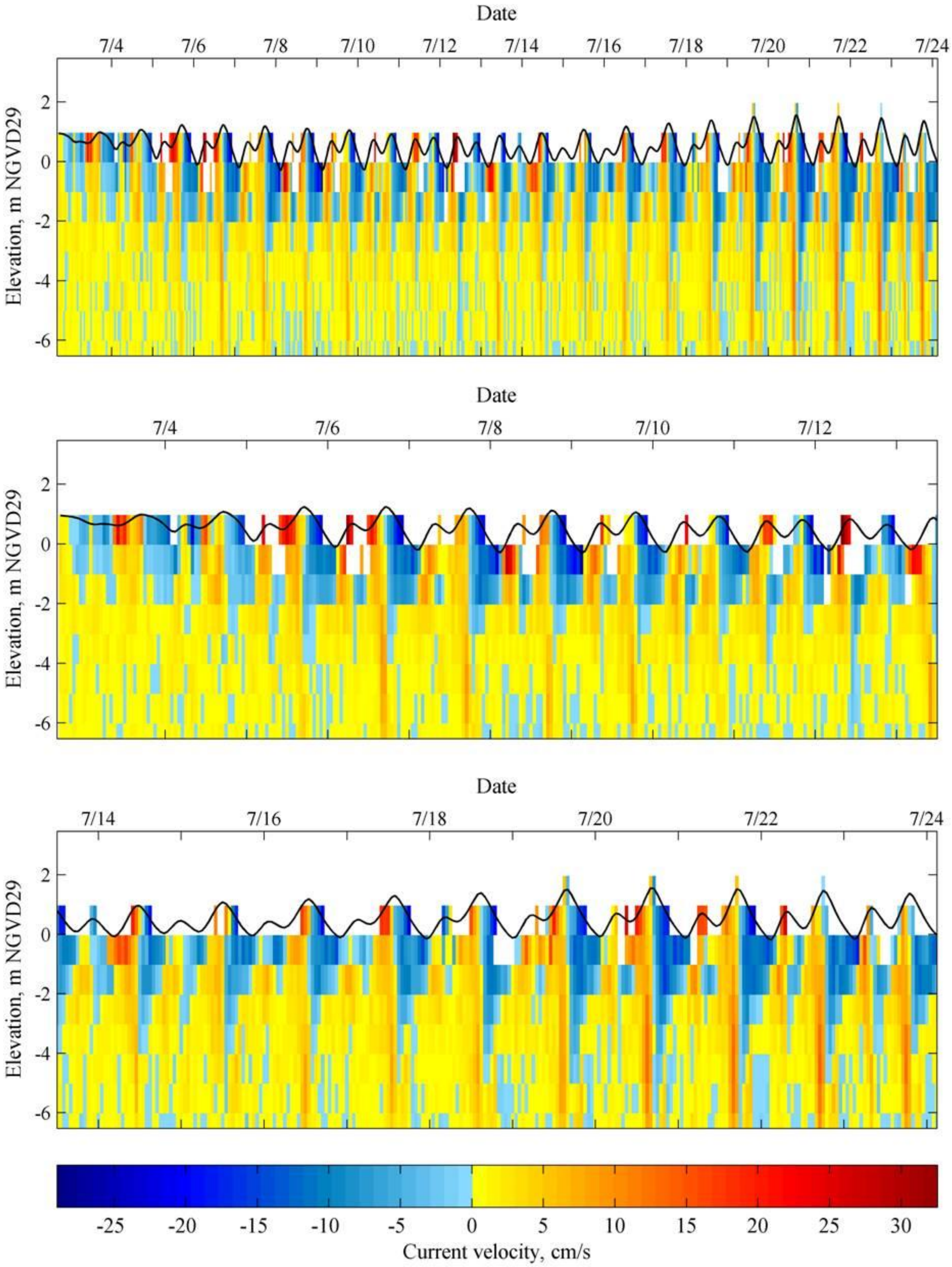

Figure 8.1 Current velocities at Patty's Rock from July 3 to July 24. Positive values denote upstream velocities

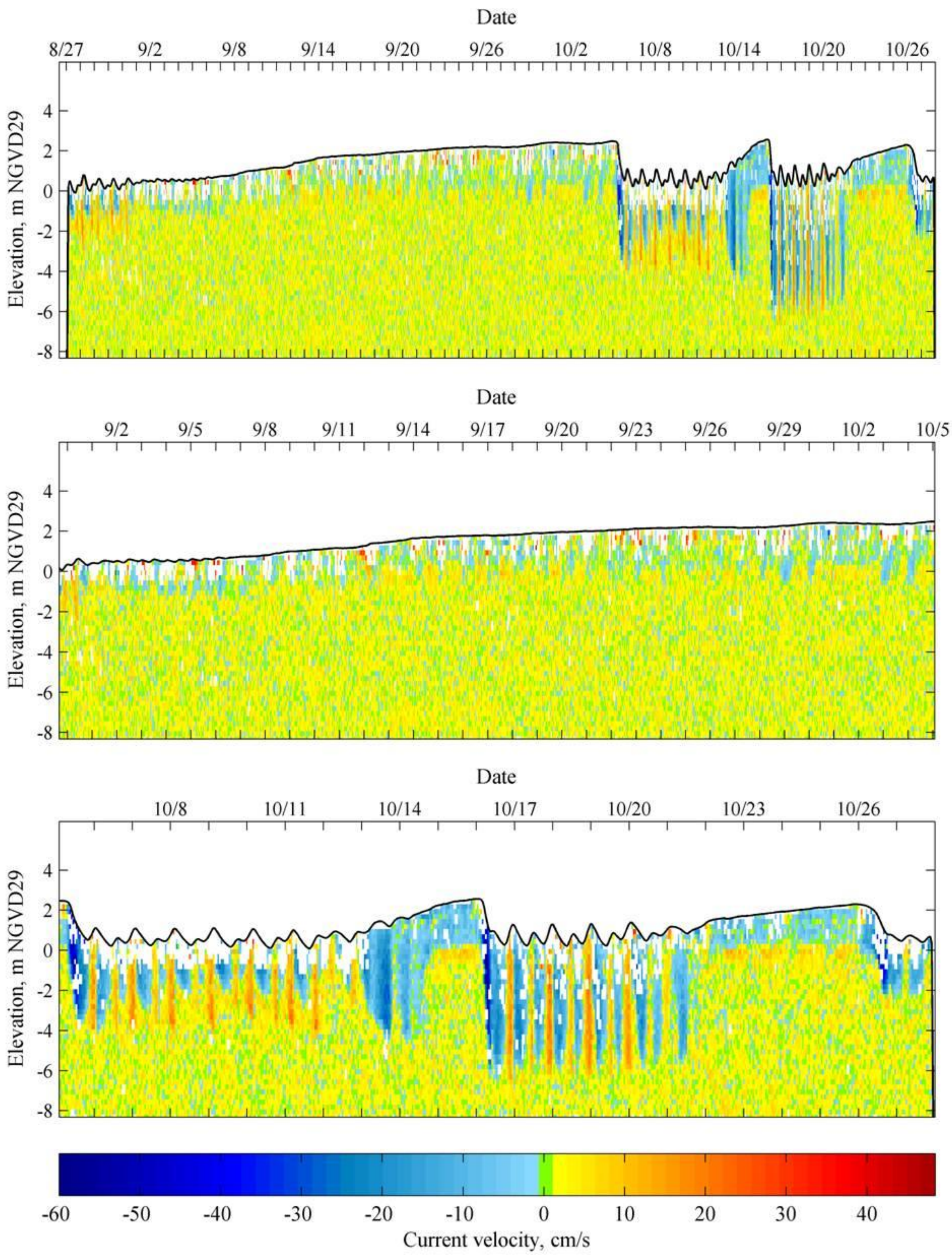

Figure 8.2 Current velocities at Heron Rookery from August 27 to October 27. Positive values denote upstream velocities. White cells represent depths where error velocities exceeded 3cm/s

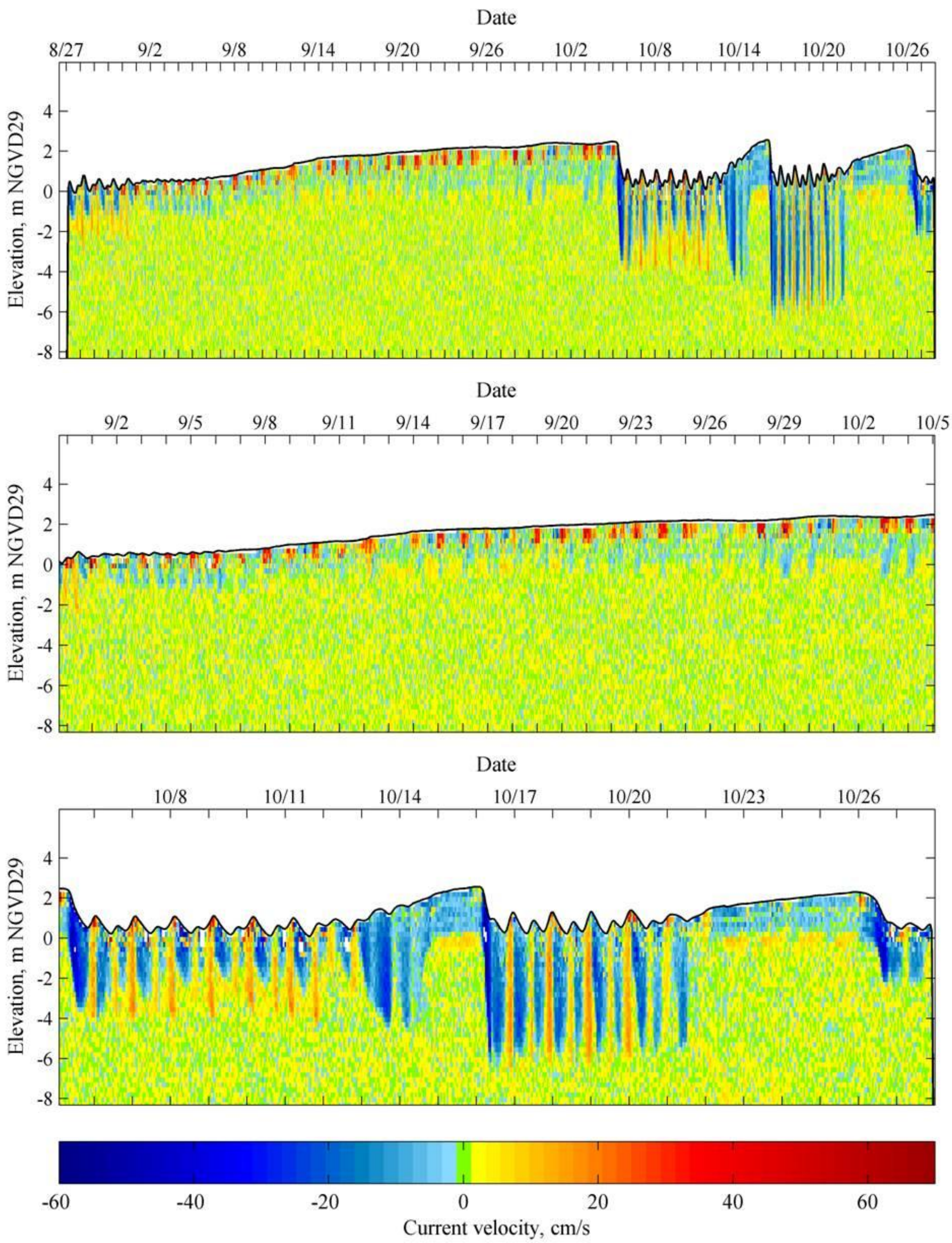

Figure 8.3 Current velocities at Heron Rookery from August 27 to October 27. Positive values denote upstream velocities. Cells with error velocities above 3cm/s are not omitted.

9. CTD Data

A profiling CTD (conductivity-temperature-depth instrument) with peripheral dissolved oxygen sensor was used to make boat-based surveys of salinity, dissolved oxygen and temperature in the estuary. Table 2 lists the dates, times and locations of profiles included in this report. CTD profiles included in this section were checked for errors before inclusion. Many profiles were taken which were not included, resulting from a pump malfunction. This mostly affected dissolved oxygen (DO) measurements upstream of Willow Creek, but on some days prevented the accurate measurements of salinity and temperature.

Profiles were generated by lowering the CTD through the water column while it took measurements at 4 Hz. The real-time water surface elevation at each station (obtained from water level recorders, see Section 2) was used to convert depth measurements into elevations referenced to the NGVD29 datum.

Plots of estuary salinity, temperature, and dissolved oxygen were generated in Matlab using the profiles and their upstream location (along the channel centerline). These plots use a cubic interpolation to fill in values between profiling locations. A longitudinal thalweg profile is superimposed on these plots for spatial context. This profile was generated in Matlab from a 10 x 10m raster grid of estuary bathymetry calculated from the 2008 EDS survey results.

Three subsections below describe the results shown in the estuary plots. They are provided in chronological order, but are explained in terms of their context regarding the three observed inlet conditions: (1) fully tidal, (2) overflow channel and (3) closed.

Table 2. Timing of CTD profiles

Date	Mouth	Patty's Rock	Bridgehaven	Willow Creek	Sheephouse Creek	Osprey Rookery	Heron Rookery	Freezeout Creek	Moscow Bridge
July 20	15:07	15:31	15:43	15:57	16:13				
July 31	15:38	16:03	16:18	16:31	16:48				
Aug 9	15:01	15:19	15:29	15:39	15:56	16:21			
Aug 10	14:56	15:13	15:22	15:31	15:43	15:56	16:12		
Aug 11		15:09	15:18	15:28	15:40	15:53	16:06	16:51	
Aug 14		17:33	17:41	17:51	18:00		18:25		
Aug 31		17:22	17:28	17:36	17:48	17:59	18:09	18:31	
Sep 1	16:58	16:43	15:55	15:55	15:48	15:41	15:30	15:19	14:27
Sep 2	11:09	11:21	11:25	11:30	11:38	11:51	12:01	12:21	
Sep 7	10:43	10:59	11:04	11:12	11:24	11:37	11:49	12:11	
Sep 8	9:52	10:03	10:07	10:14	10:20	10:32	10:42	11:02	
Sep 9	9:35	9:49	9:58	10:06	10:12	10:23	10:33	10:53	
Sep 10	10:00	10:12	10:17	10:24	10:30	10:40	10:50	11:05	
Sep 11	8:26	8:39	8:49	8:57	9:04	9:12	9:21		
Sep 13	16:38	16:54	17:02	17:09	17:16	17:26			
Sep 15	15:37	15:49	15:53	16:00	16:18	16:23	16:30		
Sep 17	11:48	12:16	12:21	12:28	12:34	12:41	12:46	12:57	
Sep 20	15:11	15:27	15:32	15:41	15:47	15:54	16:00	16:10	16:18
Sep 26	16:24	16:40	16:46	16:54	17:02	17:09	17:15	17:23	17:30
Sep 30	10:41	10:54	11:00	11:08	11:14	11:20	11:26	11:35	11:42
Oct 1	9:53	10:06	10:12	10:21	10:28	10:35	10:40	10:49	10:57
Oct 2	8:49	9:03	9:09	9:14	9:21	9:28	9:33	9:42	9:49
Oct 5(1)	13:07	13:21	13:27	13:31	13:37	13:43	13:51	13:59	14:05
Oct 5(2)	17:11	17:23	17:28	17:32	17:37	17:43	17:47		

Table 2. (Continued)

Date	Mouth	Patty's Rock	Bridgehaven	Willow Creek	Sheephouse Creek	Osprey Rookery	Heron Rookery	Freezeout Creek	Moscow Bridge
Oct 6(1)	9:15	9:27	9:37	9:45	9:51	10:03	10:13	10:32	
Oct 6(2)	13:20	13:34	13:39	13:48	13:54	14:02	14:08	14:22	
Oct 7(1)	10:29	10:42	10:47	10:56	11:02				
Oct 7(2)	11:56	12:11	12:16	12:23	12:28				
Oct 7(3)	13:26	13:39	13:44	13:51	13:57	14:04	14:09	14:23	
Oct 7(4)	15:19	15:32	15:37	15:41	15:52				
Oct 8	14:24	14:40	14:44	15:52	14:58	15:06	15:11	15:33	
Oct 9	15:10	15:26	15:31	15:37	15:44	15:51	15:56	16:12	16:20
Oct 10	16:07	16:19	16:23	16:29	16:35	16:41	16:46		
Oct 15	16:32	16:44	16:48	16:53	17:00	17:05	17:10	17:25	
Oct 16(1)	12:00	12:13	12:17	12:22	12:28	12:34	12:39	12:53	
Oct 16(2)	15:18	15:30	15:35	15:39	15:45				
Oct 16(3)	16:17	16:30	16:35	16:40	16:46				
Oct 16(4)	17:30	17:43	17:48	17:53	17:59				
Oct 25	16:12	16:26	16:31	16:36	16:42	16:47	16:52	17:03	9:37

9.1. Dissolved Oxygen Contour Plots

Although not highly resolved temporally or spatially, the CTD profiles taken during July and August indicate that during fully tidal conditions, the DO concentration throughout the estuary is high. The exception to this is the low DO concentration observed near the bottom of the Sheephouse Creek pool on August 14. This feature developed sometime after July 20, when the entire depth was high in DO.

During the period of September 1 - September 7, when the inlet was nearly an overflow channel (See figures 2.1, 2.2), oxygen levels decreased in the lower estuary, between 2 and 5 km upstream of the inlet, as shown in Figures 9.1.3 and 9.1.4. After closure, Figure 9.1.5 shows that by September 13, the pool at the Mouth station had become anoxic, and that the pool at Sheephouse Creek was anoxic at least as early as September 15. At least as early as September 26, most of the estuary from the Mouth to Heron Rookery was anoxic below an elevation of -2m NGVD29 (Figure 9.1.7). This was the case for the remainder of the closure period.

Until October 2, the boundary between low- and high-oxygen water maintained a longitudinal gradient, with the Mouth station having the lowest elevation of the boundary. As shown in Figure 9.1.8, by October 5, that boundary had become nearly horizontal, leaving a uniform, 3m thick layer of high DO water at the surface.

After the breach event on October 5, the remaining figures indicate an incremental restoration of the DO in the estuary, beginning at the mouth and extending upstream. By October 10, the DO in the estuary nearly resembled those of the conditions on September 1, when the inlet had first begun to close. The DO response during the two October closure events (Figures 9.1.12 and 9.1.13) were much different than that of the September closure event. In both cases, DO was high throughout the estuary even three days after closure.

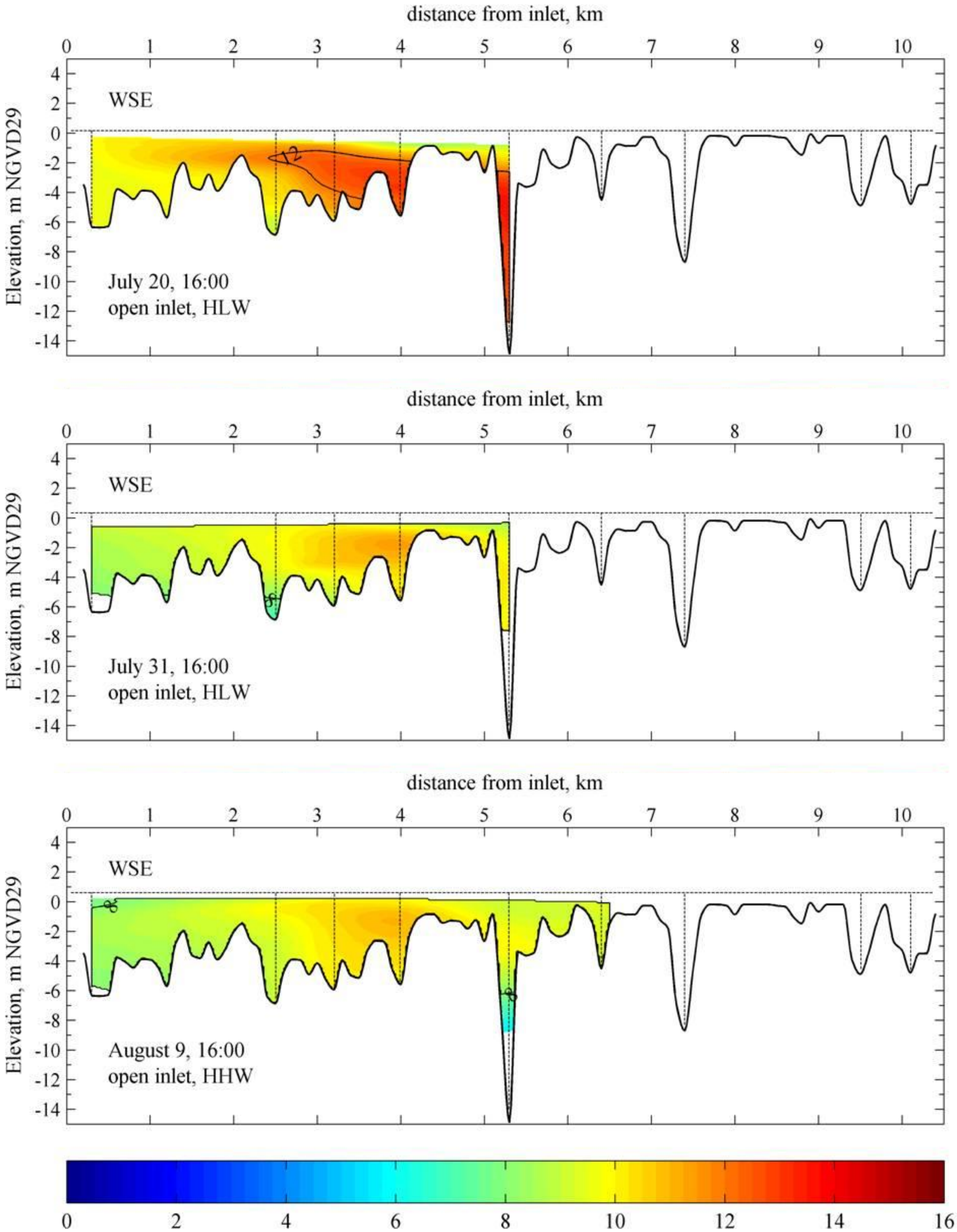

Figure 9.1.1 Estuary DO structure on **(top)** July 20, **(mid)** July 31 and **(bottom)** August 9. Units of DO are mg/L.

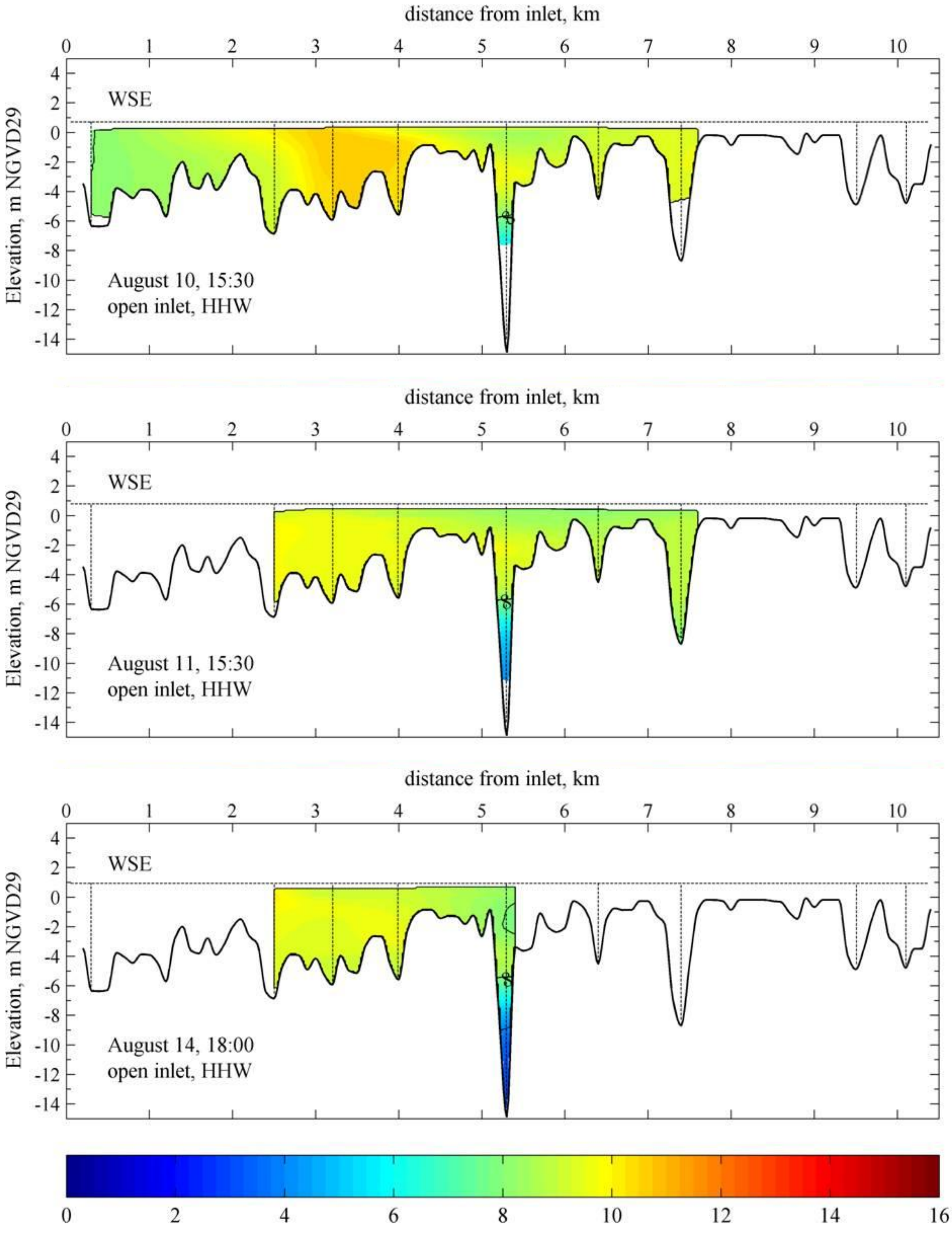

Figure 9.1.2 Estuary DO structure on **(top)** August 10, **(mid)** August 11 and **(bottom)** August 14. Units of DO are mg/L.

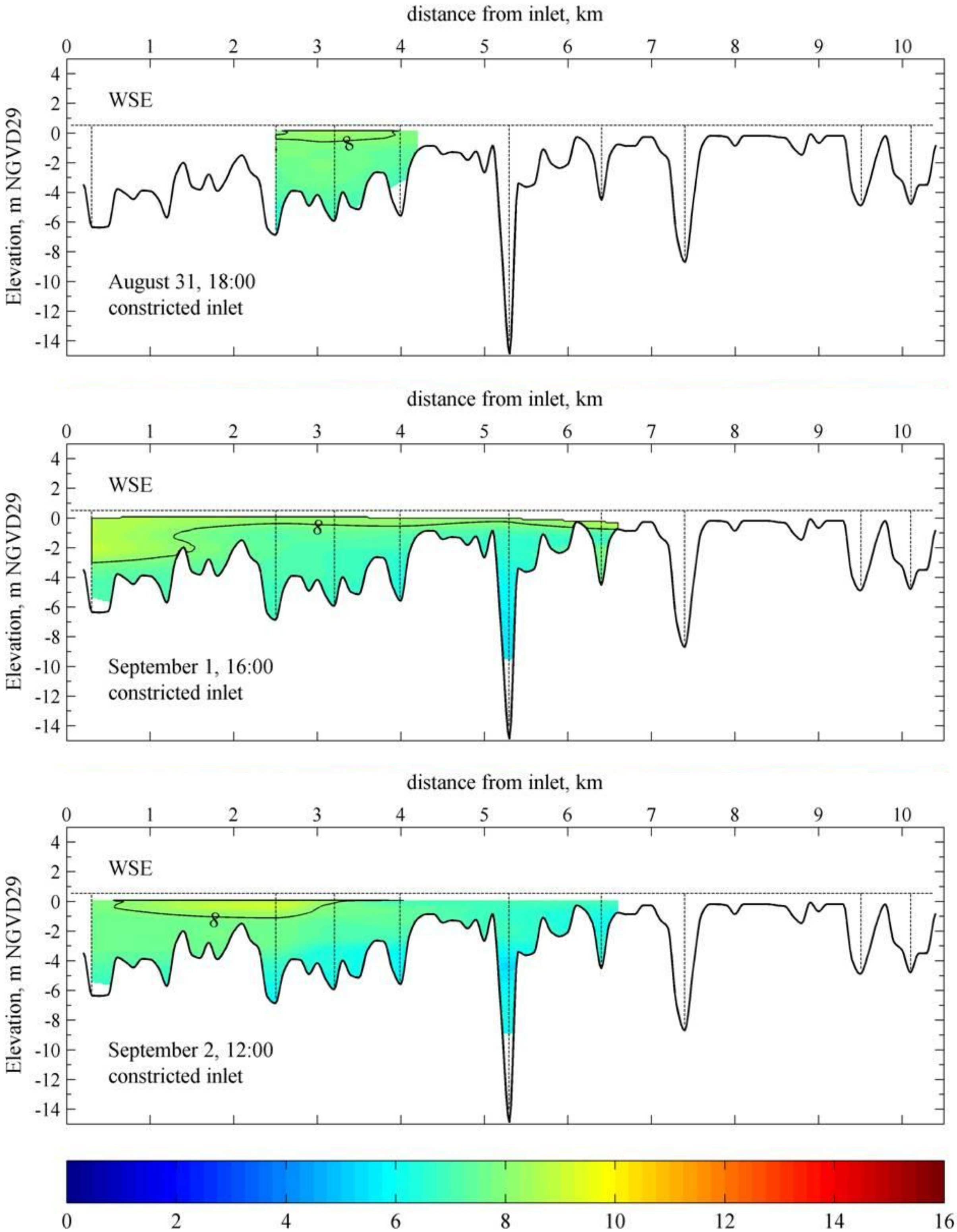

Figure 9.1.3 Estuary DO structure on **(top)** August 31, **(mid)** September 1 and **(bottom)** September 2. Units of DO are mg/L.

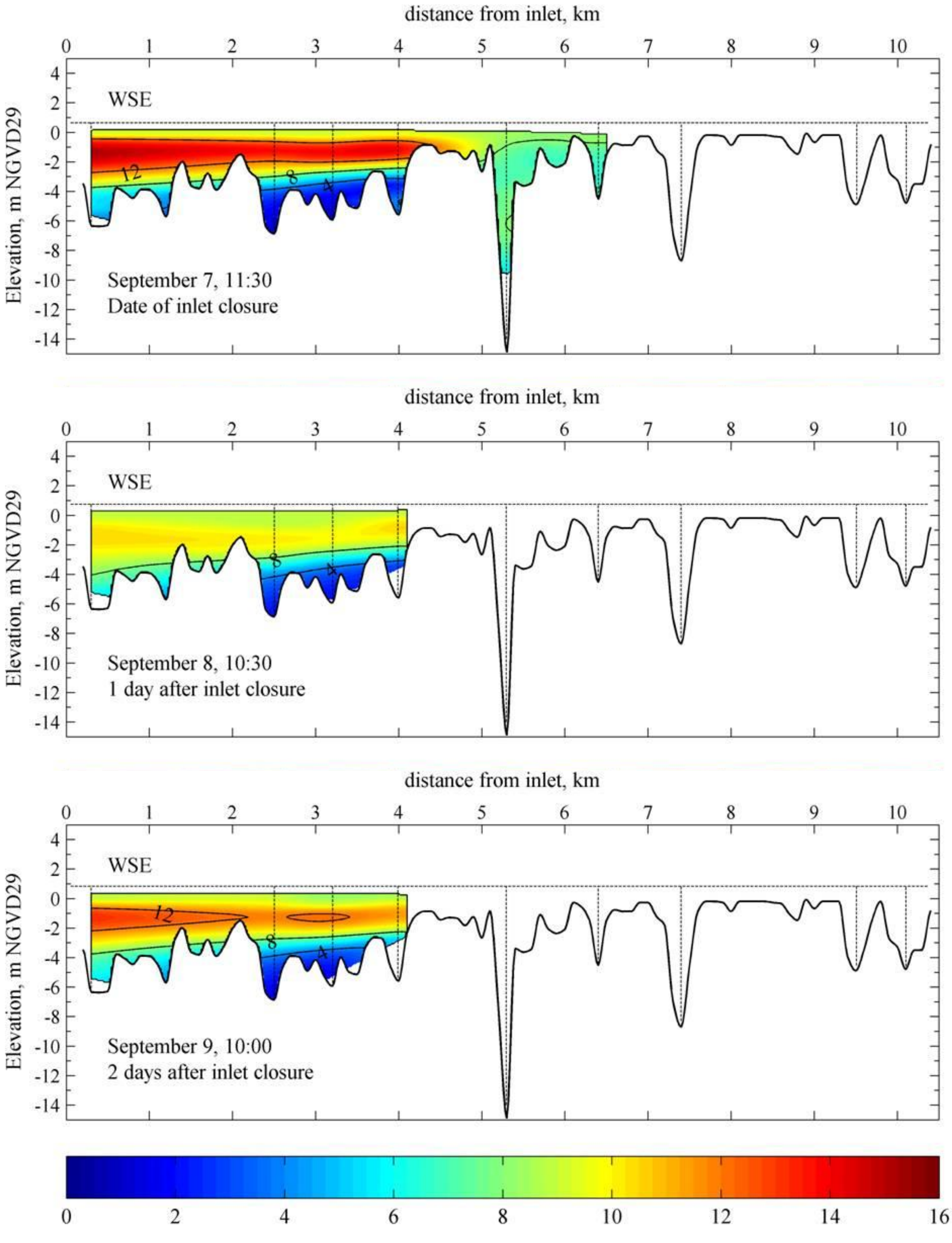

Figure 9.1.4 Estuary DO structure on **(top)** September 7, **(mid)** September 9 and **(bottom)** September 10. Units of DO are mg/L.

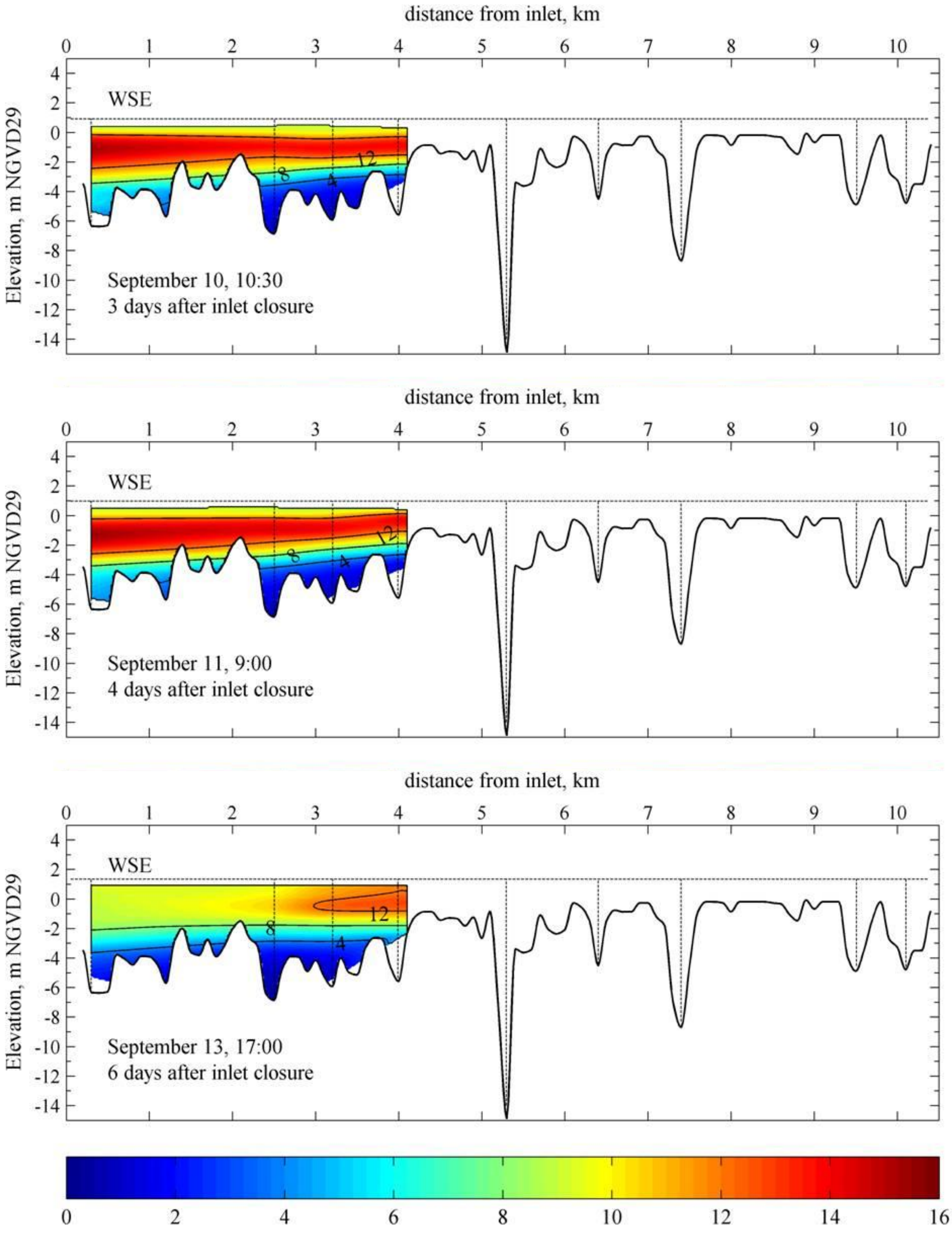

Figure 9.1.5 Estuary DO structure on **(top)** September 10, **(mid)** September 11 and **(bottom)** September 13. Units of DO are mg/L.

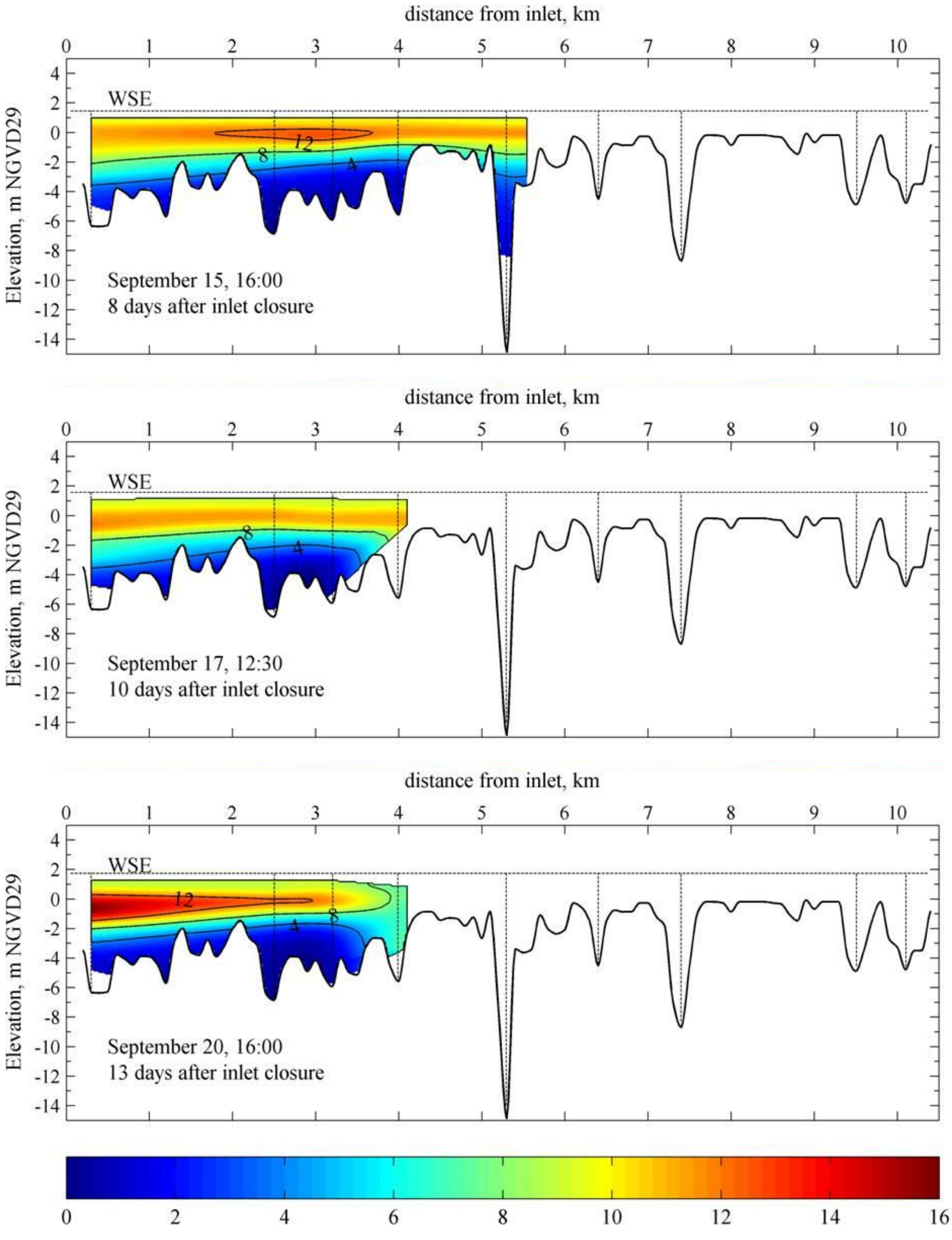

Figure 9.1.6 Estuary DO structure on **(top)** September 15, **(mid)** September 17 and **(bottom)** September 20. Units of DO are mg/L.

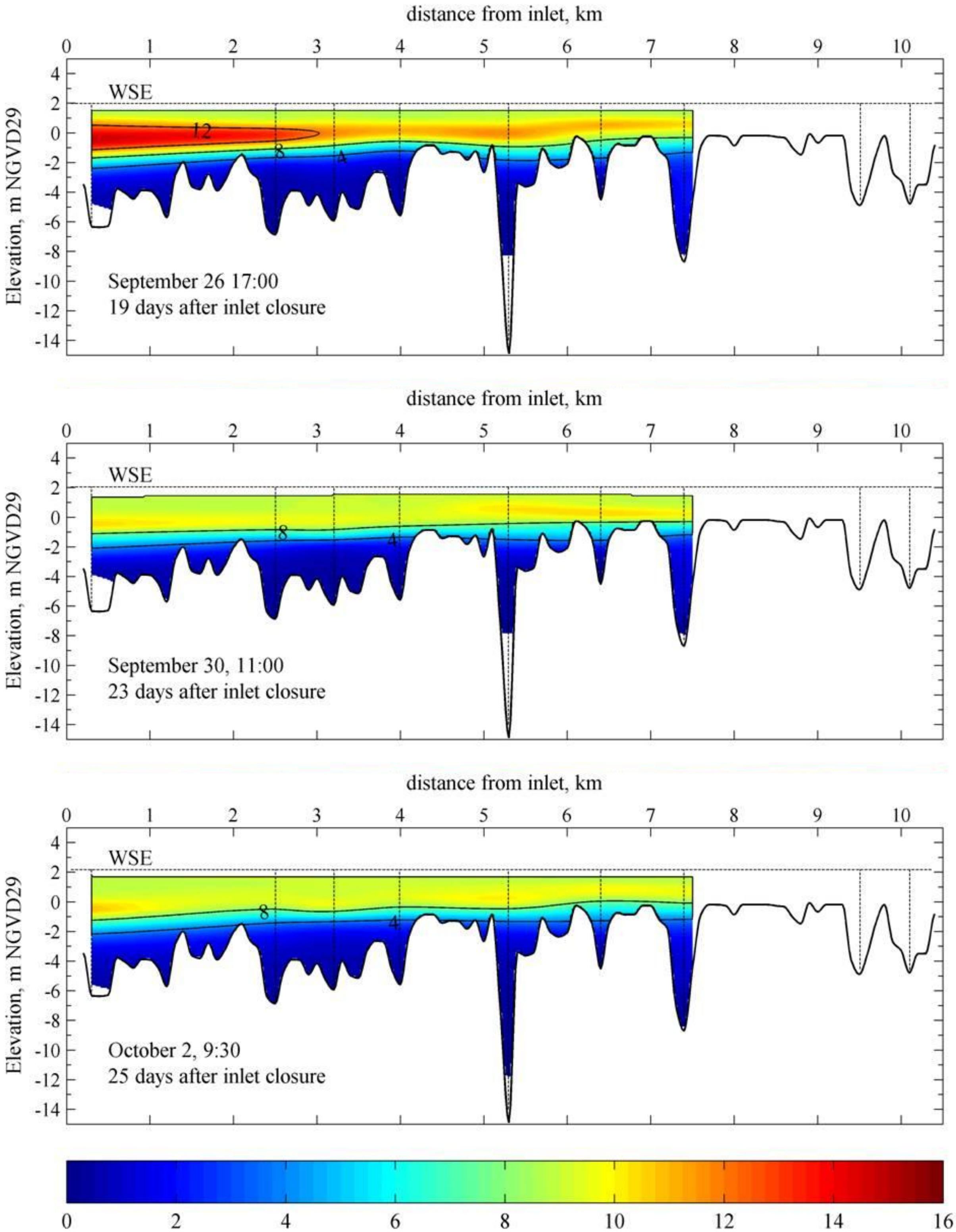

Figure 9.1.7 Estuary DO structure on **(top)** September 26, **(mid)** September 30 and **(bottom)** Oct 2. Units of DO are mg/L.

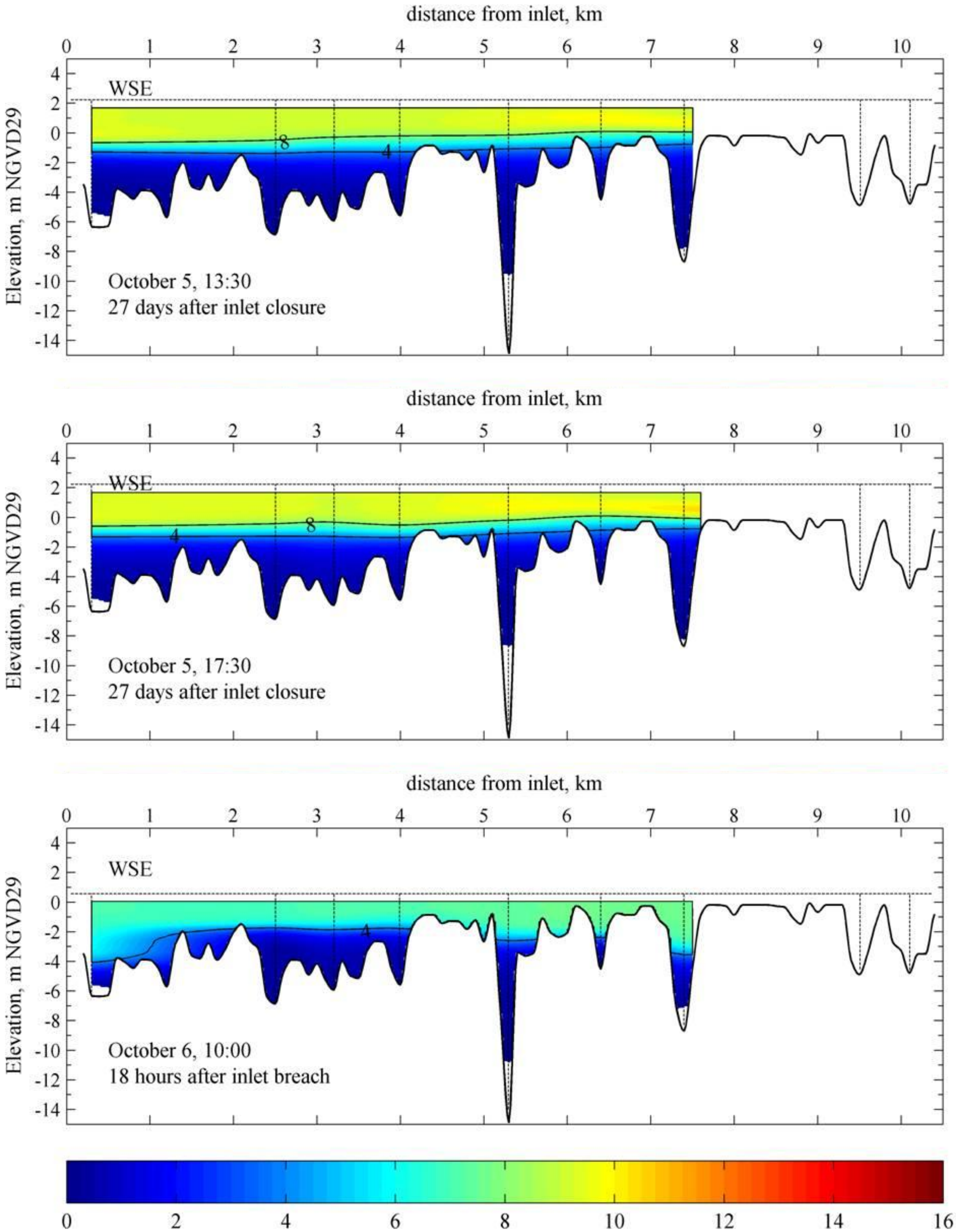

Figure 9.1.8 Estuary DO structure on **(top)** Oct 5, 13:30, **(mid)** Oct 5, 17:30 and **(bottom)** Oct 6, 10:00. Units of DO are mg/L.

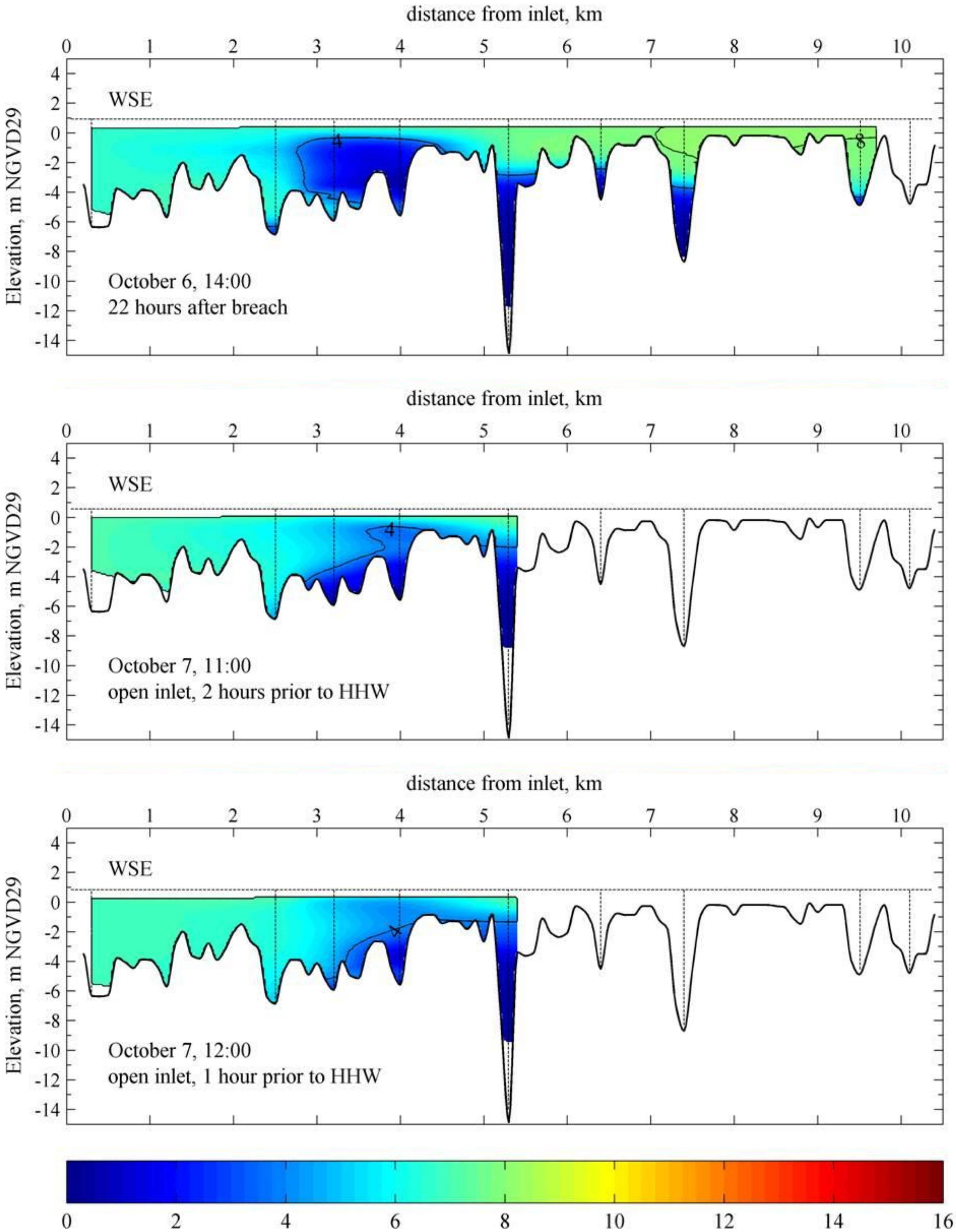

Figure 9.1.9 Estuary DO structure on **(top)** Oct 6, 14:00, **(mid)** Oct 7, 11:00 and **(bottom)** Oct 7, 12:00. Units of DO are mg/L.

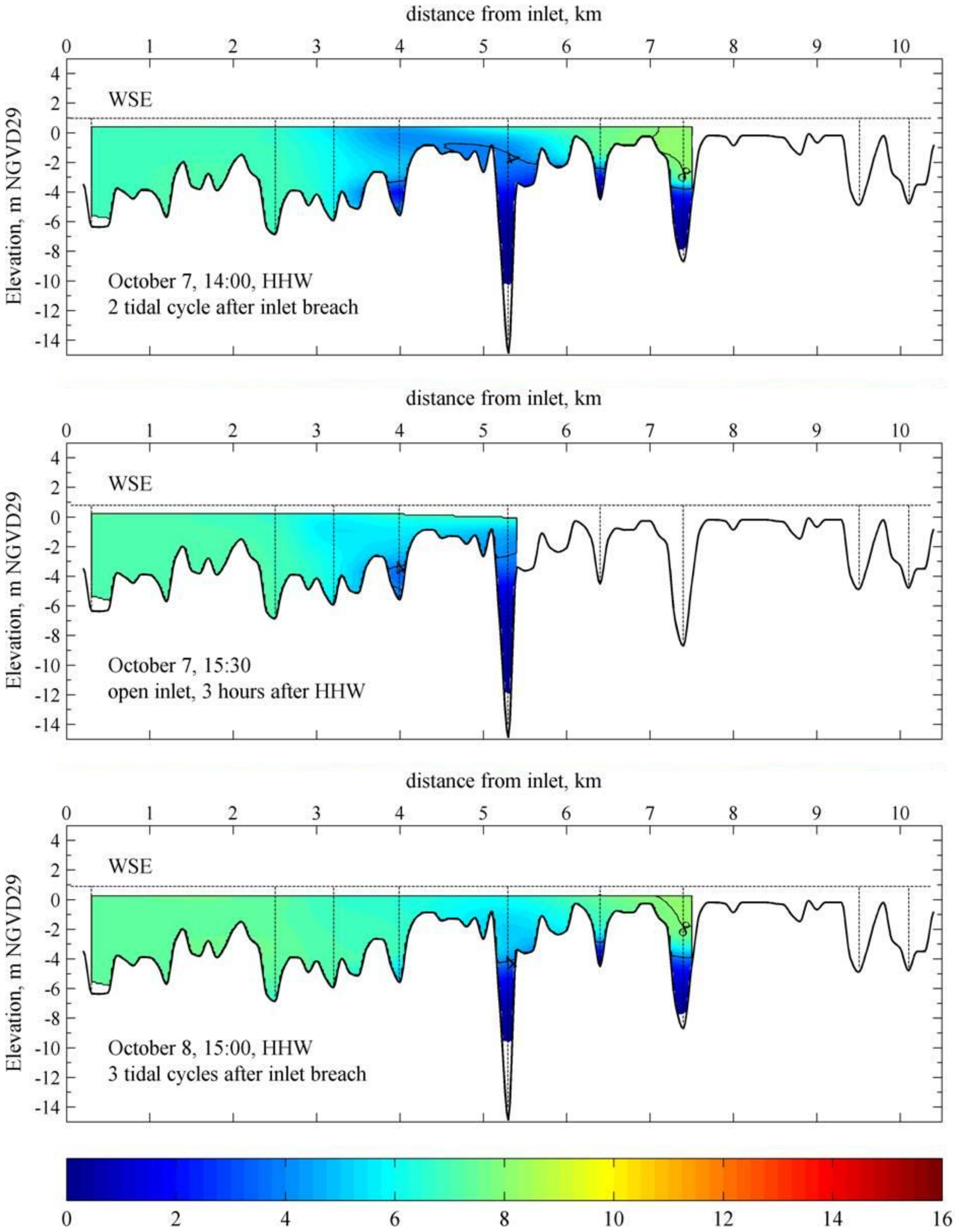

Figure 9.1.10 Estuary DO structure on **(top)** Oct 7, 14:00, **(mid)** Oct 7, 15:30 and **(bottom)** Oct 8, 15:00. Units of DO are mg/L.

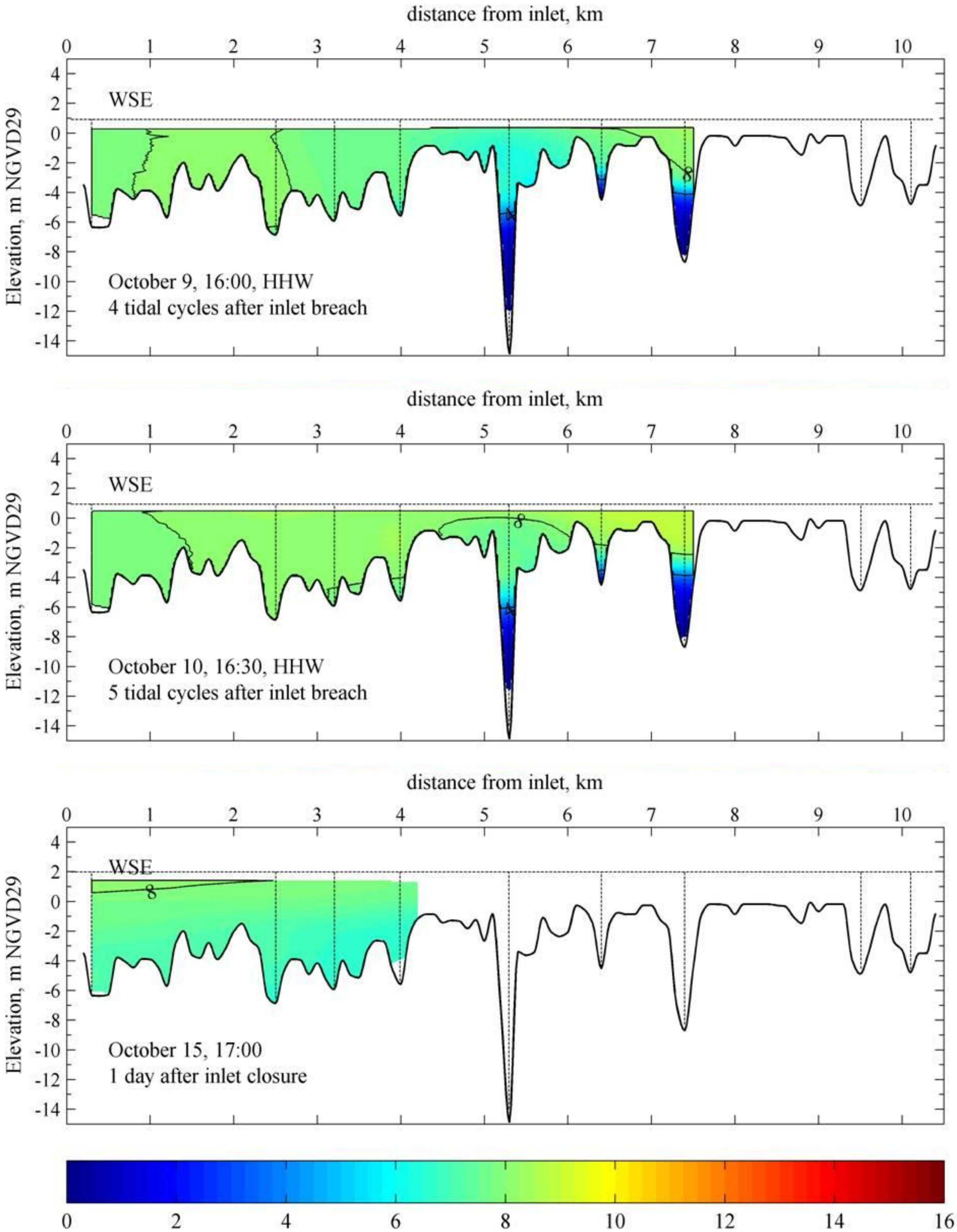

Figure 9.1.11 Estuary DO structure on **(top)** Oct 9, 16:00, **(mid)** Oct 10, 16:30 and **(bottom)** Oct 15, 17:00. Units of DO are mg/L.

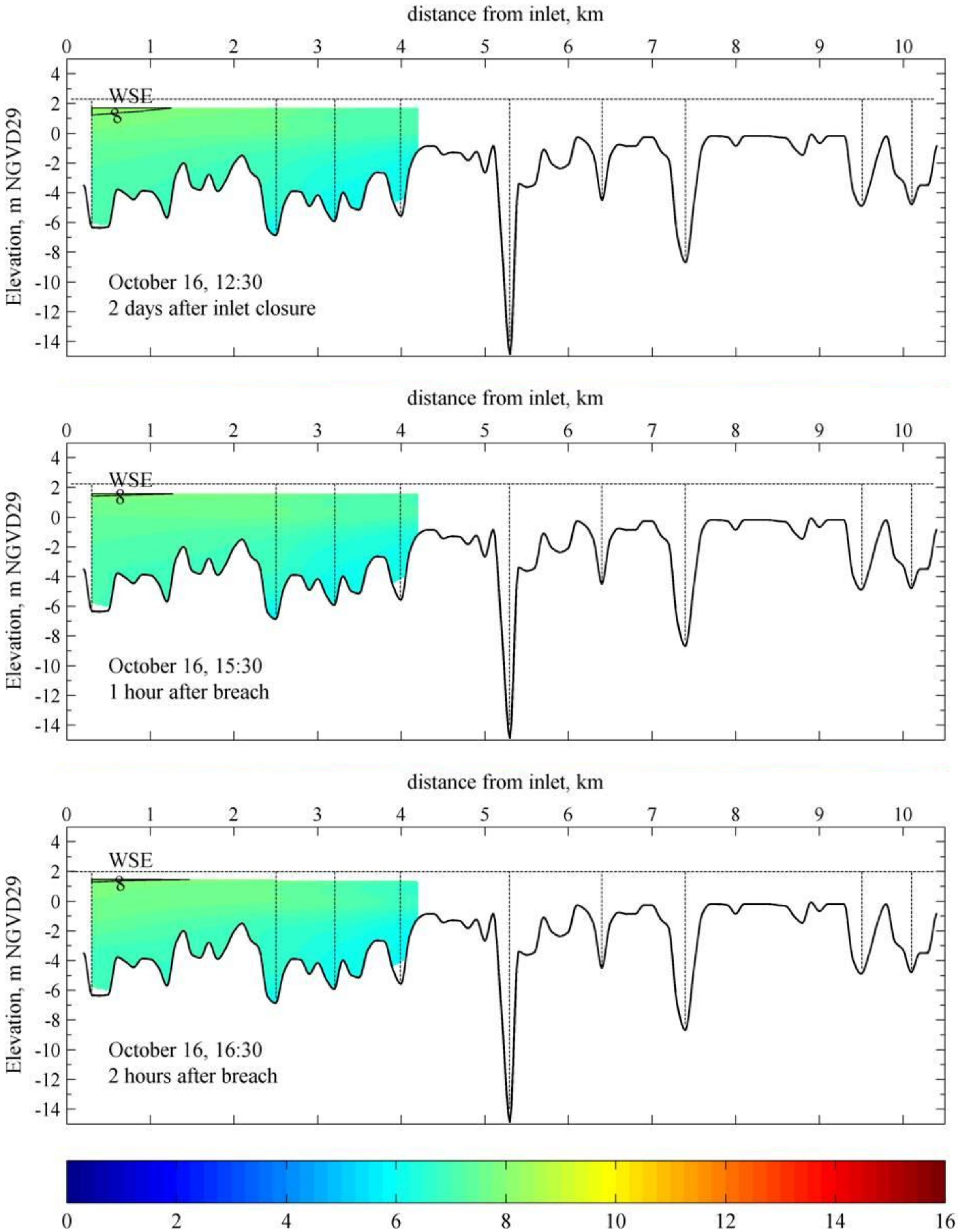

Figure 9.1.12 Estuary DO structure on **(top)** Oct 16, 12:30, **(mid)** Oct 16, 15:30 and **(bottom)** Oct 16, 16:30. Units of DO are mg/L.

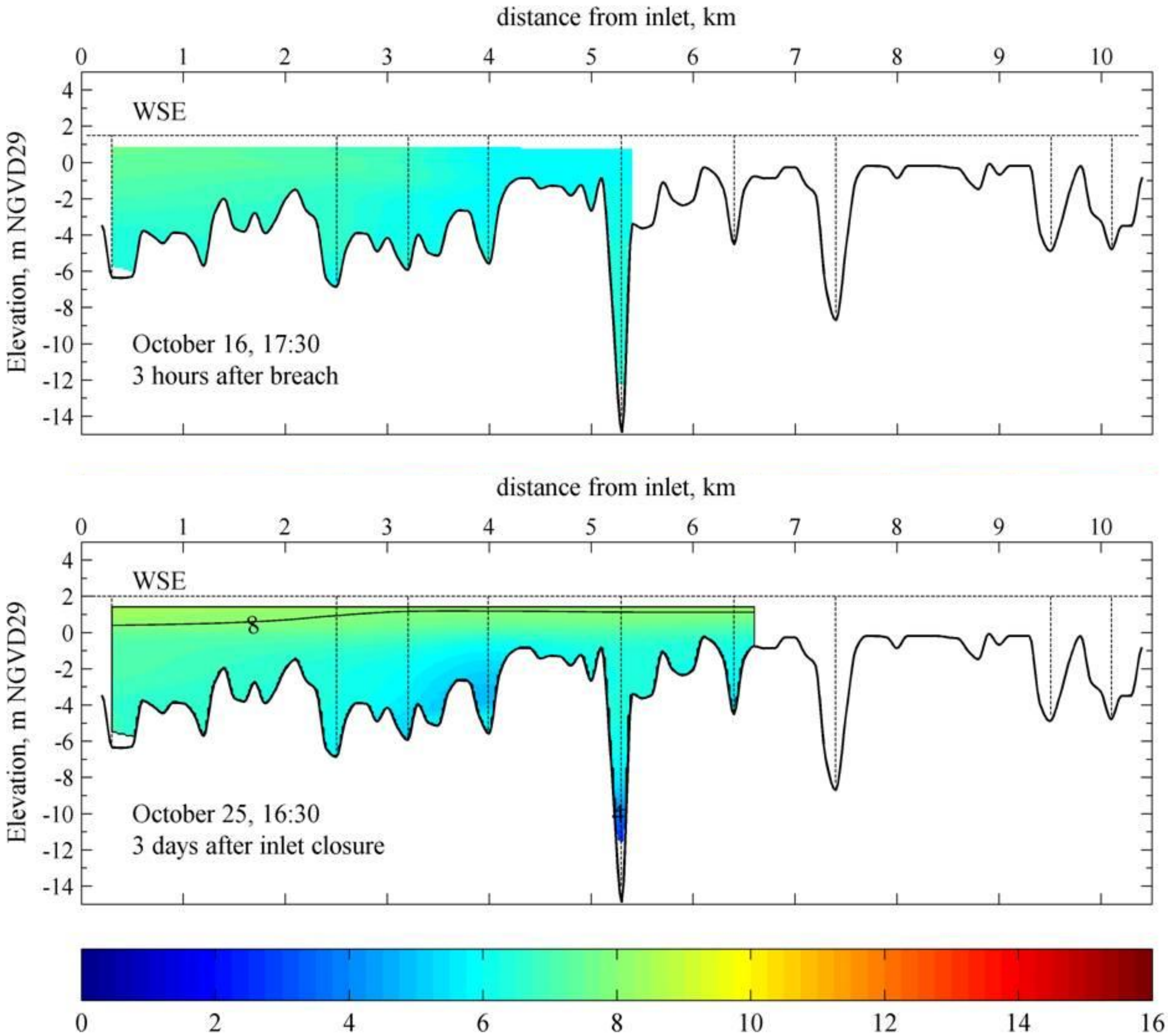

Figure 9.1.13 Estuary DO structure on **(top)** Oct 16, 17:30 and **(bottom)** Oct 25, 16:30. Units of DO are mg/L.

9.2. Temperature Contour Plots

The temperature data indicate that when the inlet was tidal, as it was during the months of July and August, it maintains a strong longitudinal temperature gradient (Figures 9.2.1 and 9.2.2). More profiling during low or ebb tide would larify how this gradient changes throughout the tidal cycle. At times other than higher high water (HHW), a thin layer of relatively warm water (> 16 ºC) extends to the lower 2 km of the estuary, while during HHW, relatively cold water (14-16 ºC) pushes this layer back to Willow Creek or farther upstream (e.g. Figure 9.2.2).

During the near-overflow conditions achieved on September 1 and 2, a layer of 16ºC water began to extend all the way to the inlet. By the time of inlet closure on September 7, the estuary already had a vertical temperature structure, as shown in Figure 9.2.4.

During the prolonged September-October closure event, the mean temperature in the estuary rose considerably. The maximum temperature rose from 22 to 24 ºC. On September 13 and 15 (Figure 9.2.5), the amount of 16ºC water at the mouth station increased sharply, and a longitudinal gradient was again formed. For the rest of the closure period, the temperature structure was mostly dominated by vertical stratification. The peak temperature was consistently located at the Osprey Rookery and Heron Rookery stations, at an elevation of 0 to -2m NGVD29, regardless of the water depth. Although the peak temperature was lower at the other stations, the same structure formed, with the maximum temperature present at the same elevation (e.g. Figure 9.2.6).

By September 30 (Figure 9.2.7), a longitudinal slope in the boundary between high and low temperature water became apparent. The temperature maximum at the Mouth was slightly lower than that of the Sheephouse Creek station.

When the inlet was breached on October 5, the first water to exit the estuary was the relatively warm water in the upper 3-4m of the water column. The temperature maximum at Heron Rookery lowered to the bottom of the pool, and the estuary temperature initially became more homogeneous. In subsequent tidal cycles, the estuary incrementally became colder, with a strong longitudinal temperature gradient re-forming between the Mouth and Sheephouse Creek.

The closure events on October 14 and October 22 did not generate similar temperature structures to that of the prolonged September-October event. In both cases, a vertical structure was formed, with the highest temperature (16-18 ºC) at the surface.

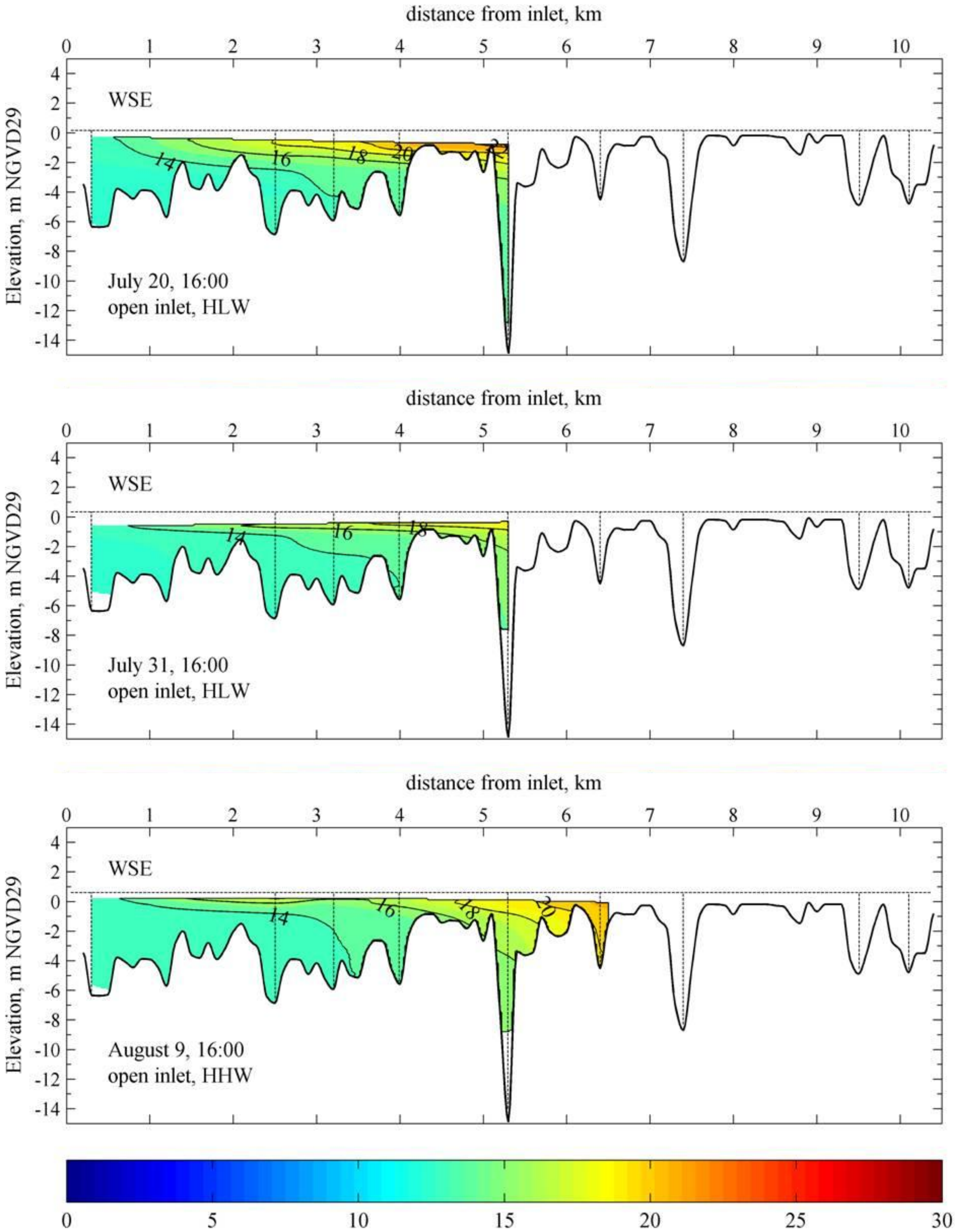

Figure 9.2.1 Estuary temperature structure on **(top)** July 20, **(mid)** July 31 and **(bottom)** August 9. Temperature units are ºC.

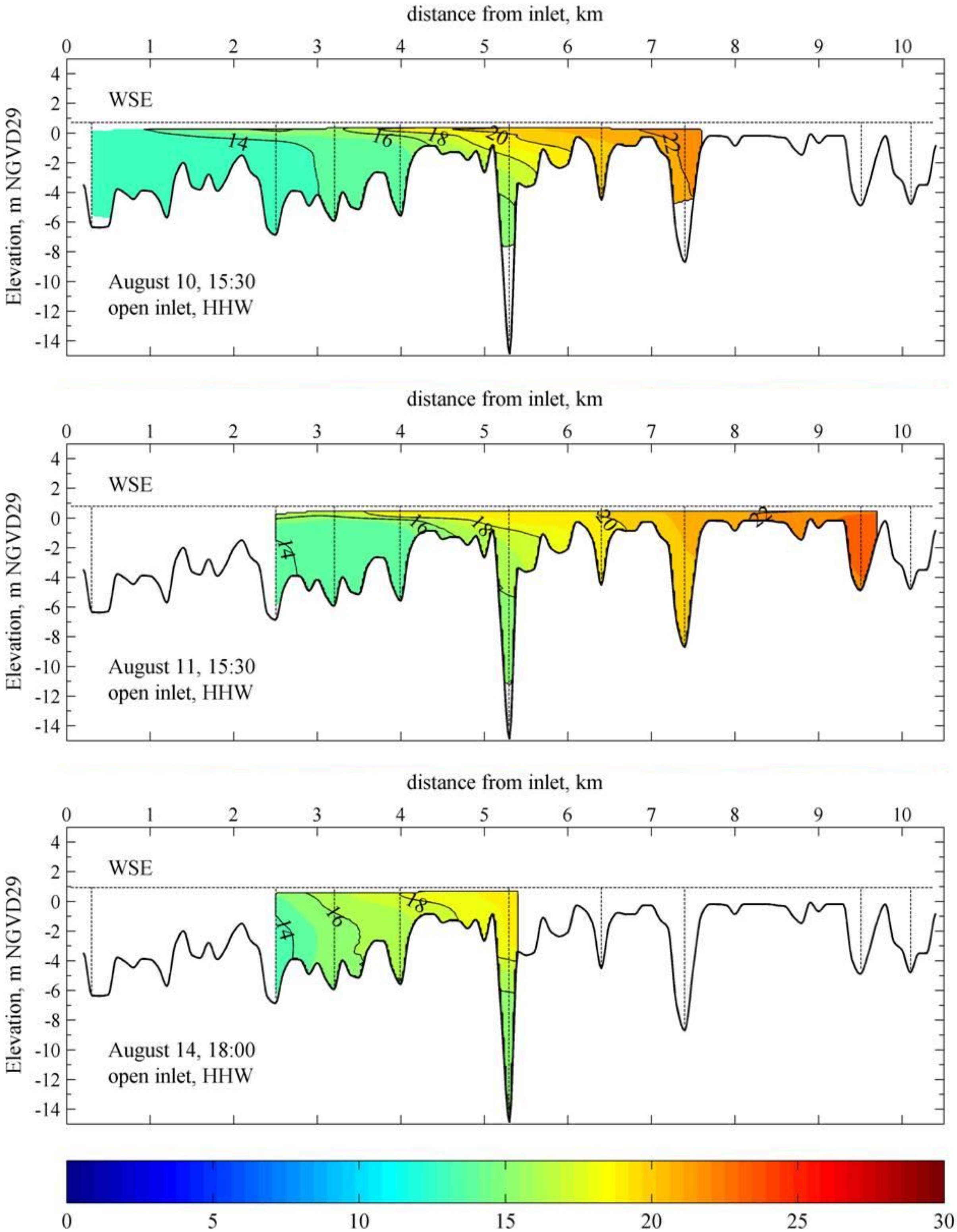

Figure 9.2.2 Estuary temperature structure on **(top)** August 10, **(mid)** August 11 and **(bottom)** August 14. Temperature units are ºC.

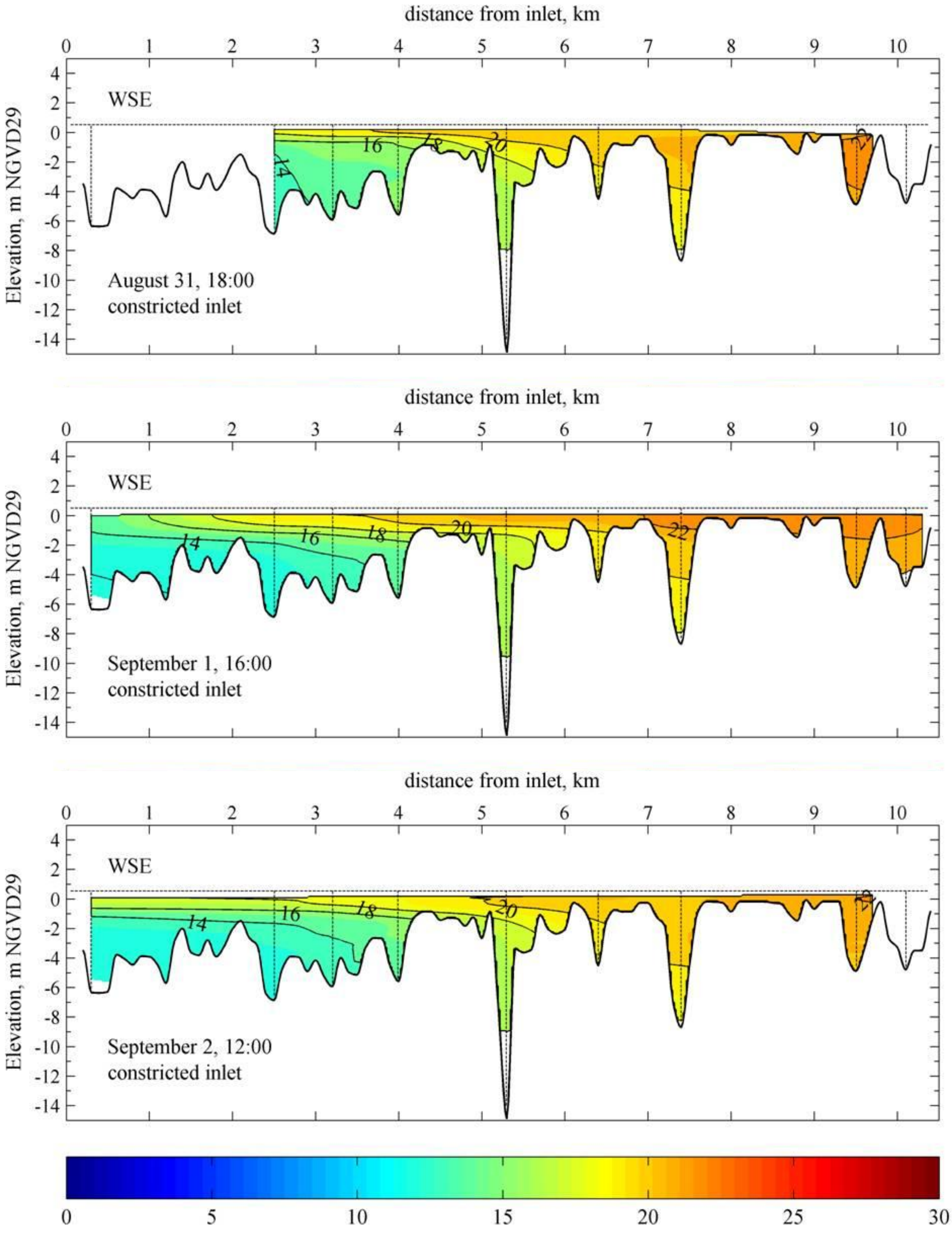

Figure 9.2.3 Estuary temperature structure on **(top)** August 31, **(mid)** September 1 and **(bottom)** September 2. Temperature units are ºC.

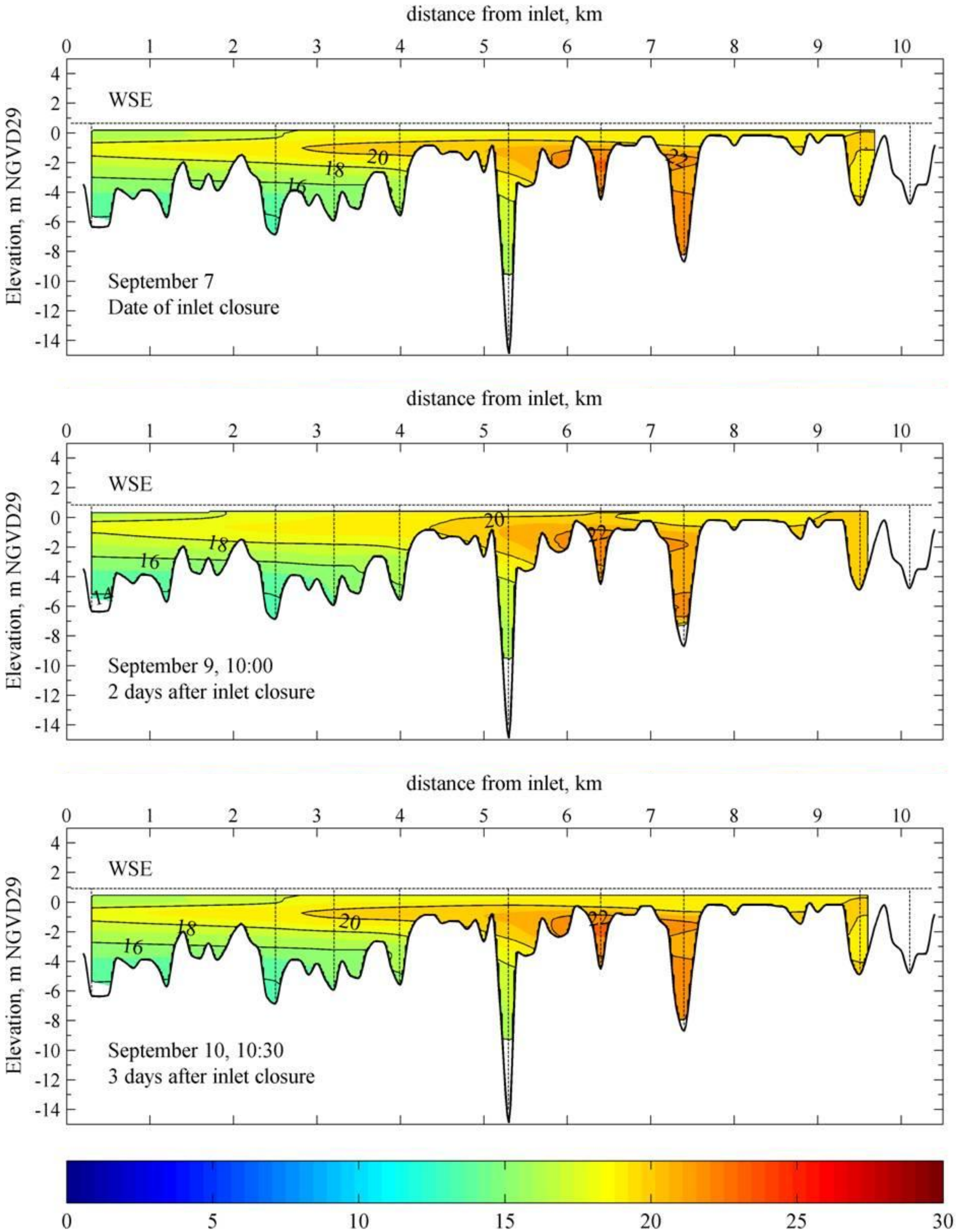

Figure 9.2.4 Estuary temperature structure on **(top)** September 7, **(mid)** September 9 and **(bottom)** September 10. Temperature units are ºC.

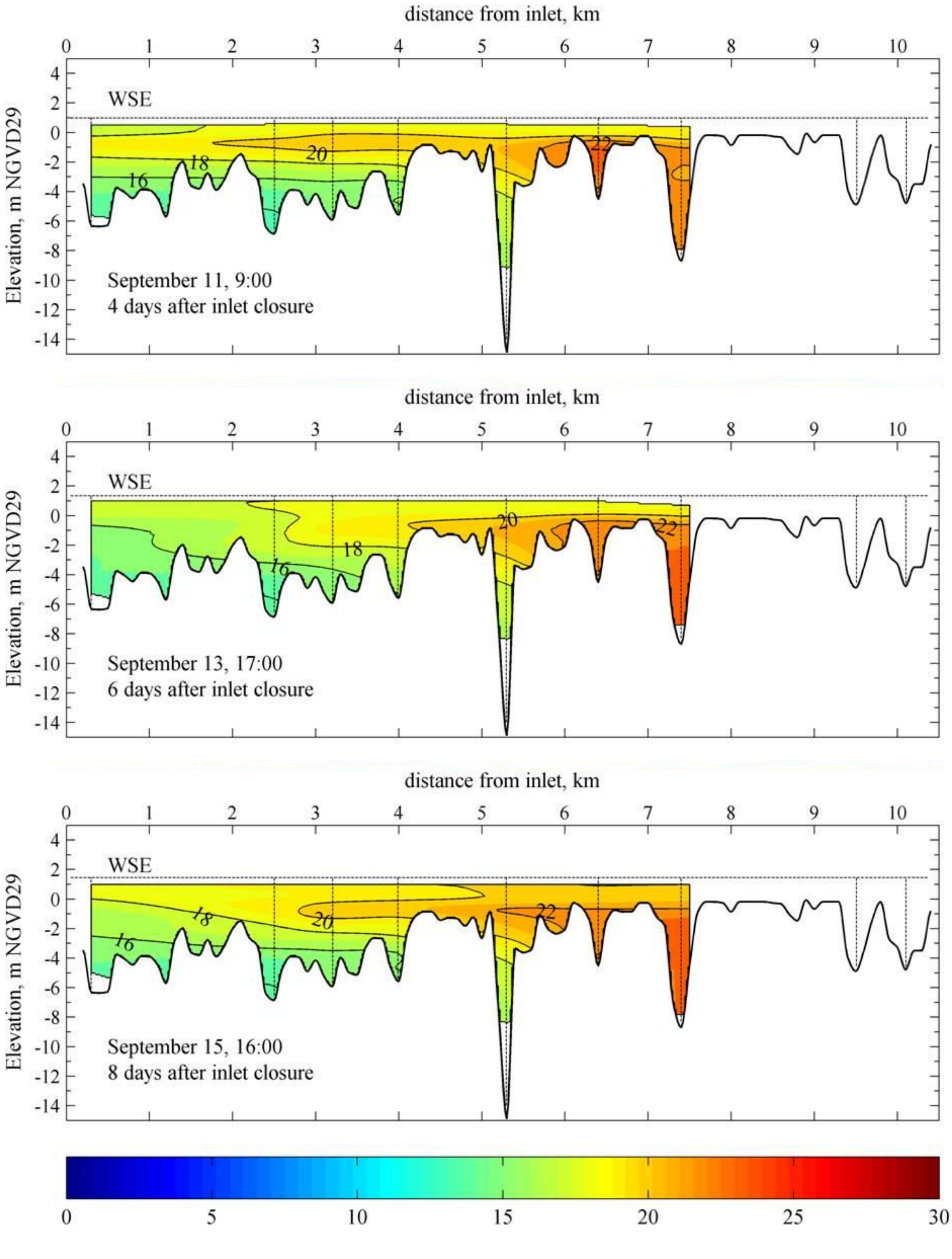

Figure 9.2.5 Estuary temperature structure on **(top)** September 11, **(mid)** September 13 and **(bottom)** September 15. Temperature units are ºC.

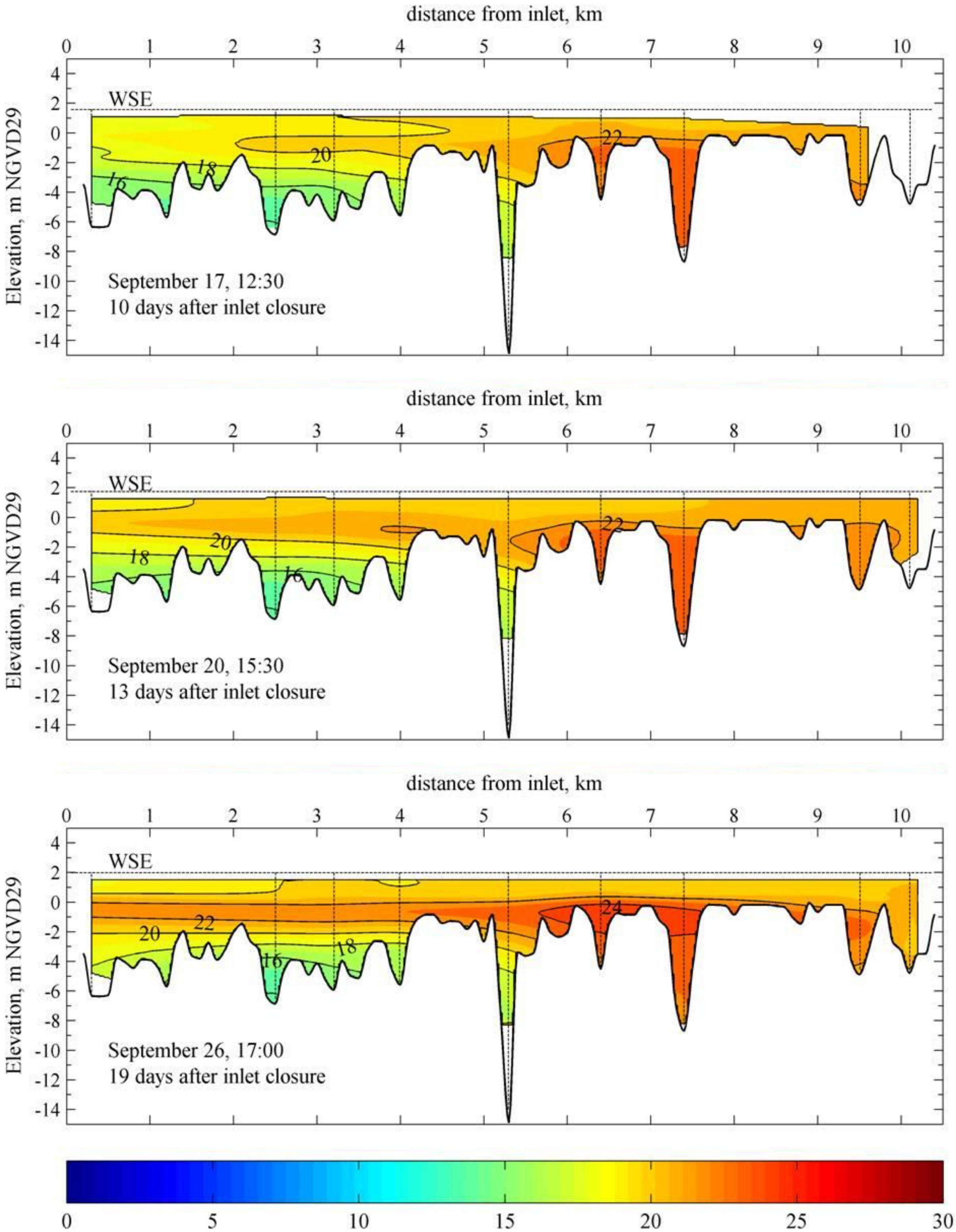

Figure 9.2.6 Estuary temperature structure on **(top)** September 17, **(mid)** September 20 and **(bottom)** September 26. Temperature units are ºC.

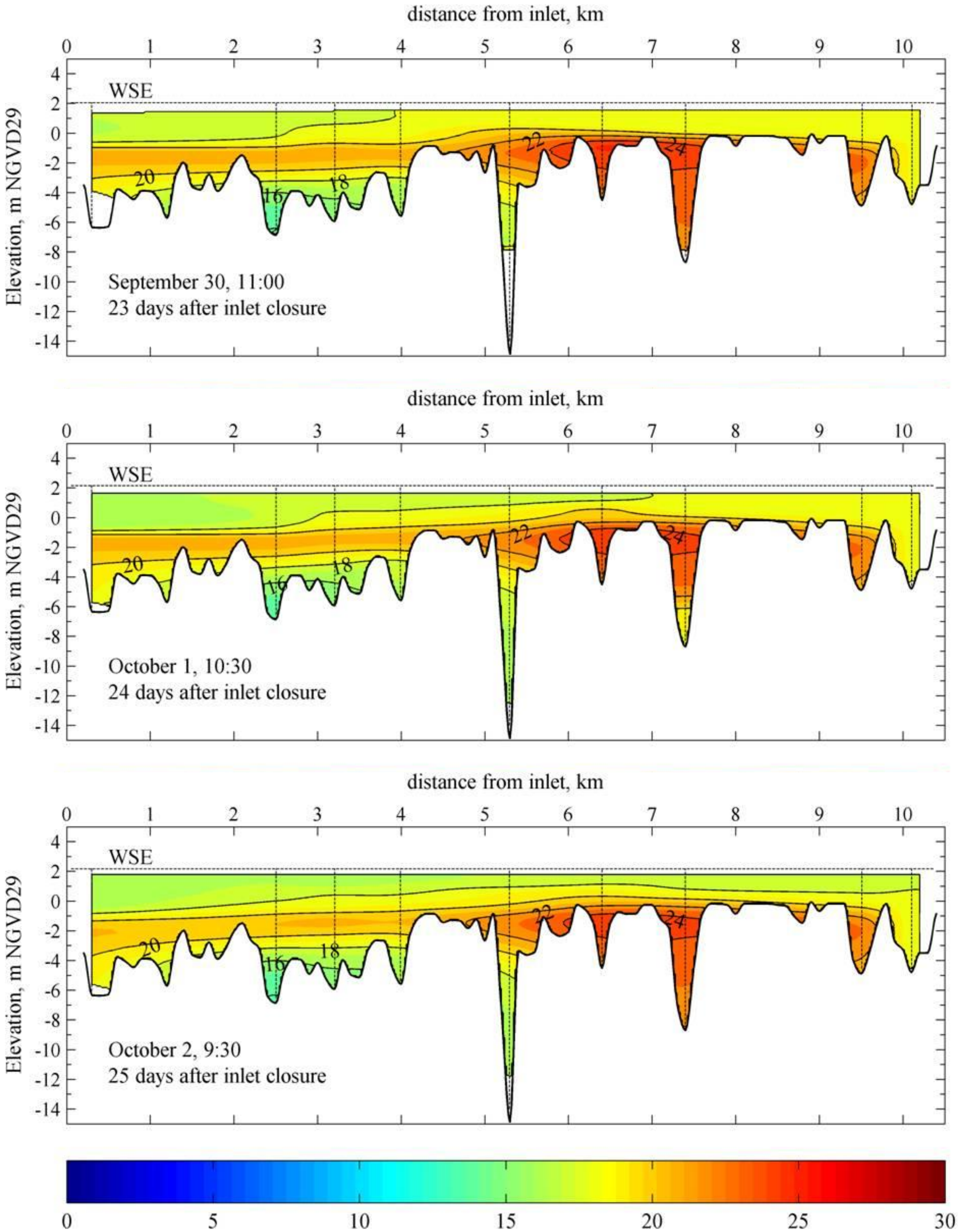

Figure 9.2.7 Estuary temperature structure on **(top)** September 30, **(mid)** October 1 and **(bottom)** October 2. Temperature units are ºC.

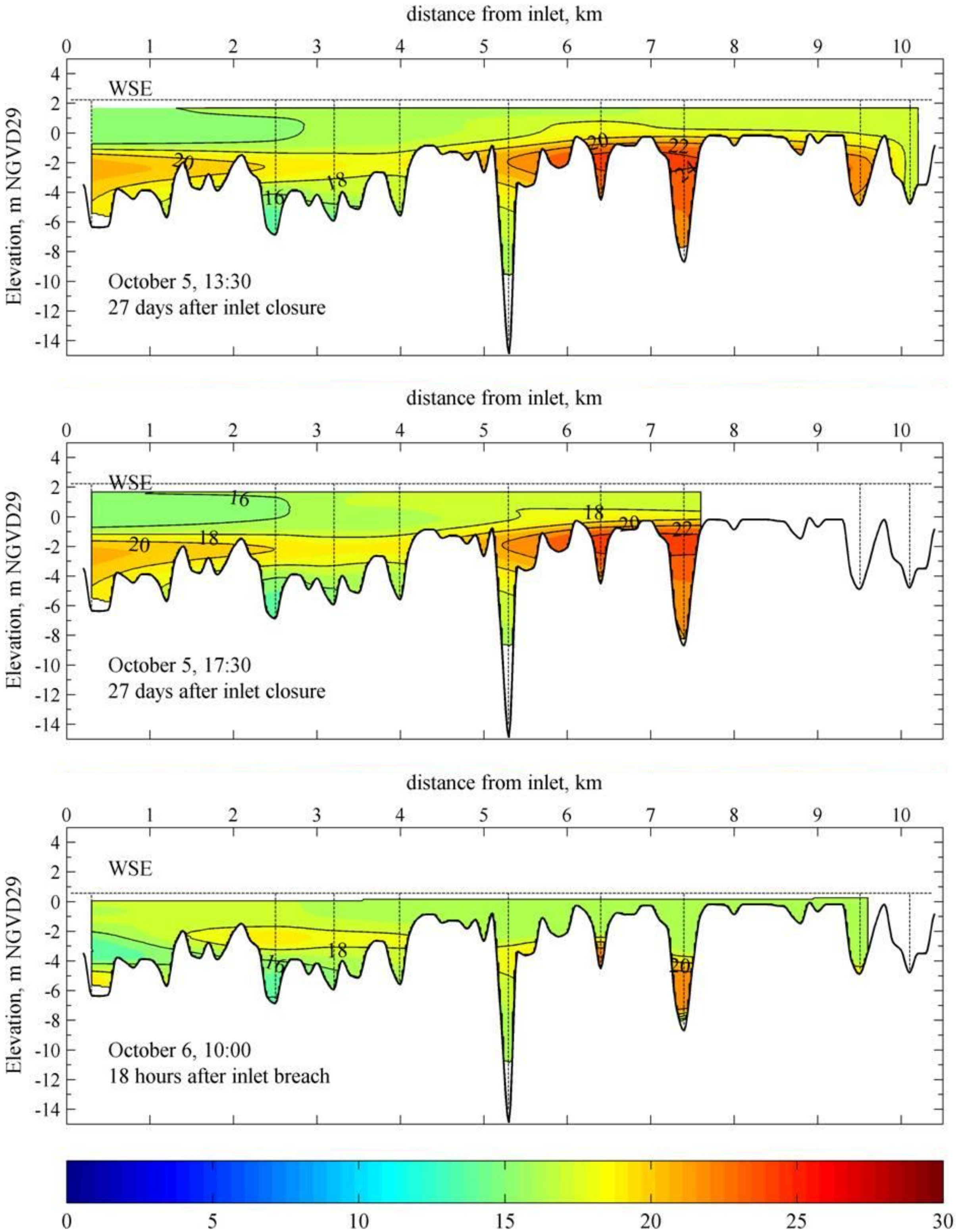

Figure 9.2.8 Estuary temperature structure on **(top)** October 5, 13:30, **(mid)** October 5, 17:30 and **(bottom)** October 6, 10:00. Temperature units are ºC.

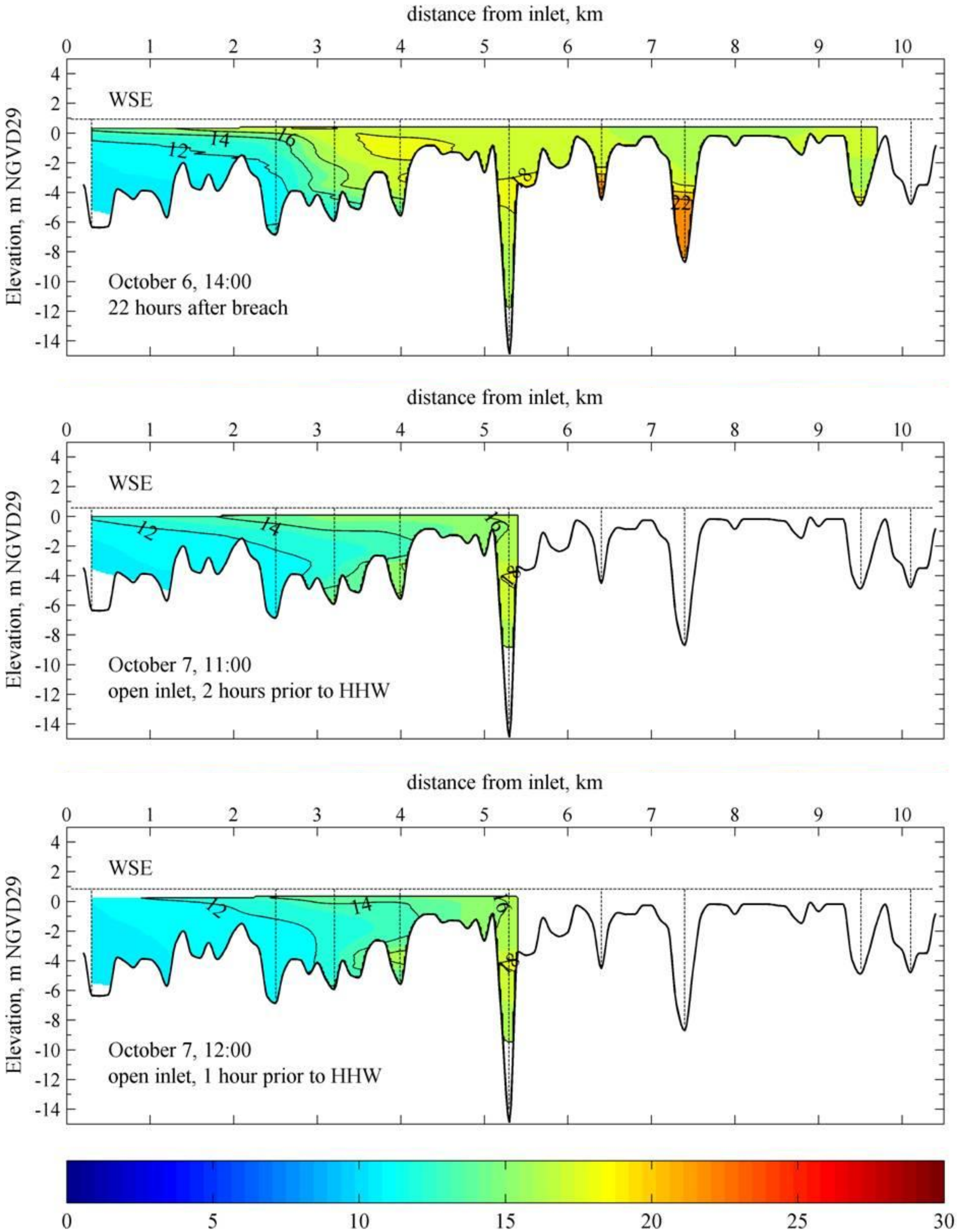

Figure 9.2.9 Estuary temperature structure on **(top)** October 6, 14:00, **(mid)** October 7, 11:00 and **(bottom)** October 7, 12:00. Temperature units are ºC.

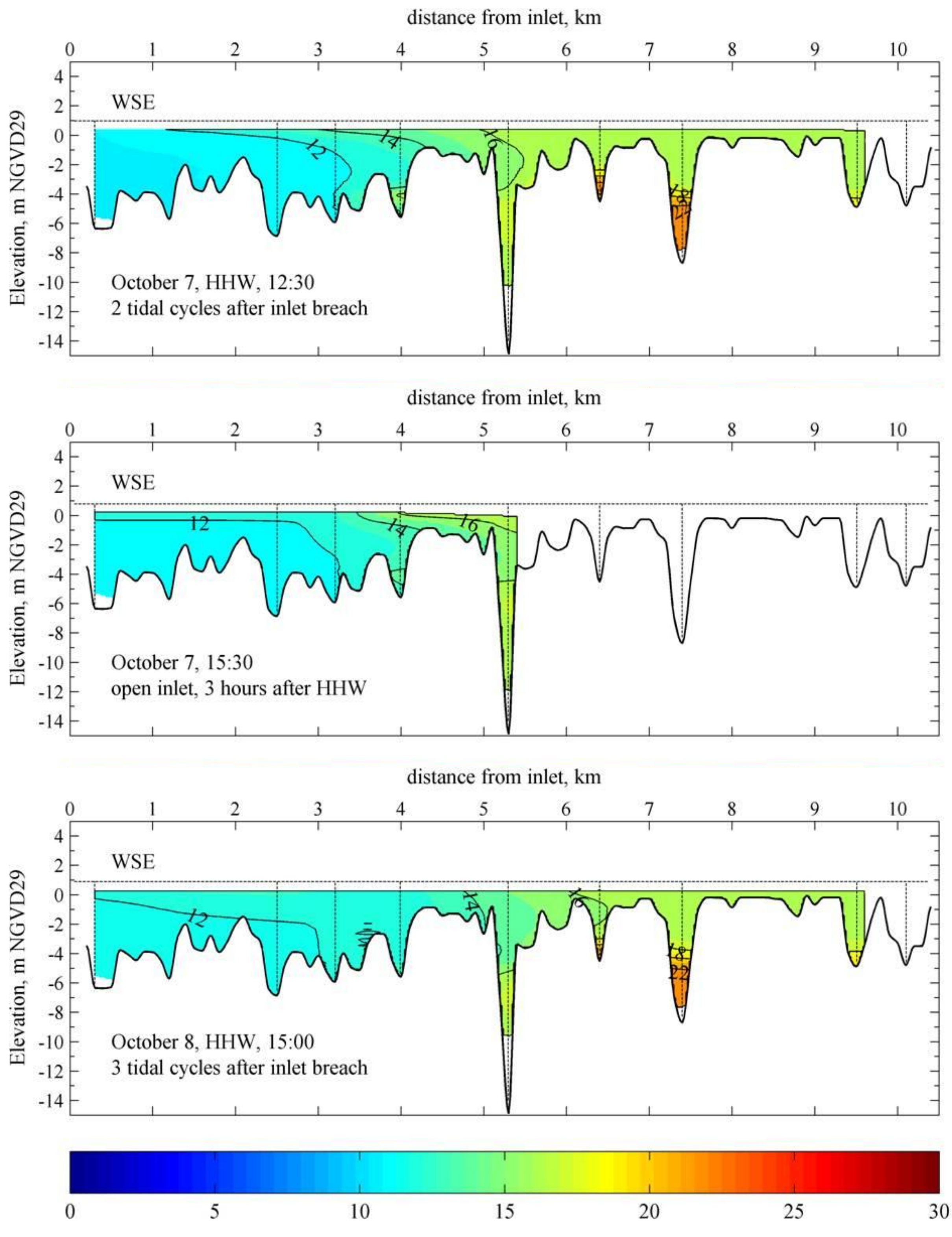

Figure 9.2.10 Estuary temperature structure on **(top)** October 7, 12:30, **(mid)** October 7, 15:30 and **(bottom)** October 8. Temperature units are ºC.

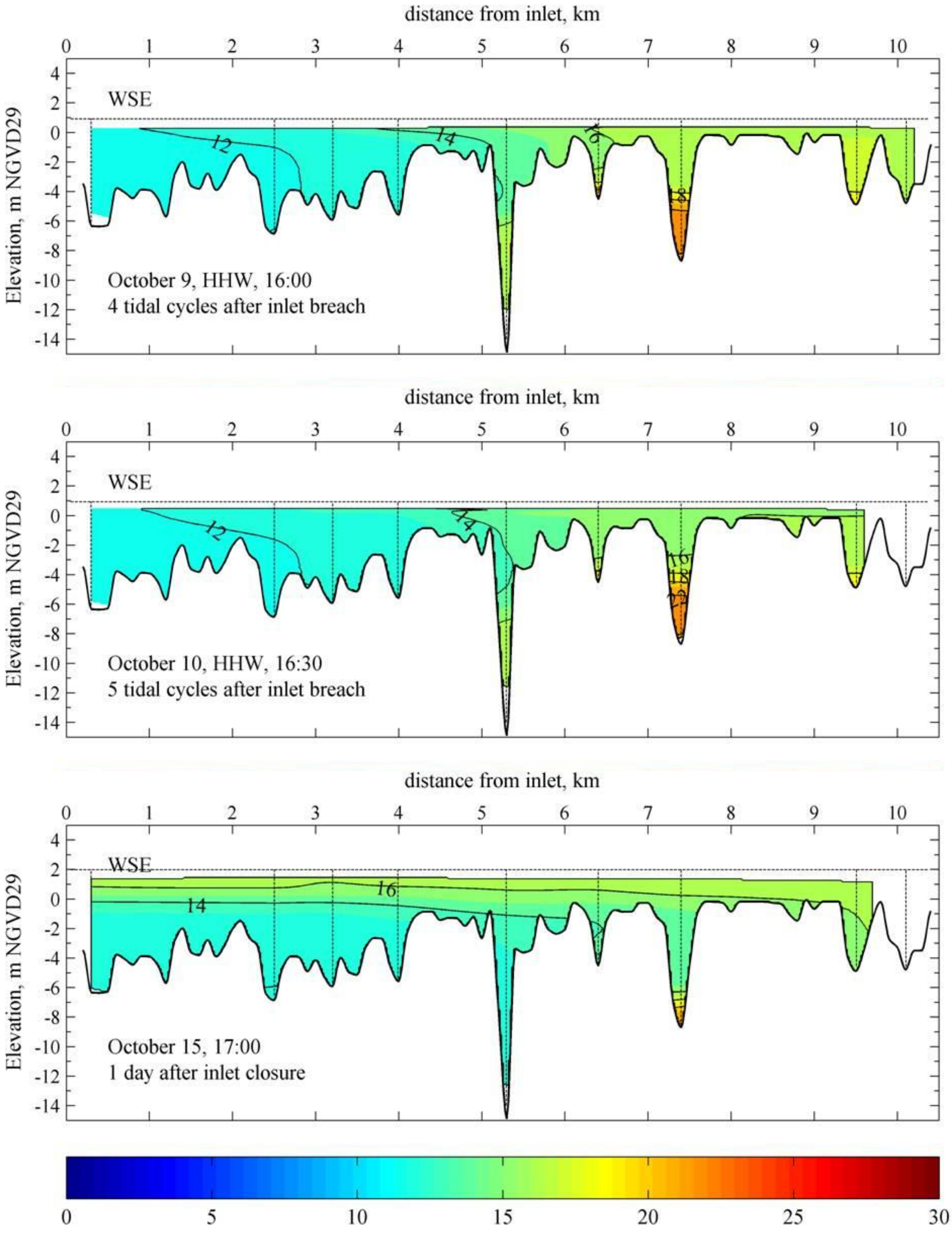

Figure 9.2.11 Estuary temperature structure on **(top)** October 9, **(mid)** October 10 and **(bottom)** October 15. Temperature units are ºC.

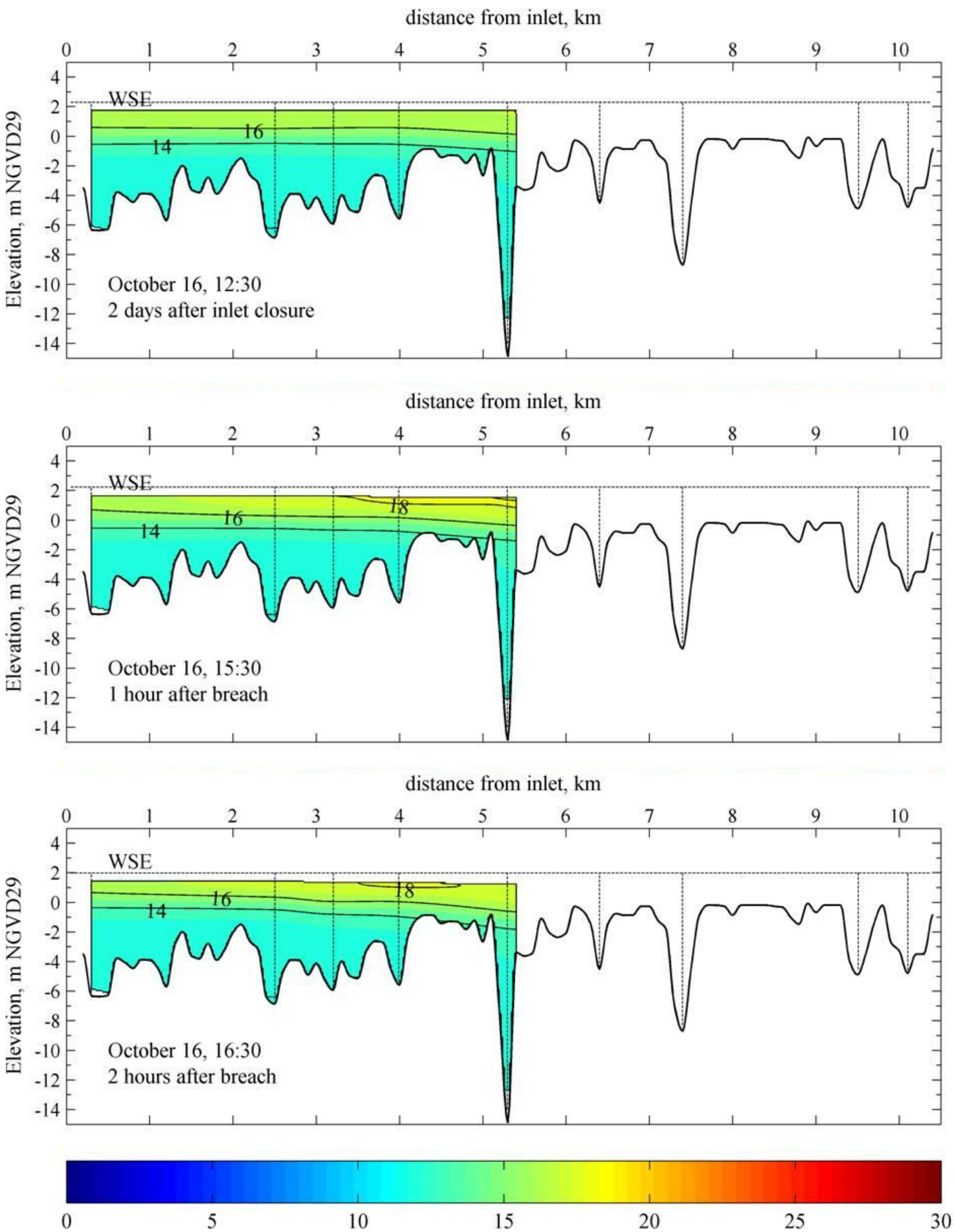

Figure 9.2.12 Estuary temperature structure on **(top)** October 6, 12:30, **(mid)** October 6, 15:30 and **(bottom)** October 6, 16:30. Temperature units are ºC.

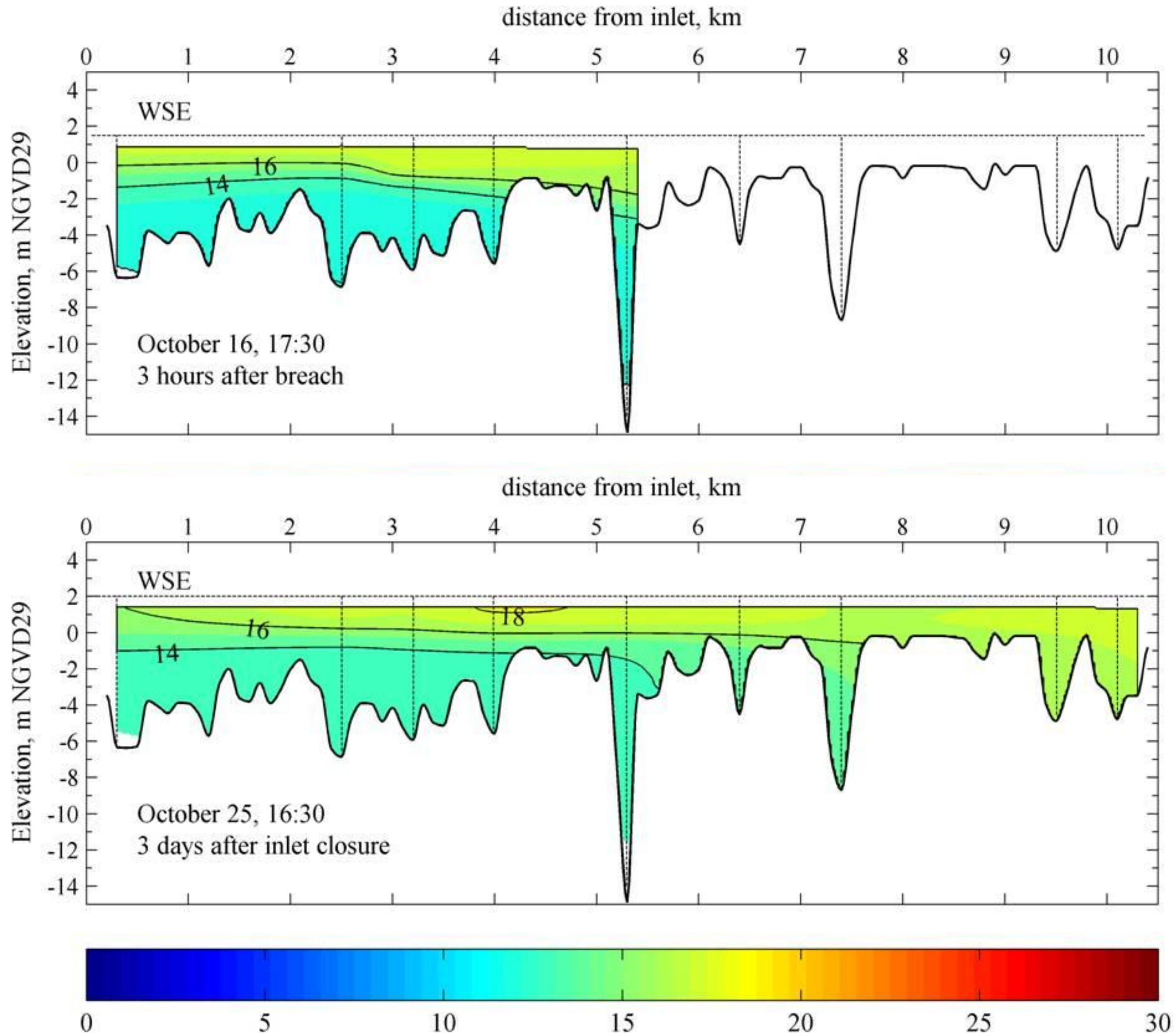

Figure 9.2.12 Estuary temperature structure on **(top)** October 16, 17:30, and **(bottom)** October 25. Temperature units are ºC.

9.3 Salinity contour plots

Salinity structure in the estuary was similar to that of temperature during tidal conditions. A strong longitudinal gradient was present, with relatively high salinity (>30 psu) water dominating the water column at the mouth (e.g. Figure 9.3.1). Figure 9.3.2 shows that when the tide was not at HHW, a layer of relatively low-salinity water was observed at the top of the water column extending to the lower estuary. When near-overflow conditions were present on September 1 and 2 (Figure 9.3.3), this layer extended to the Mouth station.

After the inlet closed on September 7, sharp vertical stratification was already present. For the first several weeks of the closure period, the halocline was approximately 1m higher in the lower 5 km of the estuary than at Sheephouse Creek. Between Sheephouse Creek and Heron Rookery, the halocline lowered substantially. An event between September 11 and September 15, shown on Figure 9.3.5, increased the amount of saline water in the lower 5 km of the estuary.

By September 26, the halocline was nearly horizontal. The halocline was lower at the Mouth station and higher upstream, at Heron Rookery and Freezeout Creek, than it had been before. After September 15, the Mouth station continually lost salt from the bottom of the water column. By the end of the closure period, none of the water at the Mouth was 30 psu or above.

When the inlet was breached on October 5 (Figure 9.3.8), the relatively fresh water near the surface was the first to exit the estuary, but halocline dropped in all locations. After one tidal cycle, a longitudinal salinity gradient was again formed, and the salt extended incrementally farther upstream each day after the closure.

The salinity structures during the October 14 and October 22 closure events were similar to that of the prolonged September-October event (see Figures 9.3.11- 9.3.13).

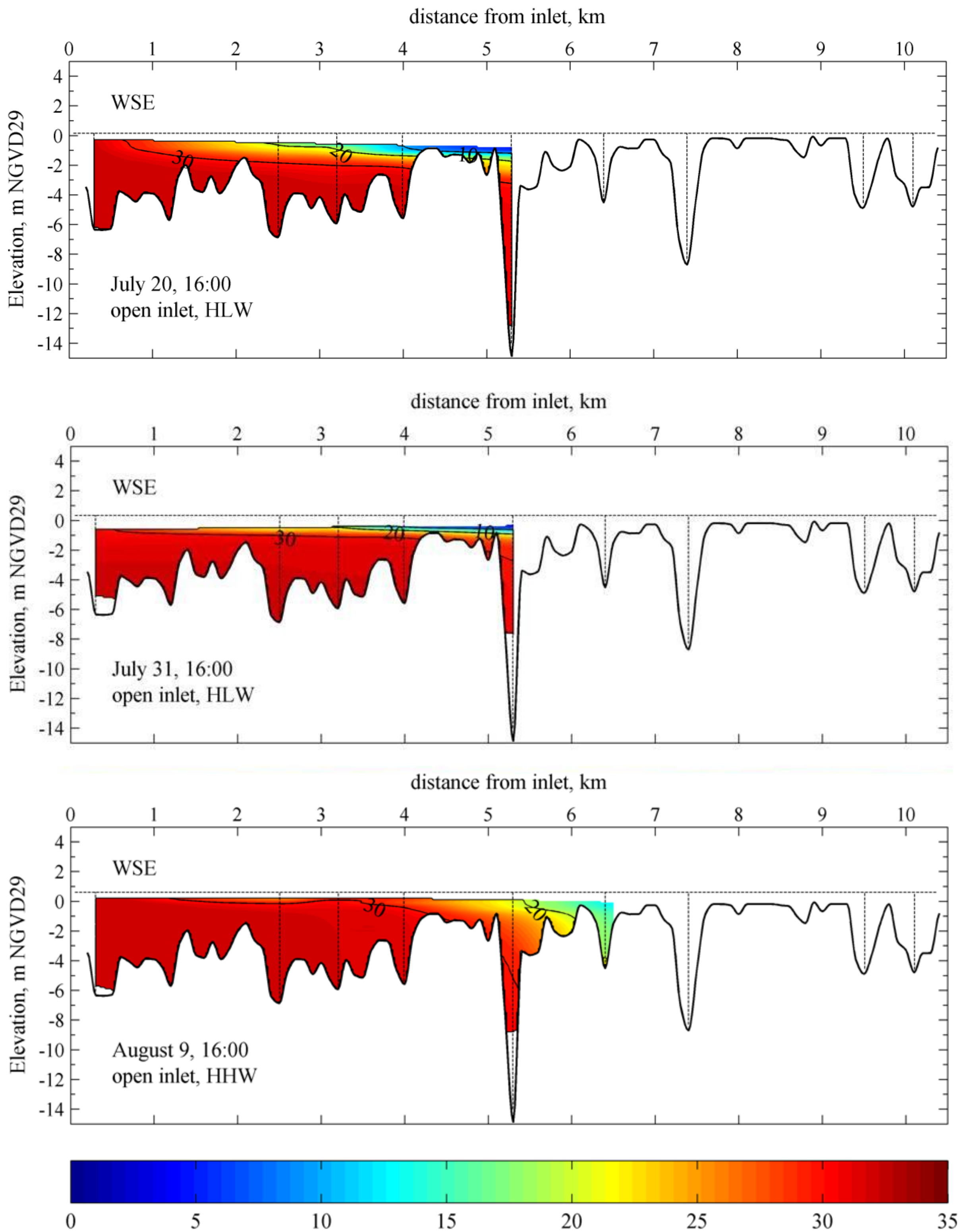

Figure 9.3.1 Estuary salinity structure on **(top)** July 20, **(mid)** July 31 and **(bottom)** August 9. Salinity units are psu.

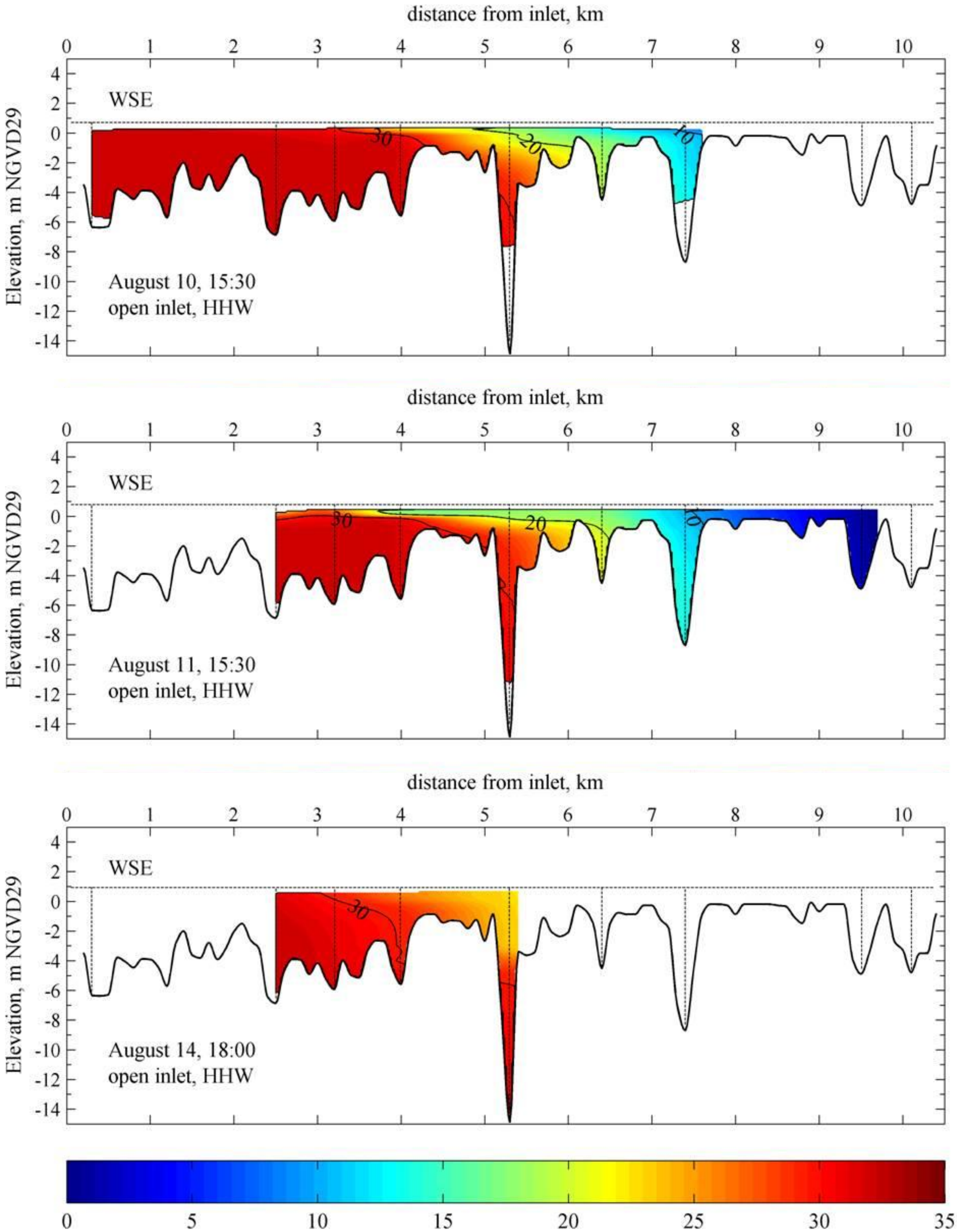

Figure 9.3.2 Estuary salinity structure on **(top)** August 10, **(mid)** August 11 and **(bottom)** August 14. Salinity units are psu.

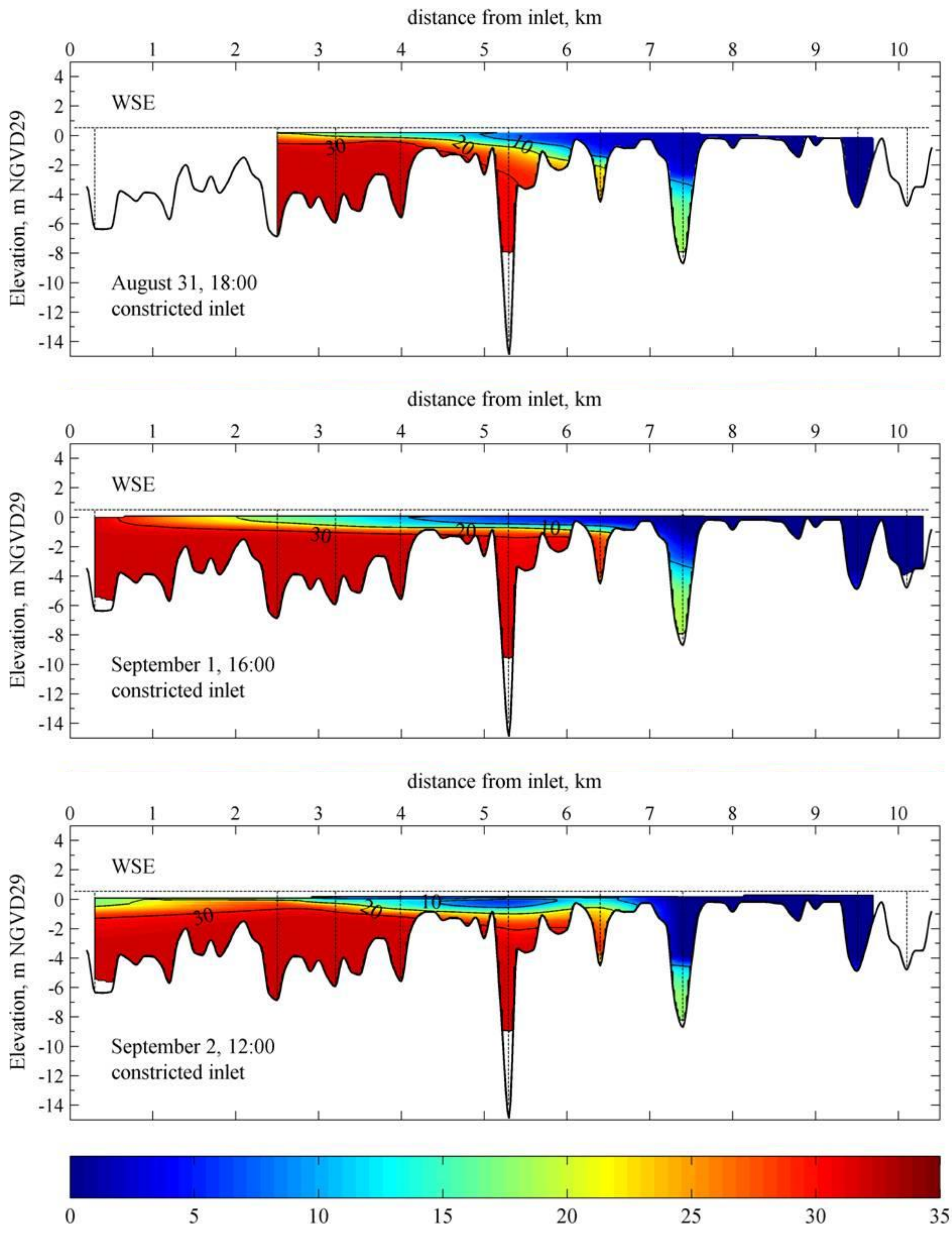

Figure 9.3.3 Estuary salinity structure on **(top)** August 31, **(mid)** September 1 and **(bottom)** September 2. Salinity units are psu.

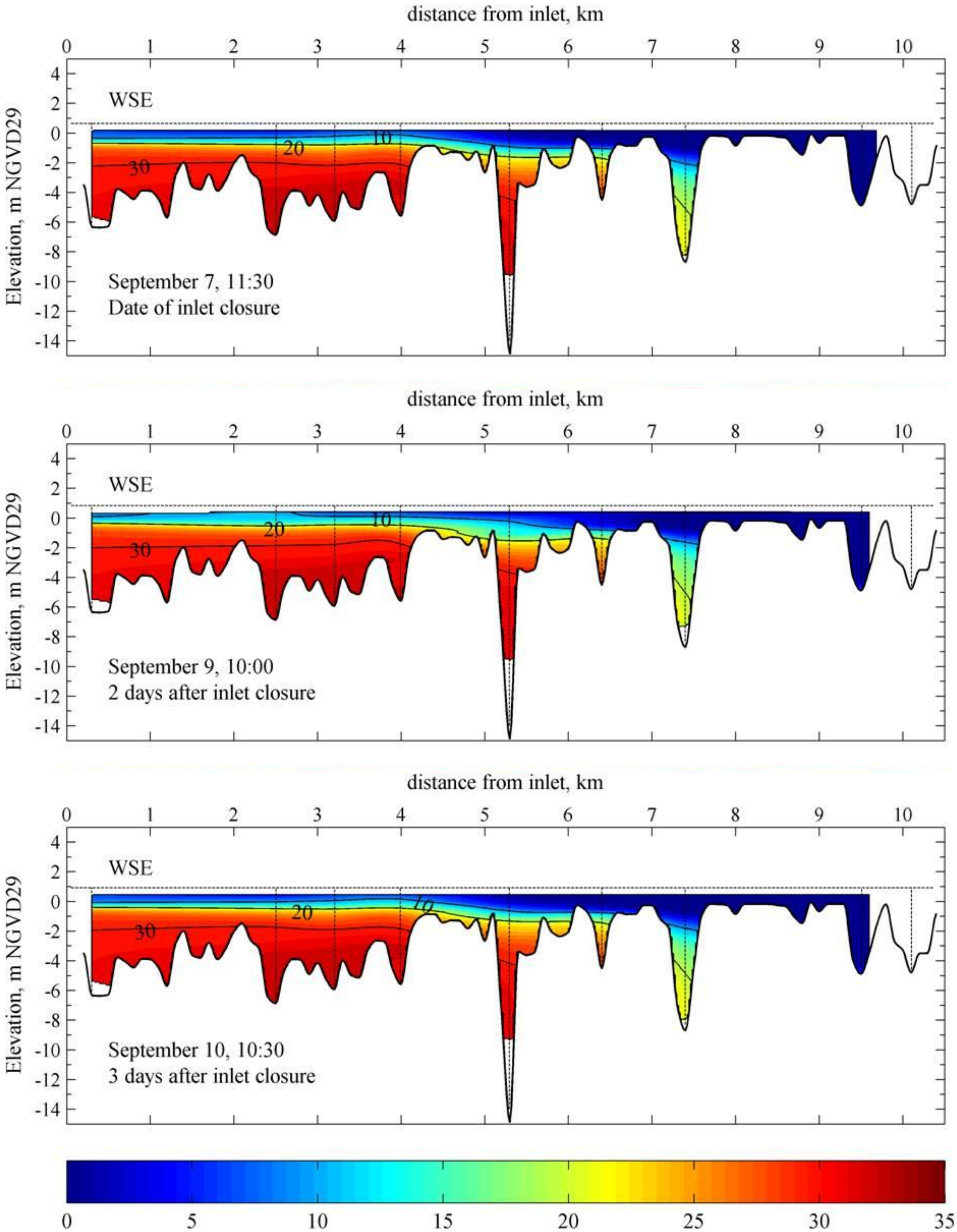

Figure 9.3.4 Estuary salinity structure on **(top)** September 7, **(mid)** September 9 and **(bottom)** September 10. Salinity units are psu.

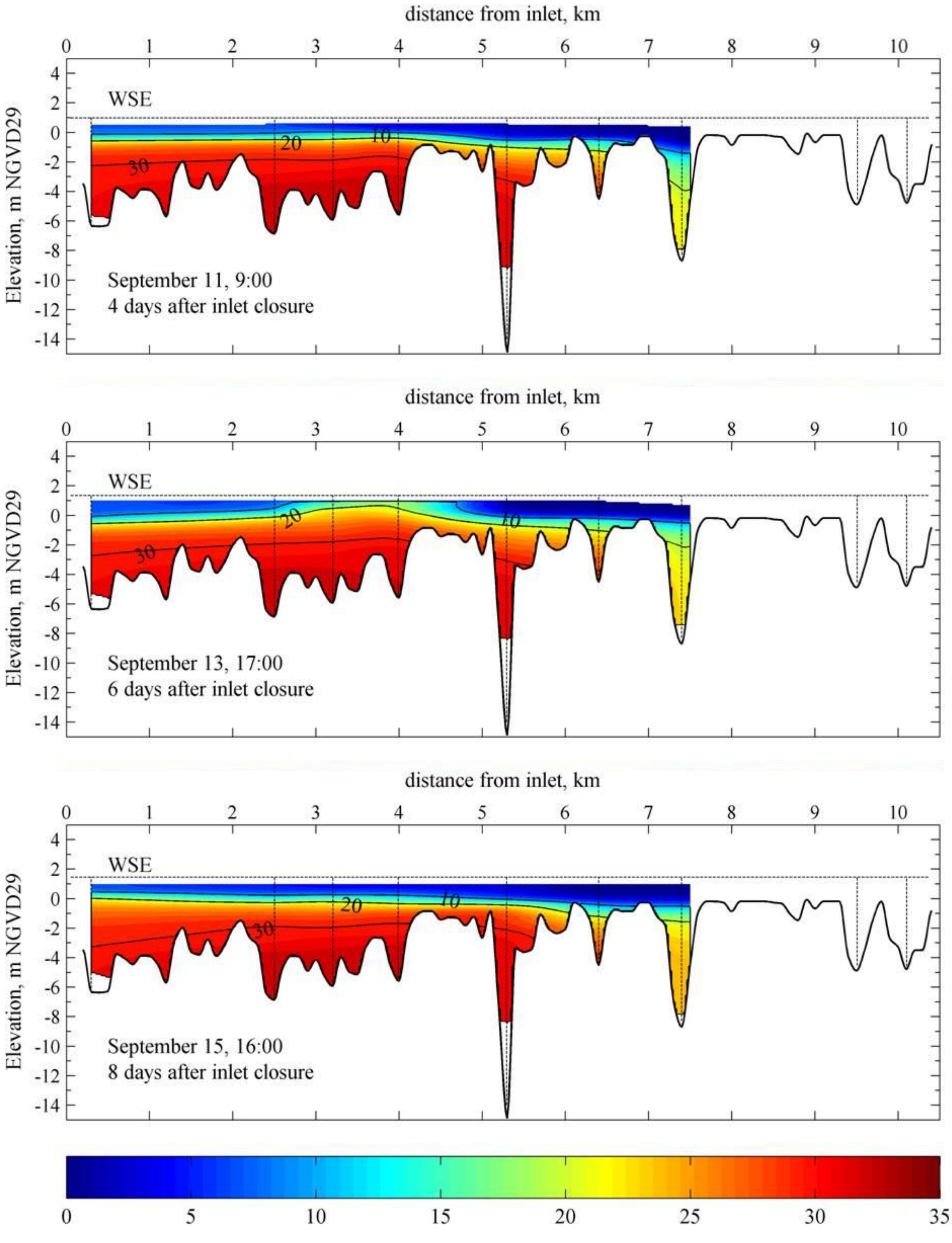

Figure 9.3.5 Estuary salinity structure on **(top)** September 11, **(mid)** September 13 and **(bottom)** September 15. Salinity units are psu.

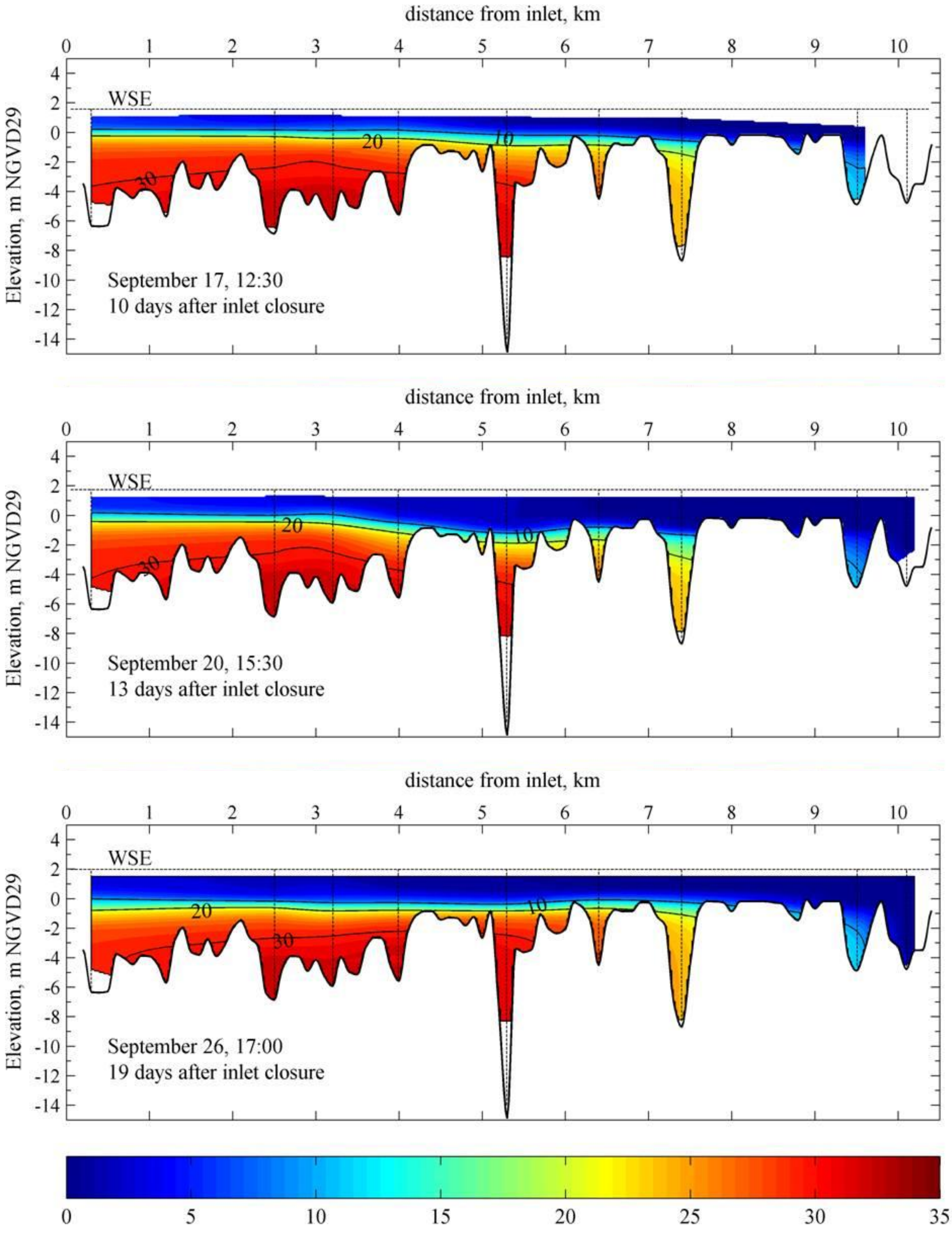

Figure 9.3.6 Estuary salinity structure on **(top)** September 17, **(mid)** September 20 and **(bottom)** September 26. Salinity units are psu.

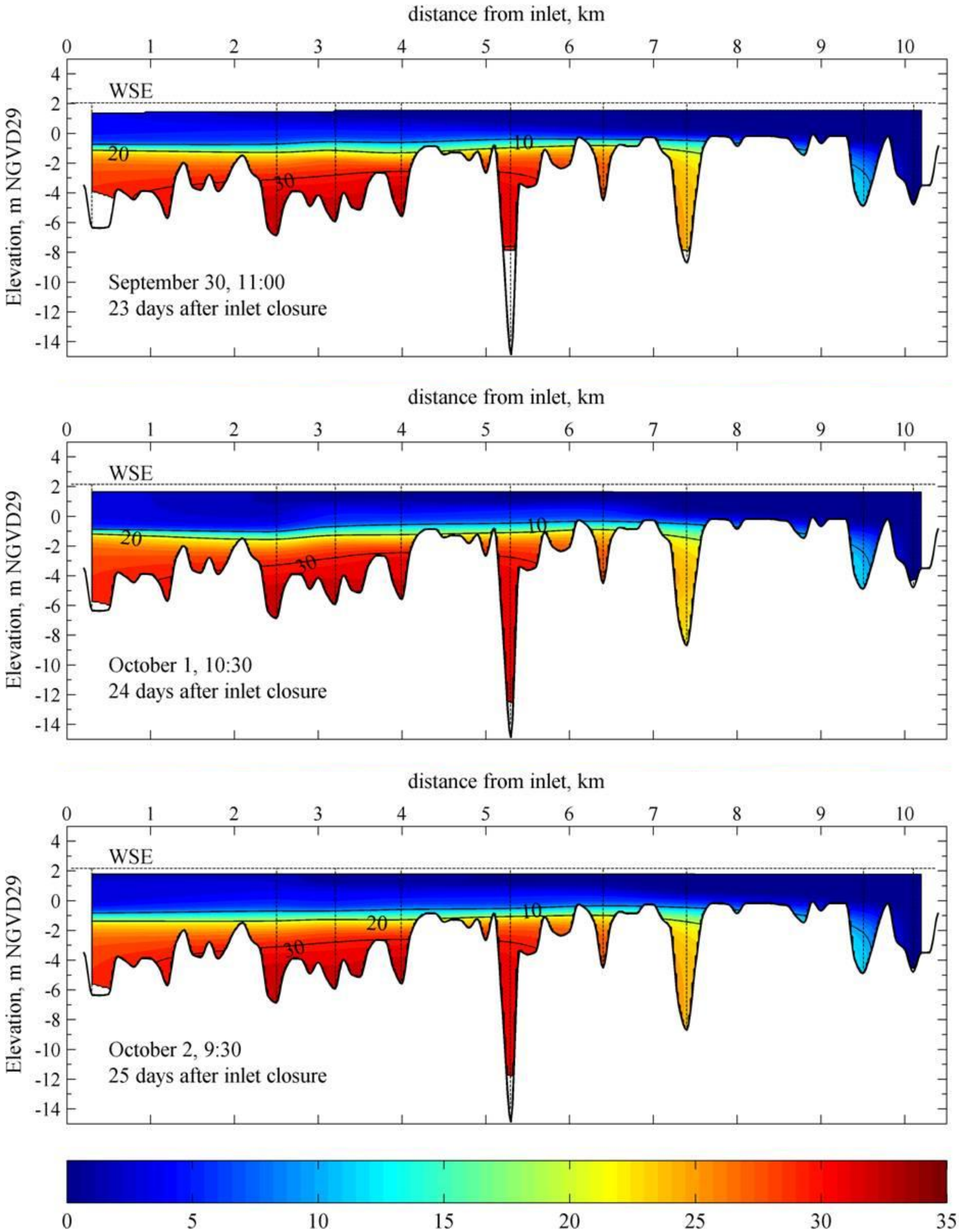

Figure 9.3.7 Estuary salinity structure on **(top)** September 30, **(mid)** October 1 and **(bottom)** October 2. Salinity units are psu.

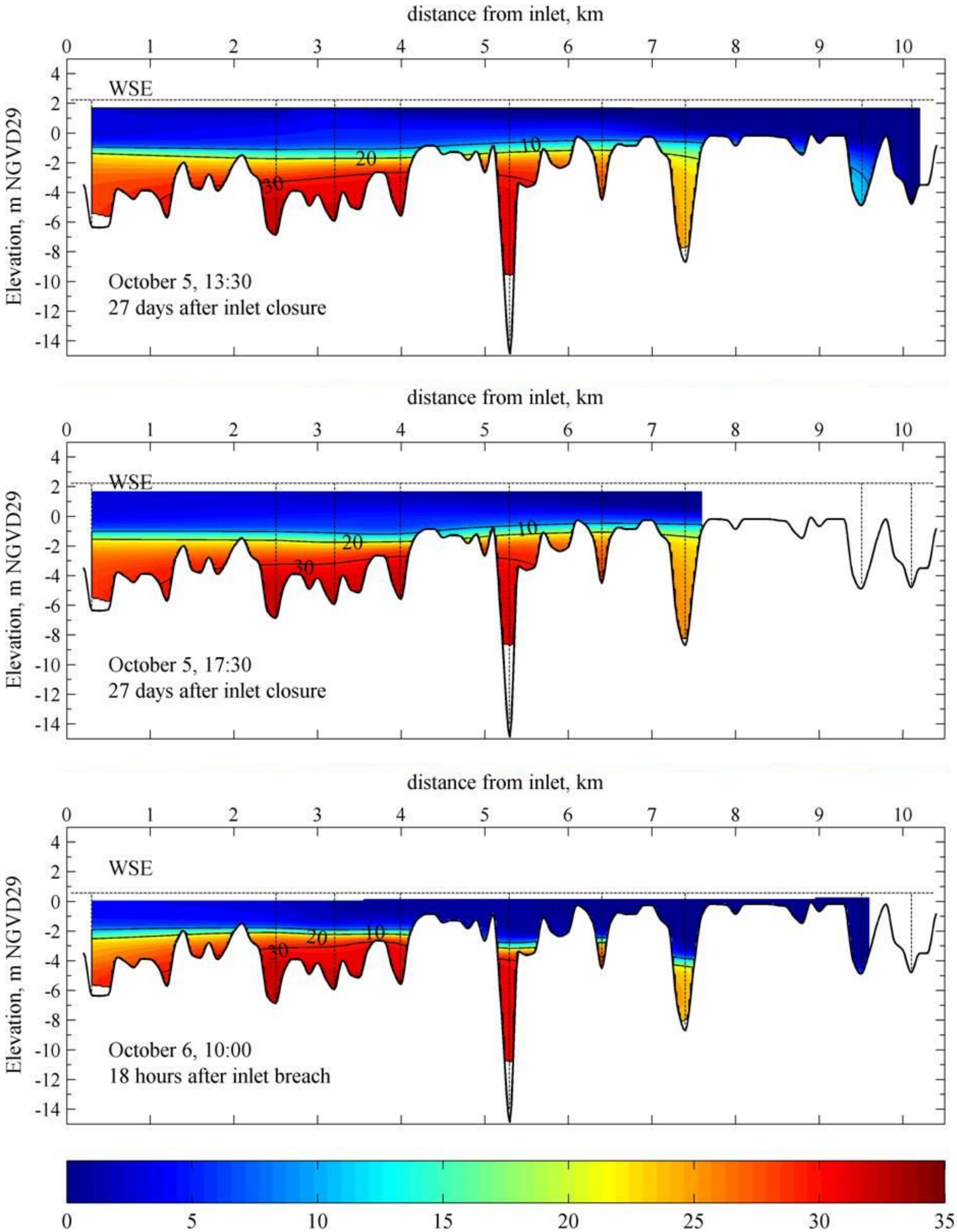

Figure 9.3.8 Estuary salinity structure on **(top)** October 5, 13:30, **(mid)** October 5, 17:30 and **(bottom)** October 6, 10:00. Salinity units are psu.

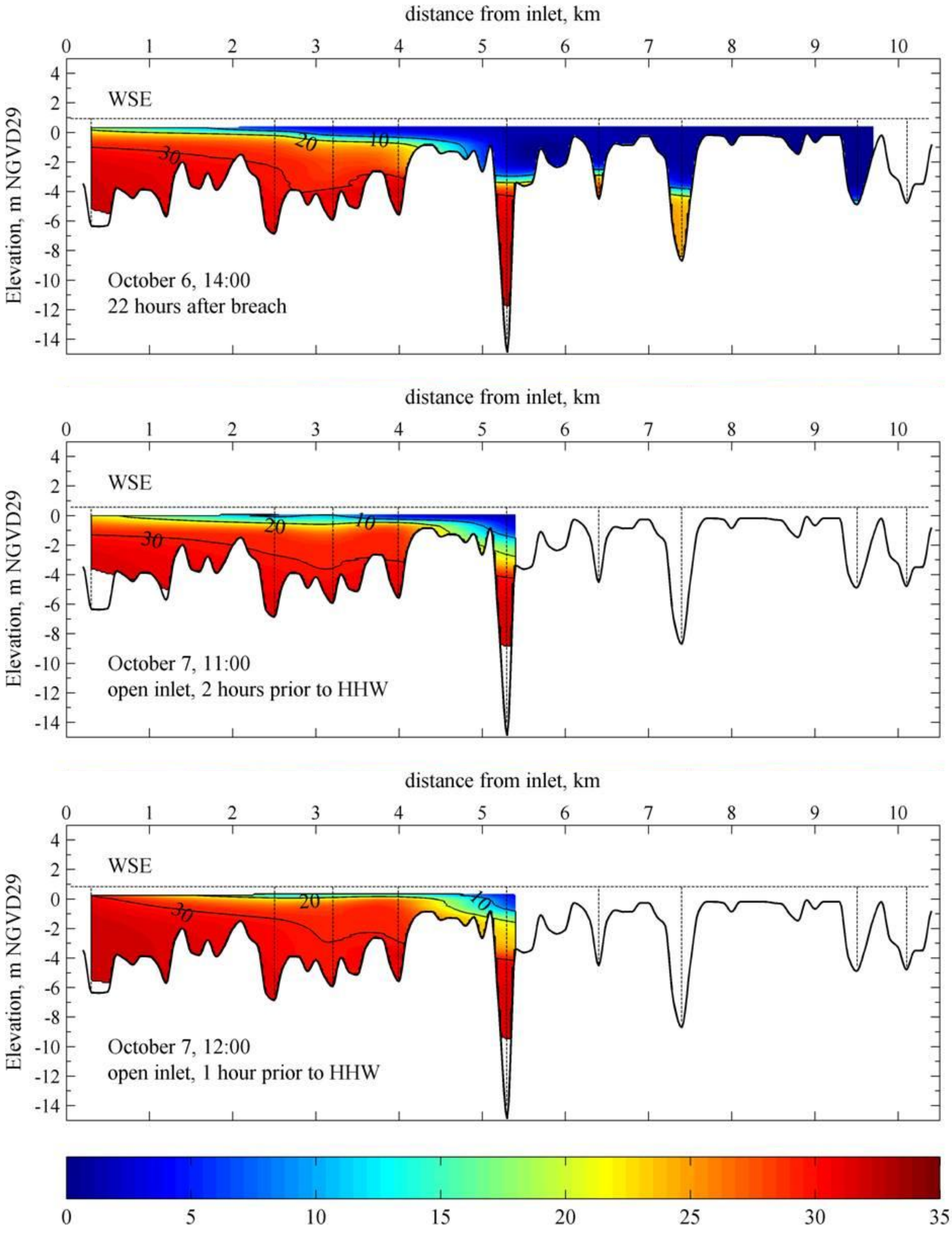

Figure 9.3.9 Estuary salinity structure on **(top)** October 6, 14:00, **(mid)** October 7, 11:00 and **(bottom)** October 7, 12:00. Salinity units are psu.

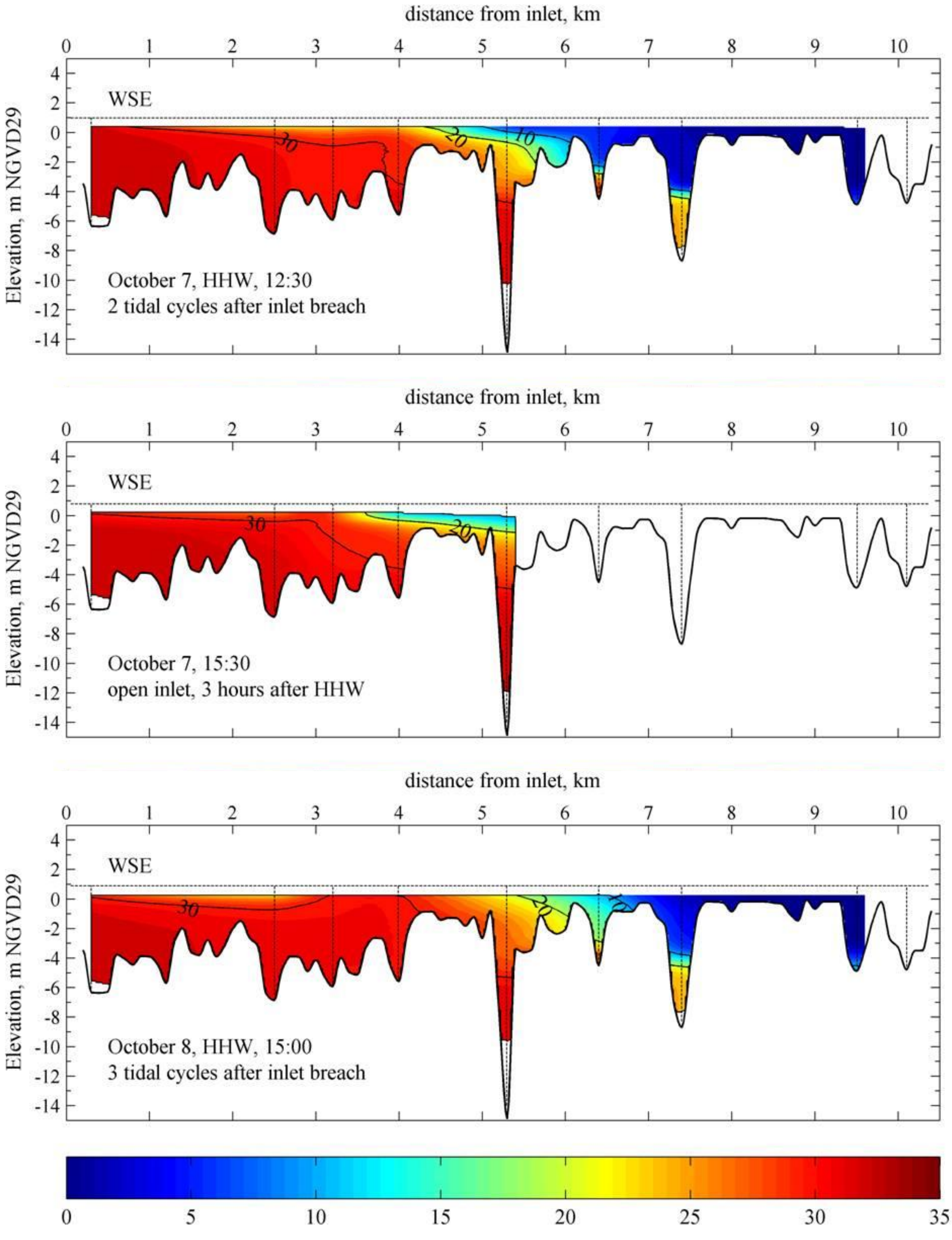

Figure 9.3.10 Estuary salinity structure on **(top)** October 7, 12:30, **(mid)** October 7, 15:30 and **(bottom)** October 8. Salinity units are psu.

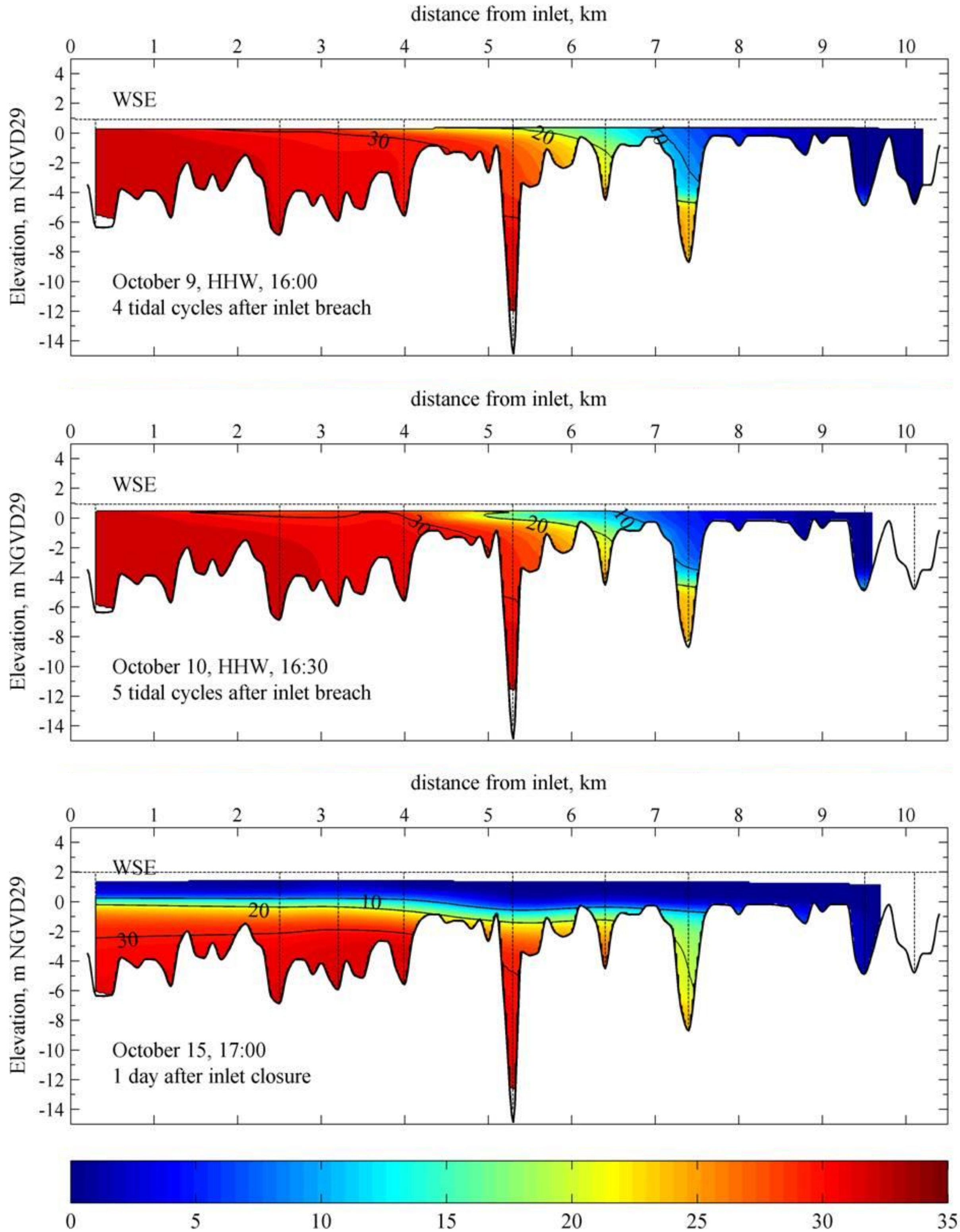

Figure 9.3.11 Estuary salinity structure on **(top)** October 9, **(mid)** October 10 and **(bottom)** October 15. Salinity units are psu.

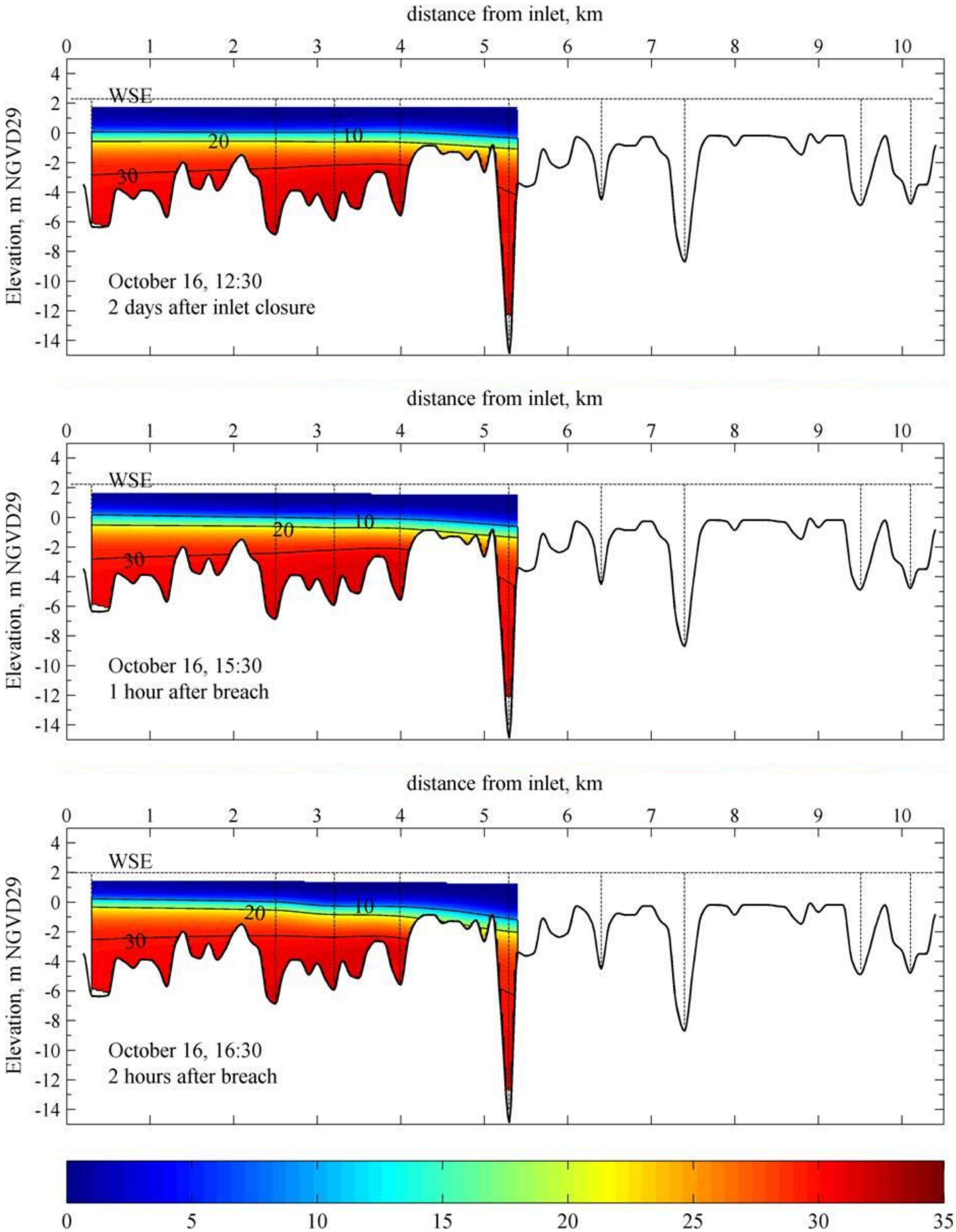

Figure 9.3.12 Estuary salinity structure on **(top)** October 6, 12:30, **(mid)** October 6, 15:30 and **(bottom)** October 6, 16:30. Salinity units are psu.

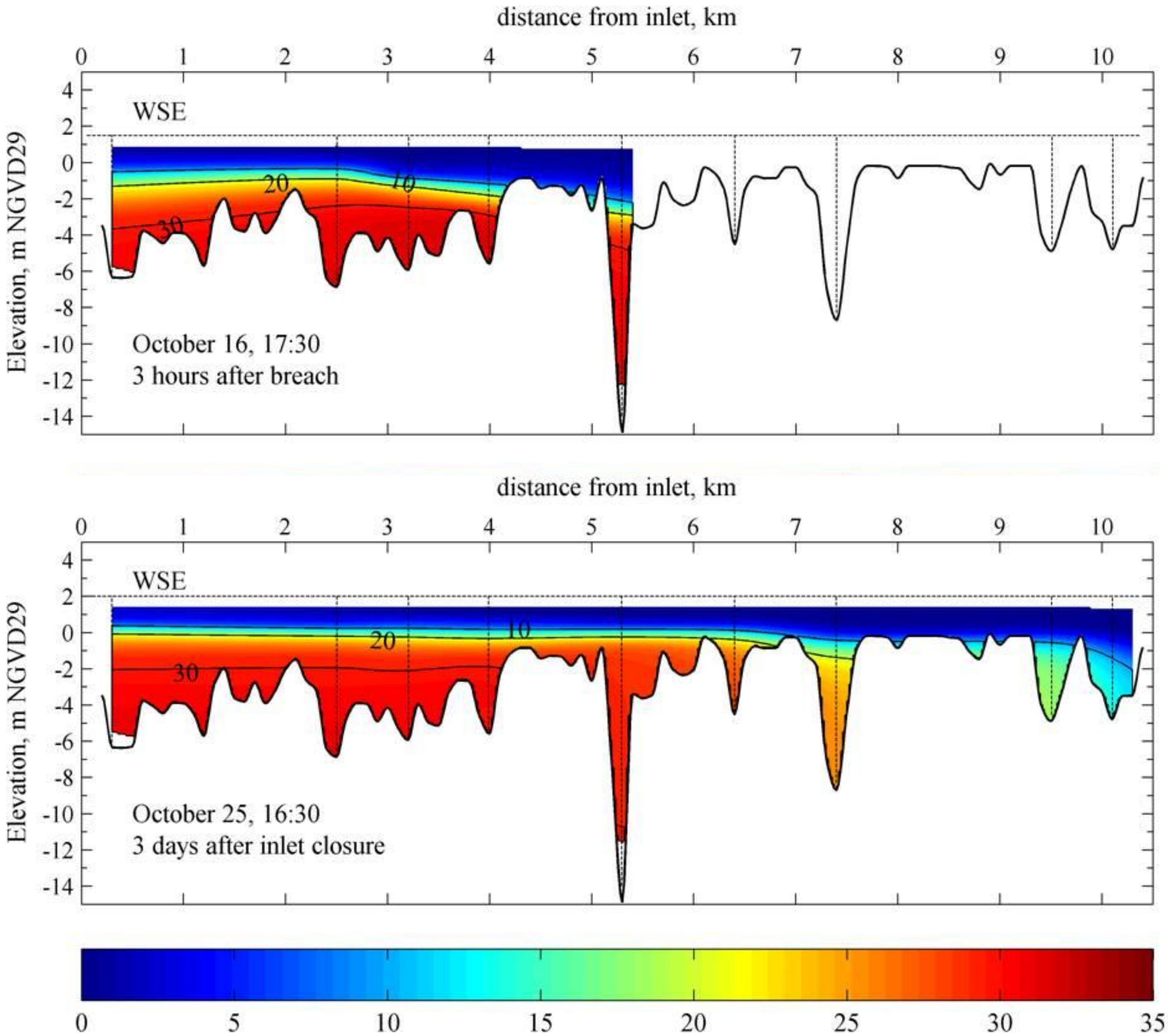

Figure 9.3.12 Estuary salinity structure on **(top)** October 16, 17:30, and **(bottom)** October 25. Salinity units are psu.